

University of Alberta

Separation of Pyrolusite and Hematite by Froth Flotation

By

Marc Donald Parrent

A thesis submitted to the Faculty of Graduate Studies and Research in partial fulfillment of the requirements for the degree of

Master of Science
in
Materials Engineering

Department of Chemical and Materials Engineering

©Marc Donald Parrent
Fall 2012
Edmonton, Alberta

Permission is hereby granted to the University of Alberta Libraries to reproduce single copies of this thesis and to lend or sell such copies for private, scholarly or scientific research purposes only. Where the thesis is converted to, or otherwise made available in digital form, the University of Alberta will advise potential users of the thesis of these terms.

The author reserves all other publication and other rights in association with the copyright in the thesis and, except as herein before provided, neither the thesis nor any substantial portion thereof may be printed or otherwise reproduced in any material form whatsoever without the author's prior written permission.

ABSTRACT

Due to challenges faced by the Wabush mine, the separation of pyrolusite and hematite using froth flotation was investigated. Using sodium oleate as a collector, micro-scale flotation testing identified conditions for selective separation of pyrolusite and hematite. When applied to Wabush iron ore on a bench-scale, direct flotation produced hematite concentrates meeting the target of 90% mass pull at 40% Mn rejection. Two separate bench-scale conditions achieved the target; the first at pH 11 using 200 g/t sodium oleate, and the second at pH 9 using 200 g/t sodium oleate and 250 g/t potato starch. Fourier transform infrared spectroscopy (FTIR) was used to study adsorption of oleate on pyrolusite and hematite. At pH 11 oleate was bound to hematite via a mixture of inner-sphere monodentate mononuclear (ISMM) and open-sphere surface hydration-shared (OS-HS) modes, while adsorption on pyrolusite was primarily ISMM with contributions from (OS-HS) and inner-sphere bidentate binuclear (ISBB) modes.

ACKNOWLEDGMENTS

Of the many people who provided me with encouragement and support during my studies, I would first like to thank Dr. Liu. Graduate school is not a path I would have taken had it not been for his encouragement and guidance over the past few years.

For financial support I would like to thank NSERC. I am also indebted to COREM for both financial support, and supplying me with iron ore. Dr. Liming Huang of COREM must also be acknowledged for organizing the assays of my bench flotation products.

I also owe thanks to Dr. Allen Pratt of CANMET and Dr. Jeff Harris of Harris Exploration Services for their contributions to my mineralogy study, as well as Gayle Hatchard for helping with SEM analysis.

I also need to thank Shiraz Merali for conducting XRD analysis, as well as Dr. Dimitre Karpuzov, Dr. Anquang He, and Shihong Xu of ACSES for their training and patience.

To Dr. Mingli Cao and my fellow group members, I owe thanks for both technical support and good company. I would also like to thank my colleagues Stephen Gibson, Patrick Kerr, Kevin Scott, Nicole Lee Robertson, and Katherine Jonsson for their understanding, friendship, and inspiration.

To my family I owe thanks for their support, and showing me what can be done with drive and determination.

Finally I would like to thank my beloved Nicole, who has been steadfast in her support for me during my studies. With you, anything is possible.

TABLE OF CONTENTS

1. INTRODUCTION.....	1
1.1 Wabush Iron Ore Mine.....	1
1.2 Challenges in Iron Ore Production	2
1.3 Organization of the Thesis.....	4
2. Literature Review.....	6
2.1 Flotation Theory	6
2.2 Hematite Flotation	9
2.2.1 Zeta Potential of Hematite.....	9
2.2.2 Flotation of Pure Hematite	9
2.2.3 Cations in Hematite Flotation	18
2.2.4 Depressants and Modifiers in Hematite Flotation.....	19
2.2.5 Flotation of Iron Ores.....	23
2.3 Pyrolusite Flotation	23
2.3.1 A Note on Manganese Dioxide	23
2.3.2 Zeta Potential of Pyrolusite.....	24
2.3.3 Flotation of Pure Pyrolusite	25
2.3.4 Cations in Pyrolusite Flotation	30
2.3.5 Depressants and Modifiers in Pyrolusite Flotation.....	33
2.3.6 Flotation of Manganese Oxide Ores	35
2.4 Manganese and Iron Bearing Mineral Flotation	36
2.5 Oxide Mineral Hydrolysis and Flotation.....	40
2.6 Fatty Acid Adsorption.....	44
3. Objectives.....	47
4. Materials and Methods.....	49
4.1 Iron Ore Concentrate	49
4.1.1 Sample Description and Preparation	49
4.1.2 SEM, EDX, and EPMA Analysis	50
4.2 Pyrolusite Concentrate.....	52

4.3	Chemical Assays	53
4.4	Reagents.....	54
4.5	Micro-Scale Flotation: Single Minerals.....	55
4.6	Bench-Scale Flotation: Wabush Ore.....	56
4.6.1	Bench-Scale Flotation Procedure.....	56
4.6.2	Spiral Concentrate Grinding and Particle Size	58
4.7	Mechanism Study.....	58
4.7.1	Zeta Potential.....	58
4.7.2	FTIR Sample Preparation.....	59
4.7.3	Pure Mineral Experiment: FTIR.....	60
5.	Mineralogical Analysis	61
5.1	SEM and EDX Analysis	61
5.2	SEM and X-Ray Mapping by Harris Exploration	63
5.3	SEM and Wavelength Dispersive Spectrometry by CANMET	64
6.	Flotation and Mechanism Studies.....	67
6.1	Zeta Potential	67
6.2	Micro-Scale Flotation	69
6.3	Bench-Scale Flotation.....	76
6.3.1	Reverse Flotation	77
6.3.2	Effect of Grind Size.....	78
6.3.3	Effect of Sodium Silicate	80
6.3.4	Complexing Agents and Cations	81
6.3.5	Effect of Potato Starch	82
6.3.6	Silicate Flotation.....	84
6.3.7	Micro and Bench-Scale Correlation	87
6.4	Mechanism Study: FTIR	88
7.	Conclusions and Recommendations	99
7.1	General Findings.....	99
7.2	Recommendations for Future Work	102

8. References.....	103
Appendix I: Bench Flotation Tests	108
Appendix II: Grinding and Passing Size.....	147
Appendix III: Mineralogical Analysis by CANMET	149
Appendix IV: Harris Exploration	158
Appendix V: Micro-Scale Flotation.....	167
Appendix VI: FTIR Spectra	168

LIST OF TABLES

Table 1: Summary of the composition, zero point of charge, and crystal structure for manganese dioxides.....	24
Table 2: Summary of manganese ore flotation.....	36
Table 3: Modes of carboxyl-iron bonding	45
Table 4: FTIR frequencies for fatty acid bonding on iron oxides	46
Table 5: Chemical analysis of iron ore samples	50
Table 6: Characteristic X-ray lines and standards for EPMA.....	51
Table 7: Chemical analysis of pyrolusite concentrate.....	52
Table 8: Potential conditions for differential flotation of pyrolusite and hematite	76
Table 9: Metallurgical balance for bench-scale flotation test BI13, the flotation of Wabush spiral concentrate at pH 11 using sodium oleate, at a grind size of 80% passing 117 μm	79
Table 10: Metallurgical balance for bench-scale flotation test BI23, the flotation of Wabush spiral concentrate at pH 9 using sodium oleate and potato starch, at a grind size of 80% passing 117 μm	83
Table 11: Metallurgical balance for bench-scale flotation test BI35, the amine flotation of Si minerals from Wabush spiral concentrate, at a grind size of 80% passing 117 μm . Potato starch was used to depress iron oxide.	86
Table 12: Summary of FTIR band assignments for solid sodium oleate as well as hematite (Fe_2O_3) and pyrolusite (MnO_2) conditioned in 1.0×10^{-3} mol/L sodium oleate solution at pH 7 and 11	94

LIST OF FIGURES

Figure 1: Concentrator flowsheet for Wabush Mine	2
Figure 2: Froth flotation concept	6
Figure 3: Illustration of generalized zeta potential – pH curves for a simple indifferent electrolyte, a physisorbed surfactant, and a chemisorbed surfactant	8
Figure 4: (A) The zeta potential of hematite as a function of pH, (B) the flotation of hematite using 1×10^{-4} mol/L dodecylammonium chloride and sodium dodecyl sulfate, and (C) the flotation of hematite with 1×10^{-4} mol/L octadecylammonium chloride and sodium octadecyl sulphate	11
Figure 5: Electrophoretic mobility of ferric oxide at 2×10^{-3} mol/L NaCl	13
Figure 6: The recovery of hematite at 25°C using 2×10^{-4} mol/L potassium octyl hydroxamate as a function of pH and conditioning time.	14
Figure 7: Flotation recovery of hematite with 1×10^{-4} mol/L potassium oleate at 25°C as a function of pH and conditioning time.....	15
Figure 8: Electrophoretic mobility of ferric oxide with 2×10^{-3} mol/L NaCl as a function of pH and oleic acid dosage	16
Figure 9: Flotation recovery of hematite with 2.5×10^{-5} mol/L sodium oleate as a function of pH and conditioning time.	18
Figure 10: Flotation recovery of hematite as a function of pH, dodecylamine dosage, and starch dosage.....	20
Figure 11: Flotation recovery of pyrolusite as a function of pH using sodium alkyl aryl sulfonate and dodecyl amine at 23°C.....	25
Figure 12: Flotation recovery of γ -MnO ₂ as a function of pH using potassium octyl hydroxamate.	26
Figure 13: Flotation recovery of γ -MnO ₂ as a function of pH using sodium dodecyl sulfonate.....	27
Figure 14: Flotation recovery of pyrolusite using 1×10^{-4} mol/L potassium oleate as a function of pH at 23°C.	28
Figure 15: Flotation recovery of pyrolusite using 1×10^{-4} mol/L potassium oleate as a function of pH at 23°C and 60°C.....	29
Figure 16: Zeta potential of pyrolusite as a function of pH	31
Figure 17: Flotation of manganese oxides as a function of pH and cetyl trimethyl ammonium bromide (CTAB) concentration.....	33
Figure 18: Co-adsorption of sulphite and oleate on β -MnO ₂ at pH 7 and room temperature.....	34

Figure 19: Amount of Mn^{2+} ions formed on conditioning β - MnO_2 in sulphite solution at pH 7 and 35°C.	35
Figure 20: Flotation recovery of chromite with oleic acid as a function of pH. ...	41
Figure 21: The logarithmic concentration diagram for 1×10^{-4} mol/L Fe^{++}	42
Figure 22: (A) Flotation recovery of rhodonite with potassium octyl and nonyl hydroxamate as a function of pH. (B) The effect of Mn^{2+} addition on the zeta potential of rhodonite as a function of pH, and (C), the concentration diagram for 1×10^{-4} mol/L Mn^{2+}	43
Figure 24: Size analysis of as-received Wabush spiral concentrate	49
Figure 25 : XRD pattern for pyrolusite	53
Figure 26: "Siwek" type micro-scale flotation tube	55
Figure 27: JK Tech bottom drive flotation machine and 1.5 L cell.....	57
Figure 28: Brookhaven Instruments ZetaPALS Zeta Potential Analyzer	59
Figure 29: Nicolet 8700 spectrometer	60
Figure 30: (A) Back-scattered electron SEM Image of Wabush spiral concentrate. (B) EDX profile	61
Figure 31: (A) Back-scattered electron SEM Image of Mn bearing particle in Wabush spiral concentrate. (B) EDX profile	63
Figure 32: BI06 Concentrate. (A): BSE image with numbers 1 through 12 indicating EDX line scans. (B): X-ray map of area in (A).....	64
Figure 33: XRD Analysis of Wabush spiral concentrate..	65
Figure 34: BSE image of Wabush Spiral Concentrate and EPMA analysis of points 1-3.	66
Figure 35: Zeta Potential of IOC as a function of pH and sodium oleate dosage.	67
Figure 36: Zeta potential of pyrolusite as a function of pH and sodium oleate dosage.	69
Figure 37: Micro-scale flotation recovery of IOC and pyrolusite as a function of pH at a sodium oleate dosage of 5×10^{-5} mol/L.....	70
Figure 38: Micro-scale flotation recovery of pyrolusite as a function of pH at sodium oleate dosages of 2×10^{-5} mol/L, 5×10^{-5} mol/L, and 1×10^{-4} mol/L.....	71
Figure 39: Micro-scale flotation recovery of pyrolusite and IOC as a function of pH at a sodium oleate dosage of 5×10^{-5} mol/L. (A) sodium silicate dosage of 100 mg/L, and (B) sodium dihydrogen phosphate dosage of 100 mg/L.....	72

Figure 40: Micro-scale flotation recovery of pyrolusite and IOC as a function of pH at a sodium oleate dosage of 5×10^{-5} mol/L. (A) potato starch dosage of 50 mg/L, and (B) tannic acid dosage of 10 mg/L.....	74
Figure 41: Micro-scale flotation recovery of pyrolusite and IOC as a function of pH at a sodium oleate dosage of 5×10^{-5} mol/L. (A) CuSO_4 dosage of 50 mg/L, and (B) MnSO_4 dosage of 50 mg/L.....	75
Figure 42: Mn Recovery vs. Mass pull for bench-scale flotation of Wabush spiral concentrate.	77
Figure 43: Mn Recovery vs. Mass pull for bench-scale flotation of Wabush spiral concentrate.	78
Figure 44: Mn Recovery vs. Mass pull for bench-scale flotation of Wabush spiral concentrate.	80
Figure 45: Mn Recovery vs. Mass pull for bench-scale flotation of Wabush spiral concentrate.	81
Figure 46: Mn Recovery vs. Mass pull for bench-scale flotation of Wabush spiral concentrate.	83
Figure 47: Si mineral recovery as a function of Mn mineral recovery for bench-scale flotation of Wabush spiral concentrate.....	85
Figure 48: Si mineral recovery as a function of total rougher concentrate mass pull for bench-scale flotation of Wabush spiral concentrate.	86
Figure 49: Recovery as a function of pH and grind size for the micro-scale flotation of IOC and pyrolusite at a sodium oleate dosage of 5×10^{-5} mol/L.....	88
Figure 50: (A) FTIR (DRIFTS) spectra of solid sodium oleate in comparison to Fe_2O_3 (IOC) and MnO_2 (pyrolusite) conditioned in 1.0×10^{-3} mol/L sodium oleate solution at pH 7 over a range of $1200 - 3000 \text{ cm}^{-1}$; (B) the same conditions as (A) with a spectral range of $1200 - 1800 \text{ cm}^{-1}$	90
Figure 51: (A) FTIR (DRIFTS) spectra of solid sodium oleate in comparison to Fe_2O_3 (IOC) and MnO_2 (pyrolusite) conditioned in 1.0×10^{-3} mol/L sodium oleate solution at pH 11 over a range of $1200 - 3000 \text{ cm}^{-1}$; (B) the same conditions as (A) with a spectral range of $1200 - 1800 \text{ cm}^{-1}$	92
Figure 52: FTIR (DRIFTS) spectra of MnO_2 (pyrolusite) conditioned in 1.0×10^{-3} mol/L sodium oleate solution at pH 7 and 11 over a range of $1200 - 1800 \text{ cm}^{-1}$	95

LIST OF UNITS AND NOMENCLATURE

atm	atmospheres
°C	degrees Celsius
g	gram
g/T	grams per tonne
km	kilometer
kV	kilovolt
kWh	kilowatt hour
mg/L	milligrams per liter
mol/L	moles per liter
nA	nanoampere
μm	micrometer
δ	deformation mode for infrared spectra
ν	vibrational stretching mode for infrared spectra
ν _s	vibrational symmetric stretching mode for infrared spectra
ν _{as}	vibrational asymmetric stretching mode for infrared spectra
ω	vibrational wagging mode for infrared spectra

1. INTRODUCTION

1.1 Wabush Iron Ore Mine

A significant hub of iron ore mining in Canada hinges the border of Labrador and Québec; with the major commerce center in the area being Labrador City, Labrador. Several iron ore mines operate in the area including the Iron Ore Company of Canada (IOC), based out of Labrador City, Labrador; ArcelorMittal with operations at Fire Lake and Mont Wright, Québec; and Cliff's Natural Resources with the Bloom Lake mine near Fermont, Québec and Wabush mine at Wabush, Labrador. The Wabush mine has been operating since 1965 and has a current operating capacity of 5.6 million tonnes annually [1]. Iron ore is concentrated at facilities in Wabush then transported by rail 445 km (275 miles) to Pointe Noire, near Sept-Isles, Québec, for pelletizing and ship loading.

The Wabush mine is based on a 1425 hectare (5.5 square mile) ore bed of quartz-specularite schists [2, 3]. The head grade of the ore averages 36 wt% Fe, with iron being present mainly as hematite (Fe_2O_3 , also called specularite in coarse-grained form) with some magnetite (Fe_3O_4) [2, 3]. Quartz and silica (SiO_2) are the major gangue minerals, accounting for approximately 50 wt% of the ore [2]. Beneficiation of the ore begins with crushing and grinding, followed by spiral concentration, producing a spiral concentrate grading 60 wt% Fe and 5 wt% silica. Tails from spiral concentration are subjected to low intensity wet magnetic separation (LIWMS) and high intensity wet magnetic separation (HIWMS). Concentrate from the spirals is subjected to high-tension electrostatic separation. Concentrates from the magnetic and electrostatic separation streams are combined to produce a final concentrate grading 64 wt% Fe, 3 wt% SiO_2 , and 1.7 wt% Mn [2, 3]. The concentrator flowsheet for the Wabush mine is shown in Figure 1, which was reproduced from Damjanovic and Goode [3].

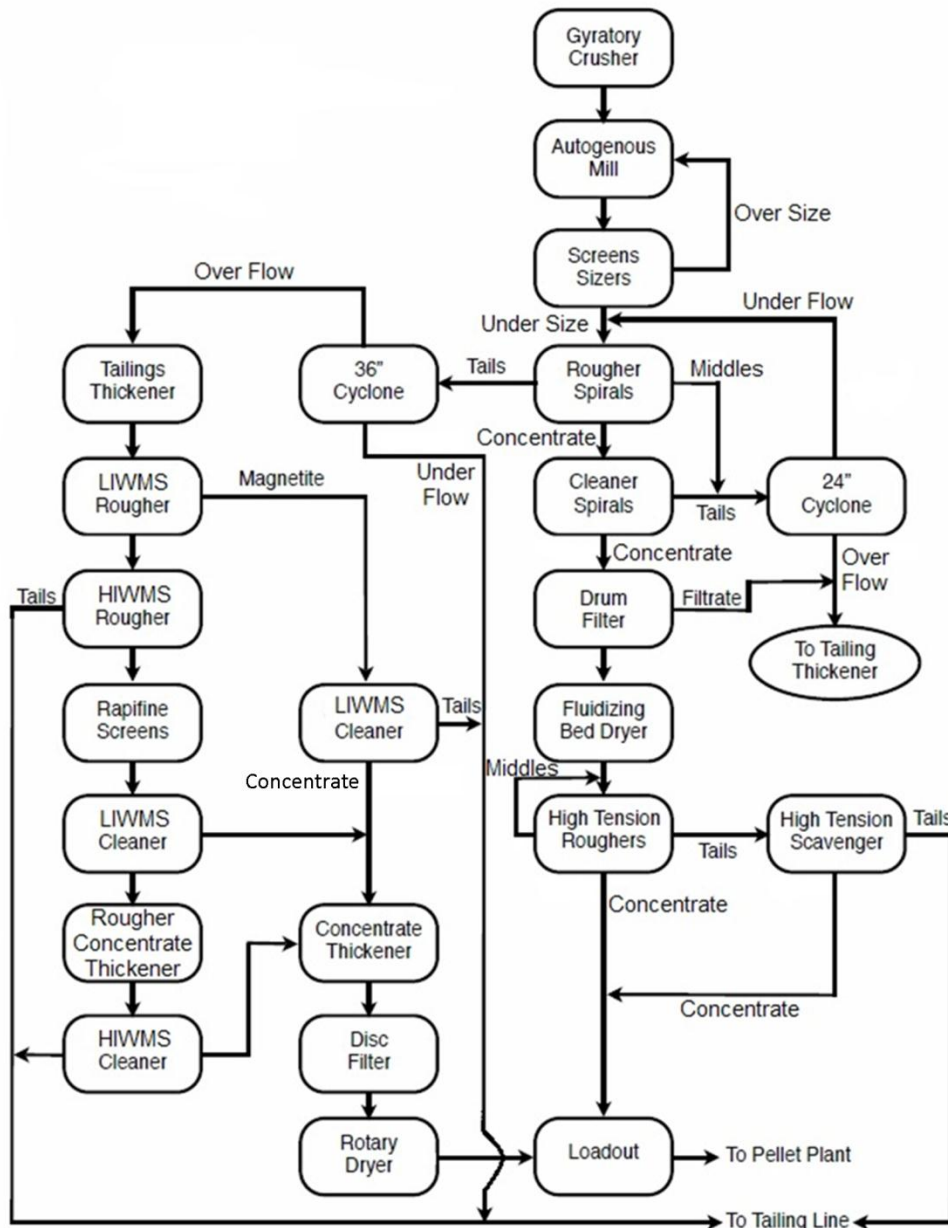


Figure 1: Concentrator flowsheet for Wabush Mine [3]

1.2 Challenges in Iron Ore Production at Wabush Mine

The major challenge faced by iron ore production at the Wabush mine is manganese content. Manganese content of the Wabush deposit can be in excess of 4 wt% Mn, present mainly as pyrolusite (MnO₂) [2]. The general requirement

of North American steel producers is the production of hot metal containing less than 0.4 wt% Mn [2]. Wabush iron ore pellets, which contain 1.2-2.0 wt% Mn, must be blended with low Mn iron ore in order to meet the Mn content specification of 0.4 wt% [2]. As North American steel producers become much less willing to accept high Mn iron ores, Wabush Mine has to ship as much as 60% of its iron ore concentrates overseas [2].

Until 2002, ore reserves at Wabush were estimated at about 250 million long tons, sufficient for about 40 years of production [2]. This reserve estimate, however, included material that graded up to 4 wt% Mn, a grade which was no longer marketable. Coupled with this was a problem of water inflow at the mine. The water inflow restricted access to the lower Mn orebody, which tended to be located in the lower sections of the deposit [2]. New reserve estimates were made considering a product content of 1.4 wt% Mn, which resulted in an estimated reserve of 58 million tonnes as of 2004, enough for production until about 2013 [2].

Reduction of manganese content in the Wabush iron ore concentrate is necessary for both marketability in North American markets, and the extension of the operation lifetime of the mine. Considering that the main manganese bearing mineral is pyrolusite (MnO_2), and that the main iron bearing mineral is hematite (Fe_2O_3), separation poses several challenges. Pyrolusite has a specific gravity of 4.7-4.9, while for hematite it is 4.9-5.3, so that gravity separation is not likely to be effective [4, 5]. Gravity separation is already the primary method of processing iron ore at Wabush mines, and no significant separation of manganese minerals is observed. Therefore, the remaining options for separation include magnetic separation, and froth flotation which is based on mineral surface properties.

Hematite is weakly magnetic while pyrolusite is nonmagnetic, presenting the possibility for magnetic separation. The current Wabush Mine flow sheet shown in Figure 1 already uses magnetic separation. However, this processing step is focused on the separation of silica from the iron ore, and it has little effect on the manganese content of the produced iron ore concentrate. The Wabush Mine has built a pilot magnetic separation facility (manganese reduction plant) for removing pyrolusite, but the plant has been running with mixed results.

Froth flotation may be an effective means of removing pyrolusite from the Wabush iron ore, although there is currently no equivalent example in the industry. Literature data shows that there is potentially enough difference in the surface charges of pyrolusite and hematite so that they may be separated via flotation. In the case of hematite, the zero point of charge (PZC) values can range from pH 4.0 to 8.9 [6]. Fuerstenau and Rice have reported PZC values for pyrolusite from pH 4.2 to 7.4, while Abeidu has reported an isoelectric point (IEP) of pH 3.8 [7, 8]. The great variation in the surface charge values for either mineral is dependent on the mineral's origin. While these ranges are ambiguous, they show that depending on the nature of the samples in question, the difference in surface charge of hematite and pyrolusite could be significant enough for flotation to be an effective means of separation.

1.3 Organization of the Thesis

This thesis begins with Chapter One, which introduces the main problem investigated by this study, while also providing a brief background.

Chapter Two contains a comprehensive literature review which provides a background on flotation theory, iron oxide flotation, manganese oxide flotation, oxide mineral hydrolysis, and fatty acid adsorption chemistry.

Chapter Three states the objectives of this study and methodologies used to achieve the objectives.

Chapter Four describes the materials and experimental methods used in this study. Mineral samples, reagents, and detailed experimental procedures are described.

Chapter Five presents results on the mineralogical studies of the Wabush spiral concentrate using scanning electron microscopy, energy dispersive X-ray spectroscopy, and electron probe micro analysis.

Chapter Six contains results and discussion from micro and bench-scale flotation tests, as well as the studies on the interaction mechanisms between flotation reagents and the mineral surfaces, primarily by Fourier transform infrared spectroscopy.

Chapter Seven concludes the thesis, and contains a summary of the findings, the important conclusions, and recommendations for future work.

2. Literature Review

While flotation separation of manganese oxides from iron oxides is apparently not common, flotation is widely utilized in the individual upgrading of manganese and iron ores. A comprehensive literature review follows which begins with an overview of flotation theory, then investigates flotation of iron and manganese ores, with a focus on hematite (Fe_2O_3) and pyrolusite (MnO_2). Reviews of flotation as a function of oxide mineral hydrolysis, and fatty acid adsorption on iron oxides conclude this chapter.

2.1 Flotation Theory

Froth flotation is a mineral separation process which utilizes differences in physico-chemical surface properties [9]. An illustration of the basic froth flotation concept is shown in Figure 2 [9]. A pulp of ground mineral particles in water is agitated while bubbles of air are injected into the pulp at the base of a flotation cell. As the air bubbles rise through the pulp, hydrophobic (water repellent) particles attach to the air bubbles and float to the pulp surface forming a froth layer. Hydrophilic (water attracting) mineral particles remain in the pulp.

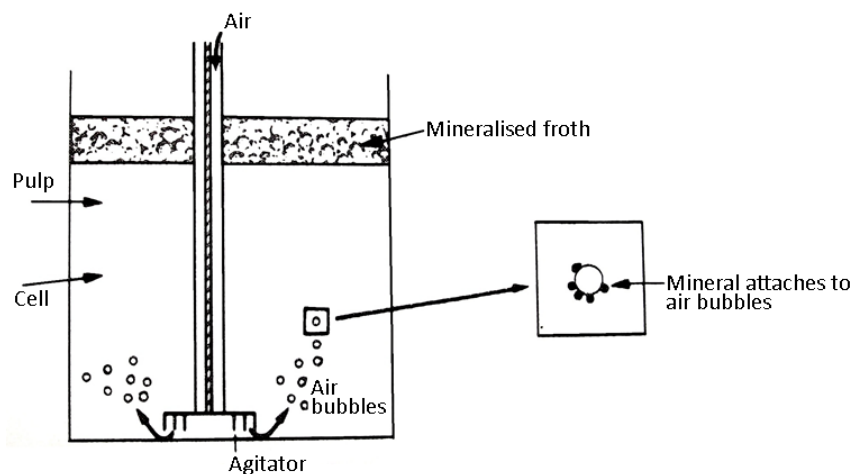


Figure 2: Froth flotation concept [9]

Minerals can be rendered hydrophilic or hydrophobic by the adjustment of pulp pH, as well as by the addition of reagents to the flotation pulp. Flotation reagents can generally be classified into the following categories:

Frothers: The role of a frother is stabilization of the froth layer. Frothers are typically heteropolar organic compounds, such as alcohols. The polar group is hydrated by water molecules, while the hydrocarbon tail is forced into the air phase, stabilizing the air bubbles in the froth layer by increasing their resistance to breakage [9].

Modifiers: A broad range of reagents can be classified under the umbrella of modifiers. Modifiers define any reagent added to the flotation pulp that makes flotation more selective, including depressants, activators, and pH regulators [9].

Depressants: A depressant plays the role of making specific minerals hydrophilic during flotation, thus keeping them in the flotation pulp [9]. While their role is the same, depressants vary greatly in form and behaviour.

Activators: Typically soluble salts, activators interact with the mineral surface promoting collector adsorption, and therefore increasing mineral hydrophobicity [9].

Collectors: Collectors are reagents which render minerals hydrophobic, causing attachment to air bubbles and collection in the froth phase. Collectors are typically heteropolar organic reagents with a non-polar section and polar section. Cationic collectors have a positively charged functional group, while anionic collectors have a negatively charged functional group.

Collectors can be further classified by the way they adsorb on a mineral surface. In physisorption, or physical adsorption, collectors adsorb via ion exchange or electrostatic attraction [10]. Physisorption is typically observed at low surfactant concentrations and low mineral surface charge densities [10]. Chemically adsorbing collectors form a chemical bond with the mineral surface. Examples of

chemisorbing collectors are fatty acids, which are known to form metal-carboxylate complexes with mineral surfaces [10]. Figure 3 illustrates the effect of physisorbing and chemisorbing collectors on the surface charge, or zeta potential, of a mineral and was adapted from Han, Healy, Fuerstenau [10]. As chemisorbing collectors form a chemical bond with the mineral surface, their adsorption will modify the point of zero charge (PZC) for the mineral, or the pH at which the charge of the mineral surface is zero. Physically adsorbing collectors cannot modify the PZC of a mineral, only the magnitude of charge above or below the PZC.

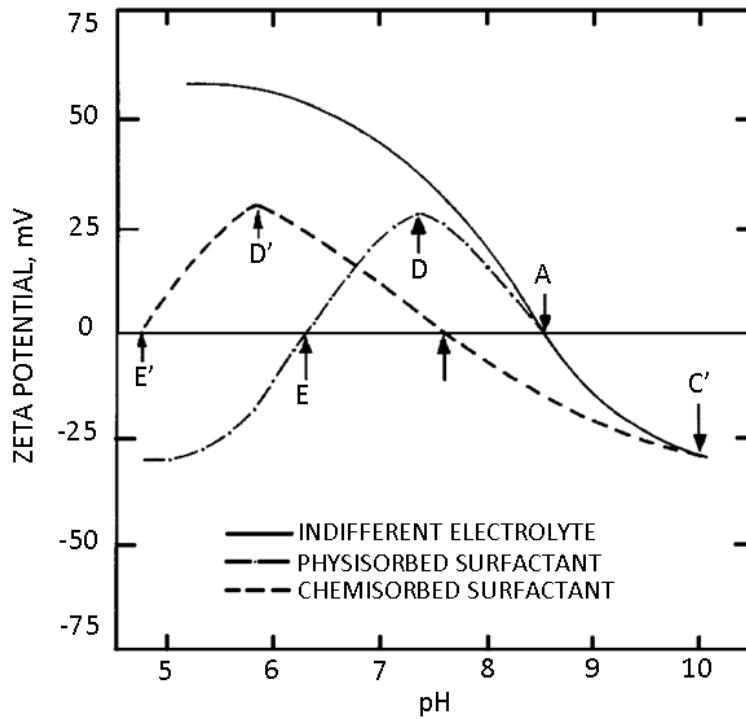


Figure 3: Illustration of generalized zeta potential – pH curves for a simple indifferent electrolyte, a physisorbed surfactant, and a chemisorbed surfactant. Point A indicates the PZC of the oxide, and point B indicates the PZC due to a chemically adsorbed collector [10]

2.2 Hematite Flotation

2.2.1 Zeta Potential of Hematite

A range of values has been reported for the zero point of charge (PZC) of natural hematite. Parks reported values for the PZC of pH 5.3 and 6.7 for natural hematite, and pH 8.6 for synthetic hematite [11]. Parks observed that PZC values occurred in “clusters” within certain pH ranges, depending on the nature of the mineral and techniques used; therefore, two values of PZC were reported for natural hematite. Wide ranging isoelectric point (IEP) values have been reported for hematite, from pH 2.7 to 7.8 [12–15]. These values appear to depend largely on the purity of the mineral sample used. Kulkarni measured an IEP of pH 3.0 and a PZC of pH 7.1 from a single hematite sample using electro-phoretic mobility and titration techniques respectively [12]. The variation in values was attributed to surface contamination of silicate on the hematite surface, in which case the titration technique is less sensitive and reported a value in agreement with other references. Regardless of the possible variation in IEP due to impurities and technique, the PZC of hematite should lie in the range of pH 5.3 to 8.6.

2.2.2 Flotation of Pure Hematite

Hematite flotation has been investigated using both cationic and anionic collectors. Many resources are available concerning flotation reagents used in hematite flotation; however, a good starting point is the review by Quast of hematite flotation using 12 carbon chain collectors, which is very thorough and focused on pure mineral flotation [13].

Amine type cationic collectors are commonly used in the flotation of hematite. Flotation response using amines is a function of pH, amine dosage and amine structure. In the case of amine dosage, there is an optimum value for full recovery as observed by Partridge and Smith [16]. If amine dosage exceeds the

optimum value, hematite recovery will decrease. The relationship between amine dosage and flotation behaviour was discussed by Laskowski, and is dependent on the solubility limit of amine, above which amine precipitates will form [17]. Laskowski showed that in the case of quartz flotation with dodecylamine, increases in amine concentration above the solubility limit result in decreasing recovery in the pH regions where amine precipitation occurs [17].

The flotation and mobility behaviour of hematite with amines and sulphonates is shown in Figure 4, which was adapted from Iwasaki, Cooke, and Choi [18]. In the simplest cases amines function as physically adsorbing cationic collectors; as shown in Figure 4B [18]. When compared to Figure 4A, it can be seen that dodecyl ammonium chloride collects hematite above pH 7, which is above the IEP of pH 6.7 for this hematite. As collection only occurs when dodecyl ammonium chloride is positively charged, and hematite is negatively charged, the adsorption mechanism can be considered physical.

Amine structure has a significant effect upon flotation behaviour as can be seen by comparing Figure 4C to Figure 4B. Octadecyl ammonium chloride has the same functional NH_3 group as dodecyl ammonium chloride, but with a longer hydrocarbon chain. Due to the increased chain length, hematite is collected over a much broader pH range. In this case, the adsorption mechanism is obviously more than physical adsorption, as recovery occurs when both collector and hematite are positively charged. Iwasaki attributed the broader recovery range of the 18 C amine to a “squeezing-out” effect due to the large ionic size of the amine causing it to be preferentially associated with the hematite surface rather than water [18]. Although there has been no study directly investigating it, it seems this “squeezing-out” effect may be another way of describing the hydrophobic force, which is the preferential aggregation of the amine molecules due to the hydrophobicity of their hydrocarbon chains [19].

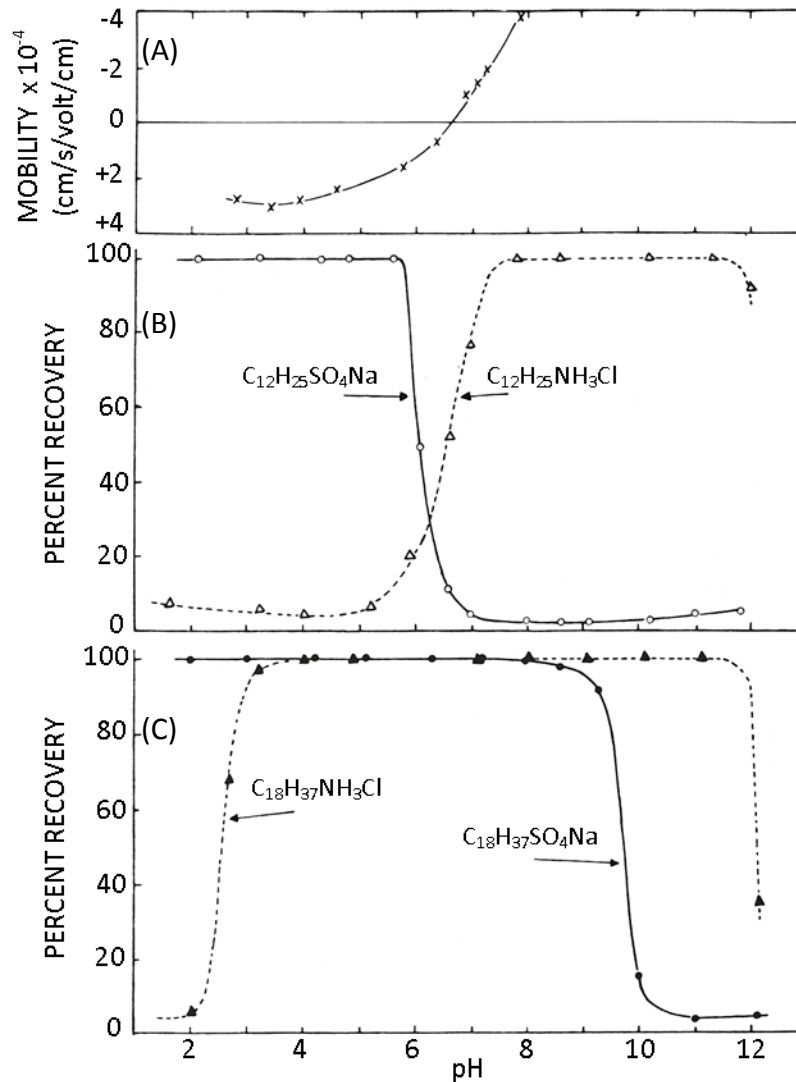


Figure 4: (A) The zeta potential of hematite as a function of pH, (B) the flotation of hematite using 1×10^{-4} mol/L dodecyl ammonium chloride and sodium dodecyl sulfate, and (C) the flotation of hematite with 1×10^{-4} mol/L octadecyl ammonium chloride and sodium octadecyl sulphate [18]

Amine type, either primary, secondary, or tertiary, also has an effect on the flotation of hematite, as investigated by Bibawy and Takeda [6, 16]. Bibawy found primary amines to be more effective hematite collectors than quaternary ammonium collectors under the same conditions [6]. Takeda observed

differences in selectivity in the flotation of a hematite-quartz mixture using mono, di, and tri-n-hexylamine as collectors [20].

Anionic flotation of hematite has primarily been conducted using fatty acids, hydroxamates, and sulphates/sulphonates. Sulphate flotation of hematite has been investigated separately by Bibawy, Iwasaki, and Han [6, 16, 19]. As shown in Figure 4B, sodium dodecyl sulphate (SDS) collects hematite in the acidic region below the IEP for this hematite of pH 6.7. Flotation of hematite only occurs in the region where hematite bears a positive charge and SDS is negatively charged; therefore, physical adsorption is the mechanism of interaction. However, when sodium octadecyl sulphate is used as shown in Figure 4C, flotation of hematite occurs over a much broader pH range, presumably due to the same reasons octadecyl ammonium chloride floats hematite over a wider pH range than dodecyl ammonium chloride. Han measured electrophoretic mobilities of ferric oxide in both SDS and sodium dodecyl sulphonate solutions, and found in both cases that changes in dosages did not affect the IEP of the ferric oxide, meaning that no chemisorption is present [10]. Han also observed that increasing collector dosages would eventually produce conditions for micelle formation, which would reverse the zeta potential of the ferric oxide [10].

Hydroxamates are another group of anionic collectors tested for hematite flotation. Hydroxamates are generally considered to be purely chemisorbing collectors [10, 21, 22]. Figure 5 shows the effect of potassium octyl hydroxamate on the electrophoretic mobility of ferric oxide, and was adapted from Han, Healy, and Fuerstenau [10]. The changing value of IEP with changing hydroxamate dosage infers that hydroxamate is chemically adsorbed on the ferric oxide surface [10]. It should also be noted from Figure 5 that there is no charge reversal at lower pH values, meaning that no formation of hemi-micelles occurs.

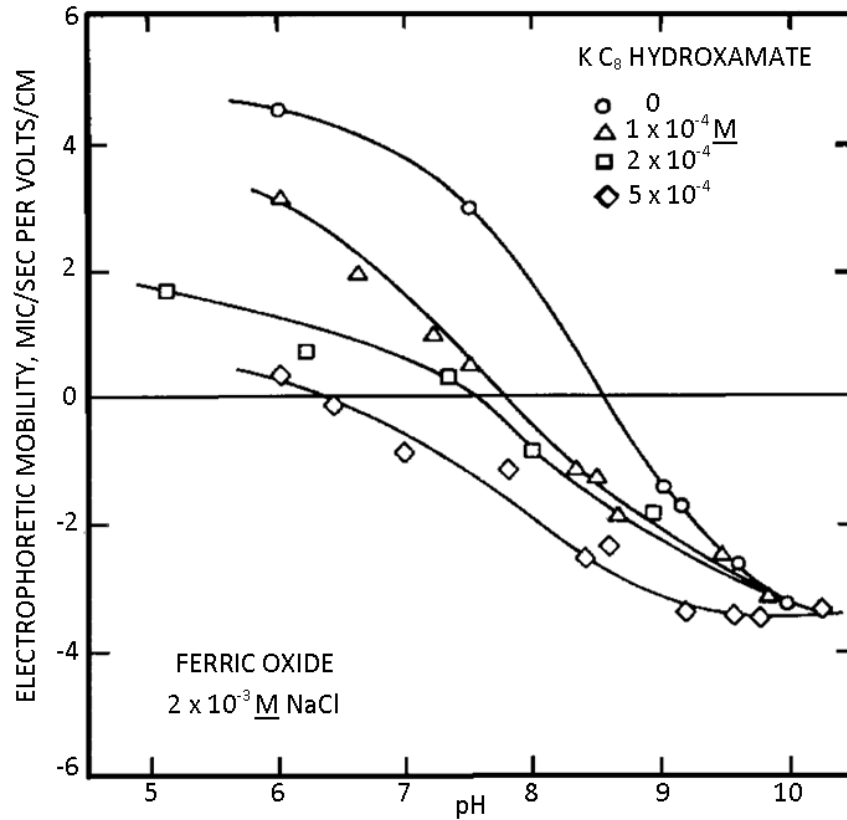


Figure 5: Electrophoretic mobility of ferric oxide at $2 \times 10^{-3} \text{ mol/L NaCl}$ [10]

Figure 6 shows the flotation recovery of hematite using potassium octyl hydroxamate [22]. A sharp peak in recovery at approximately pH 9 can be seen, with no recovery occurring in the acidic pH range. This is characteristic of chemical adsorption since the hematite used has a PZC of pH 6.7 [22]. Fuerstenau also confirmed the presence of precipitated ferric hydroxamate on the hematite surface using infrared studies, which confirms chemical adsorption of hydroxamate [22].

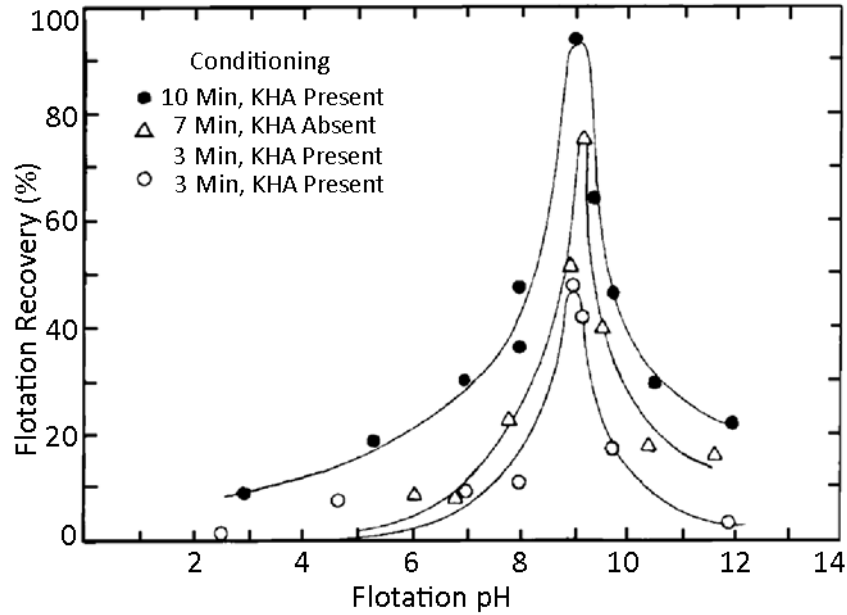


Figure 6: The recovery of hematite at 25°C using 2×10^{-4} mol/L potassium octyl hydroxamate as a function of pH and conditioning time. Adapted from Fuerstenau, Harper, and Miller [22]

Quast also investigated the flotation characteristics of hydroxamates in the flotation of hematite [21]. Quast tested three different forms of hydroxamate, which were lauryl, C7/9, and octyl. Broad pH ranges for flotation recovery were observed; pH 4 – 12 in the most extreme case [21]. The lack of selectivity was attributed to the purity of the hydroxamates used, as each type actually contained a range of carbon chain lengths [21]. The hydroxamate with the tightest composition produced the narrowest pH range for hematite recovery.

A great deal of research has been carried out investigating the flotation behaviour of hematite with fatty acids, particularly oleate or oleic acid. A great place to begin an investigation into hematite flotation with oleic acid is the review done by Quast, which includes summaries of work dealing with both iron ores and the mineral hematite [23].

An example of flotation recovery of hematite using potassium oleate as a collector is shown in Figure 7 [22]. Two distinct regions of recovery are observed.

The first is below about pH 5, and the second is from pH 6.5 to 11, with a peak at about pH 8.5. As the PZC for this particular hematite sample is pH 6.7, the lower pH region for hematite recovery is attributed to physical adsorption, while the upper pH region is attributed to chemical adsorption [22]. The region of depression at pH ~5 is not always observed, and recovery curves in other works are often a single, broad peak depending on conditioning time and dosage among other variables [18, 24–27].

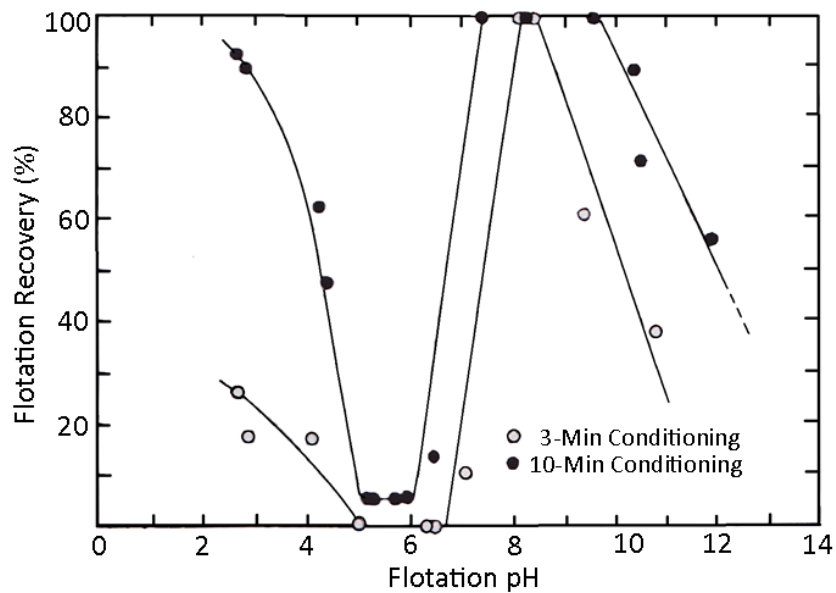


Figure 7: Flotation recovery of hematite with 1×10^{-4} mol/L potassium oleate at 25°C as a function of pH and conditioning time. Adapted from Fuerstenau, Harper, and Miller [22]

Figure 8 shows the effect of oleic acid on the electrophoretic mobility of ferric oxide [10]. Below an oleic acid concentration of 2.5×10^{-5} mol/L, no appreciable effect on electrophoretic mobility is observed, while above this concentration significant charge reversal and change of IEP is apparent, which is indicative of chemical adsorption [10].

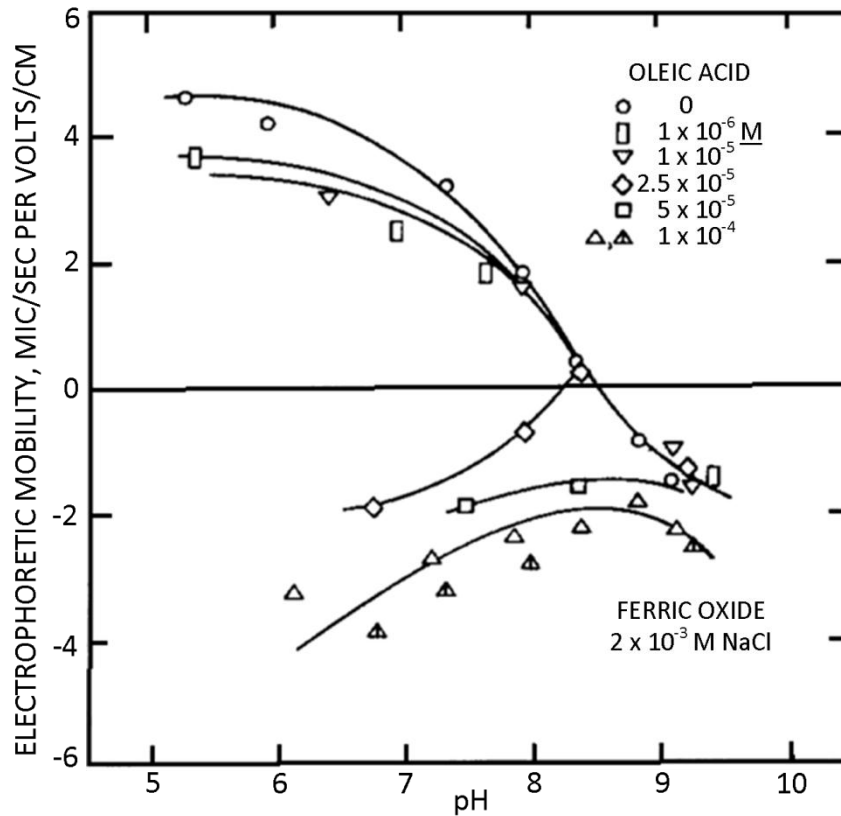


Figure 8: Electrophoretic mobility of ferric oxide with 2×10^{-3} mol/L NaCl as a function of pH and oleic acid dosage. Adapted from Han, Healy, and Fuerstenau [10]

Factors affecting the flotation of hematite with oleic acid include hematite particle size, temperature, and oleic acid solution chemistry as a function of dosage and pH.

Gutiérrez and Iskra studied the action of neutral oleic acid in hematite flotation and observed that different size fractions of the same mineral produced different adsorption behaviour [24].

Cooke et al found that in the flotation of an iron ore with oleic acid, selectivity and overall recovery were improved when the flotation temperature was increased from 25°C to 70°C [28]. Part of the increased flotation behaviour observed was attributed to increased temperatures resulting in increased ionic

mobility, meaning that solution equilibrium is reached more quickly [28]. The solubility of oleic acid is also increased with increasing temperature, leading to a greater concentration of its collecting ionic form in solution [28].

The importance of conditioning time and the solution species of oleic acid in the flotation of hematite was investigated by Laskowski et al, and Morgan et al [15, 24, 25]. By only considering adsorption of species which cause hydrophobicity of hematite, Morgan et al were able to show a general relationship between oleate adsorption and flotation recovery [25]. Peak hematite recovery was found to occur at roughly the same pH as the peak in concentration of the acid/soap complex HOI_2^- species for a given initial concentration of oleic acid, which was approximately pH 7 for an initial oleic acid concentration of 4.4×10^{-6} mol/L [25]. Work by Laskowski et al indicated that in flotation with fatty acids, the basic pH limit of flotation occurs due to the precipitation of a non-collecting molecular form [17]. Laskowski et al also found conditioning time to have a significant effect on the flotation behaviour of hematite with sodium oleate, as shown in Figure 9 [26].

Extending conditioning time has the most significant effect in the acidic region, where the solubility limit of oleic acid is the lowest. When the concentration of oleic acid is above the solubility limit, oleic acid droplets are present in solution [26]. With the presence of the oleic acid droplets, flotation resembles emulsion or oil agglomeration flotation [26]. When this is the case, the species responsible for collection diffuse slowly, and transport to the mineral surface is the limiting factor; hence longer conditioning times result in more time for species transport and greater recovery [26]. This is supported by the fact that flotation using short chain fatty acids is less sensitive to changes in conditioning time, as they are more soluble and species transport is faster [26].

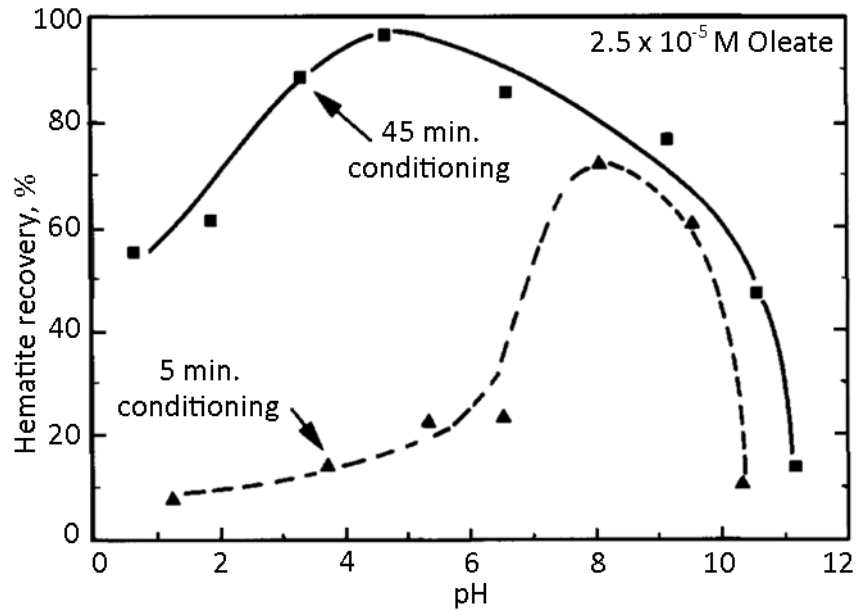


Figure 9: Flotation recovery of hematite with 2.5×10^{-5} mol/L sodium oleate as a function of pH and conditioning time. Reproduced from Laskowski and Nyamekye [26]

The effectiveness of fatty acids in the flotation of hematite is also affected by chain length, and its degree of saturation. Cooke et al observed that in the flotation of hematite, the effectiveness of C_{18} fatty acids decreases as the number of non-conjugated double bonds increases [29]. This was supported by Iwasaki et al who proposed that the presence of double bonds increases the hydrophilicity of the hydrocarbon tail [18]. In a comparison of C_6 - C_{18} saturated fatty acids, Quast observed a gradual change in properties with changes in chain length [30]. Hexanoic acid was found to have too short a chain length to impart significant recovery of hematite, while hexa and octadecanoic acid were too large and insoluble to be effective collectors [30].

2.2.3 Cations in Hematite Flotation

The interaction between metal cations and hematite in flotation has been investigated in seemingly little detail. Studies concerning iron ore flotation and cationic activators almost exclusively focus on the activation of quartz. Some

work has been done, however, on the interaction of hematite with Fe and Ca cations [16, 29, 30].

Abeidu investigated the effect of FeSO_4 on the flotation of hematite and goethite using oleic acid [31]. In the case of both hematite and goethite, minimal effect was observed on either adsorption or flotation recovery with the addition of FeSO_4 [31].

The effect of Ca^{2+} cations on the flotation of hematite was investigated by Iskra et al [27], and Iwasaki et al [18]. Iwasaki et al observed that in the flotation of hematite with oleic acid, the addition of 50 mg/L Ca^{2+} caused a slight activation from pH 10-12, but had no apparent effect otherwise [18]. Contrary to these findings, in the flotation of hematite using potassium oleate Iskra et al observed complete hematite depression above pH 8 with the addition of CaCl_2 [27]. Iskra et al also found that Ca^{2+} eliminated an adsorption maximum at pH 7.5, but otherwise had no effect on oleate adsorption on hematite [27]. A point of interest in the work by Iskra was that the combination of CaCl_2 and quebracho was a more effective hematite depressant than either component individually [27].

2.2.4 Depressants and Modifiers in Hematite Flotation

One of the most commonly used reagents in iron ore flotation is starch, being primarily used as a hematite depressant in the cationic flotation of silica. Partridge and Smith studied the effect of starch on the hematite-dodecylamine flotation system [16]. The effect of starch and amine dosage on hematite flotation is shown in Figure 10.

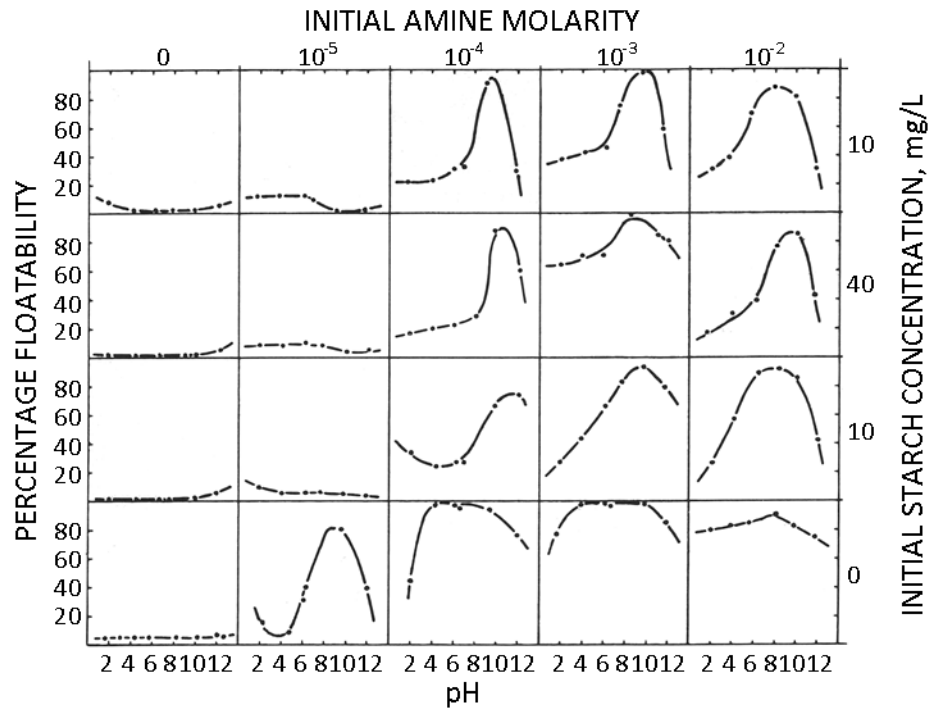


Figure 10: Flotation recovery of hematite as a function of pH, dodecylamine dosage, and starch dosage. Reproduced from Partridge and Smith [16]

The mechanism of starch adsorption on minerals has been studied in great detail by Liu and Laskowski [32]. They consider polysaccharides to interact with hydroxylated metal species on the mineral surface via an acid-base interaction, where the polysaccharide behaves as a Lewis acid. Polysaccharide adsorption can also be enhanced by surface hydrophobicity of mineral surfaces.

Starch can have a variation in composition depending on what plant it is produced from and the nature of its refinement. Pinto, Araujo, and Peres studied the effect of amylose and amylopectin, distinct components of starch, on the flotation of hematite [33]. Using dodecylamine hydrochloride as a collector, amylopectin was found to be the strongest hematite depressant, followed by natural starch and amylose [33]. Peres found that zein, the most abundant corn protein, was comparable to conventional starch and amylopectin as hematite depressants when using an ether-alkyl-amine as a collector [34]. Inferior

depression of hematite was observed when using gluten, and starch of increasing oil content [34].

Humic acid has been found to be an effective depressant of hematite when using dodecylamine as a collector [15]. Due to its relative abundance in soil and selectivity towards iron bearing minerals, dos Santos and Oliveira compared it to starch as a depressant for hematite [15]. Humic acid was found to be stronger than starch at depressing hematite at pH 10.2, and had a larger depressant effect on hematite than on quartz [15].

Turrer and Peres compared guar gum, lignosulphonates, humic acids, and carboxymethyl cellulose (CMC) to starch as a hematite depressant in reverse flotation using alkyletheramine as a collector for silica [35]. Starch was found to be the most selective depressant of those tested. Guar gum produced the next best results to starch, and produced concentrates of satisfactory grade and recovery. One form of CMC showed selective behaviour, although inferior to starch and guar gum. The lignosulphonates and humic acids tested were not selective.

The effect of polyacrylamides (PAM) on the cationic reverse flotation of iron oxide from silica was investigated by Turrer, Araujo, Papini, and Peres [36]. PAM acts as a flocculant in flotation and is available in non-ionic, cationic, and anionic forms. PAM was tested in conjunction with corn starch and FLOTIGAM EDA-B amine collector. The recovery of iron and silica was increased, 7.8% and 0.12%, respectively, by non-ionic PAM, and 5.5% and 0.12%, respectively, using cationic PAM. Flotation was not found to be affected by anionic PAM.

Another naturally occurring compound used as a hematite depressant is Quebracho, which is a tannin extract prepared from particular South American trees [27]. It has been effectively used to depress hematite in reverse soap flotation where silicates are floated [27]. In this system the effect of quebracho is

heavily dependent on pH and Ca^{2+} concentration; however, the general behaviour of quebracho was found to be the depression of hematite via competitive adsorption and reduction of collector adsorption, as well as the adsorbed quebracho imparting hydrophilicity onto the hematite [27].

Sodium silicate has been effectively utilized as a hematite depressant in the soap flotation of apatite in the pH range of 7.5 – 11 [37]. The mechanism of interaction between hematite and sodium silicate is complex and dependent on sodium silicate solution pH and ageing time, sodium silicate modulus ($\text{SiO}_2/\text{Na}_2\text{O}$), and the presence of metal salts [36, 37]. The pH and ageing time of the sodium silicate solution affects the equilibrium between silicate species and their polymerization [37]. Polymeric silicate species are stronger hematite depressants than either monomeric or colloidal species [38]. Sodium silicate solutions having a modulus of approximately 2 are more effective hematite depressants than those having a modulus of either 1 or 3 [37]. Metal salts can form complex anions with SiO_3H^- in solution, which can be beneficial or detrimental to the depression of hematite [31]. In the separation of hematite from gangue minerals, the addition of CaCl_2 or $\text{Al}(\text{SO}_4)_3$ can be beneficial, while the addition of FeSO_4 has been found to be detrimental [29, 36].

Wei and Smith investigated the role of multivalent anionic activators in the flotation of hematite with dodecylamine hydrochloride [39]. More specifically, sulfuric, chromic, selenious, ascorbic, succinic, telluric and citric acids were tested. In general, the protonated forms, HA^- , were found to be the activating species. Citric acid was found to cause activation over a much broader pH range than the other acids, which was attributed to its strong chelating effects with iron. Chromic acid also deviated from the main hypothesis and was found to be an activator in the pH region where CrO_4^{2-} is the most stable species rather than CrO_4H^- . This was attributed to the tendency of Cr^{6+} to convert to Cr^{3+} when the pH is above 6.

2.2.5 Flotation of Iron Ores

In the flotation of iron ores removal of quartz is nearly the universal problem. For an in-depth review of the separation of quartz from iron oxide a good starting point is the review by Uwadiae [40]. Fuerstenau and Fuerstenau summarized the methods developed for the flotation separation of quartz and iron ore, with the list shown below [41]. The last method shown on the list was not mentioned by Fuerstenau and Fuerstenau, but is currently widely utilized [42].

1. Hematite collection using sulphonate as a collector at pH 2-4
2. Hematite collection using fatty acids as collectors at pH 6-8
3. Quartz collection using amine as a collector at pH 6-7
4. Quartz collection using soap and calcium ion activation at pH 11-12, and starch to depress hematite
5. Hematite collection using amine as collector at pH 1.5 in the presence of hydrochloric or sulphuric acid
6. Hematite collection using hydroxamate as a collector at pH 8.5 with methyl isobutyl carbinol (MIBC) as a frother
7. Quartz collection using amine as collector at pH 10-11, and starch to depress hematite

2.3 Pyrolusite Flotation

The following is a review of the flotation characteristics of manganese minerals and ores with a focus on pyrolusite. For further reference, a concise yet thoroughly researched review was done by Fuerstenau, Han, and Miller and can be found in *Advances in Mineral Processing: A half-century of progress in application of theory to practice* [43].

2.3.1 A Note on Manganese Dioxide

Before discussing in too much detail the flotation of pyrolusite, it is important to briefly mention the diverse nature of MnO_2 . As discussed by Healy et al, MnO_2 is

nearly always oxygen deficient to some degree [44]. MnO_2 , therefore, can have several different forms varying widely in crystallographic structure and surface properties, but roughly sharing the same chemical composition. A brief summary of the different forms of MnO_2 and their properties are shown in Table 1 using information from Healy et al [44].

Table 1: Summary of the composition, zero point of charge, and crystal structure for manganese dioxides [44]

Name	Chemical Properties	PZC	Crystal Structure
$\delta\text{-MnO}_2$	O:Mn greater than 1.9	1.5 ± 0.5	NA
Manganite	O:Mn 1.7 to 1.9 $3\text{MnO}_2 \cdot \text{Mn}(\text{OH})_2 \cdot n\text{H}_2\text{O}$	1.8 ± 0.5	Hexagonal Triclinic
$\alpha\text{-MnO}_2$ (Cryptomelane)	$\text{KMn}_8\text{O}_{16}$ or $\text{NaMn}_8\text{O}_{16}$	4.5 ± 0.5	Pseudo-tetragonal Monoclinic
$\gamma\text{-MnO}_2$ (Electrolytic MnO_2)	Typically $\text{MnO}_{1.93}$	5.5 ± 0.5	Orthorhombic
$\beta\text{-MnO}_2$ (Pyrolusite)	MnO_2 (some oxygen deficiency still indicated)	7.3 ± 0.5	Tetragonal

2.3.2 Zeta Potential of Pyrolusite

The surface charge characteristics of manganese minerals in solution vary widely, depending on several factors. In the case of pyrolusite ($\beta\text{-MnO}_2$), point of zero charge (PZC) values have been reported ranging from pH 4.2 to pH 7.4 [7, 11, 44–47]. An isoelectric point (IEP) value of pH 3.8 for pyrolusite has also been reported [8]. The pyrolusite samples from the sources mentioned above are all of different origin and, therefore, will have variations in oxygen content and purity. Work done by Healy et al has shown a relationship in manganese oxides between crystal structure and PZC, as shown in Table 1 [44]. It was observed that increasing atomic packing generally has the effect of increasing the electrostatic field above the lattice, subsequently increasing the pH of PZC [44]. The following

manganese dioxides are listed in order of increasing crystallinity and increasing PZC: $\delta\text{-MnO}_2 < 3\text{MnO}_2 \cdot \text{Mn}(\text{OH})_2 \cdot n\text{H}_2\text{O} < \alpha\text{-MnO}_2 < \gamma\text{-MnO}_2 < \beta\text{-MnO}_2$ [44]. Hydration state, oxygen deficiency, and/or impurity content can also be reasons for the variation in the reported values of PZC mentioned above [11].

2.3.3 Flotation of Pure Pyrolusite

Flotation of pyrolusite using cationic collectors has been studied by Fuerstenau, Arafa, and Nayak [7, 47, 48]. Amine type collectors were used by Fuerstenau and Nayak, with Fuerstenau's results shown in Figure 11 [7]. The pyrolusite sample used by Fuerstenau for the results in Figure 11 was described as being high grade with no impurities [7]. Dodecyl amine most effectively recovers pyrolusite from pH 8 to pH 10, which is above the PZC of pH 7.4 for this particular sample. Recovery of pyrolusite only above the PZC is characteristic of dodecyl amine being physically adsorbed [7].

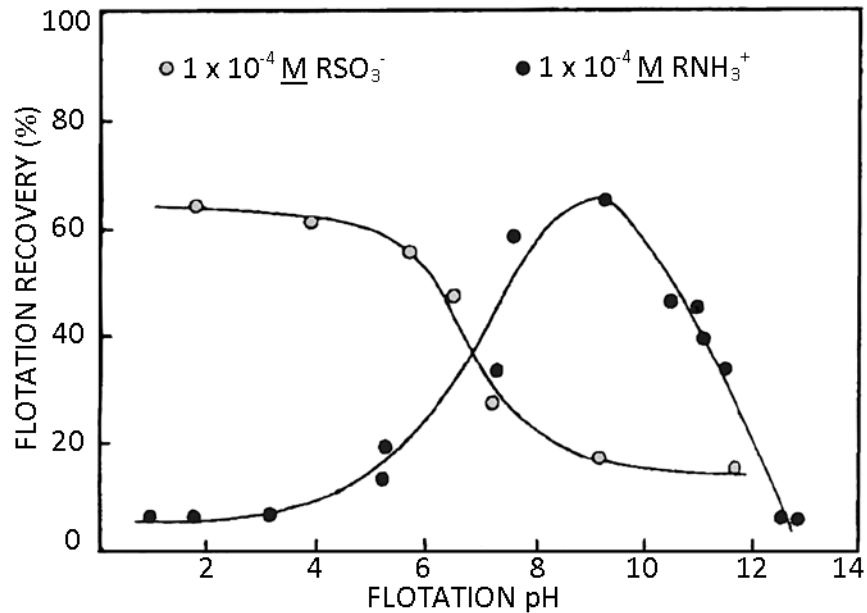


Figure 11: Flotation recovery of pyrolusite as a function of pH using sodium alkyl aryl sulfonate and dodecyl amine at 23°C. Reproduced from Fuerstenau and Rice [7]

Also shown in Figure 11 is the recovery of pyrolusite as a function of pH using sodium alkylaryl sulfonate. Recovery occurs below the PZC pH of 7.4, being strong at pH 6 and below. Since sulfonate carries a negative charge in solution, and recovery only occurs when pyrolusite carries a positive surface charge, the mechanism of sulfonate adsorption is electrostatic attraction, or physisorption [7].

The flotation behaviour of $\gamma\text{-MnO}_2$ using potassium octyl hydroxamate as a collector was investigated by Natarajan and Fuerstenau [46]. Hydroxamates are considered chelating agents and have the ability to selectively form complexes with metal cations. In the case of $\gamma\text{-MnO}_2$, the flotation response when using potassium octyl hydroxamate is shown in Figure 12, with the response using sodium dodecyl sulfonate (SDS) shown in Figure 13 [46].

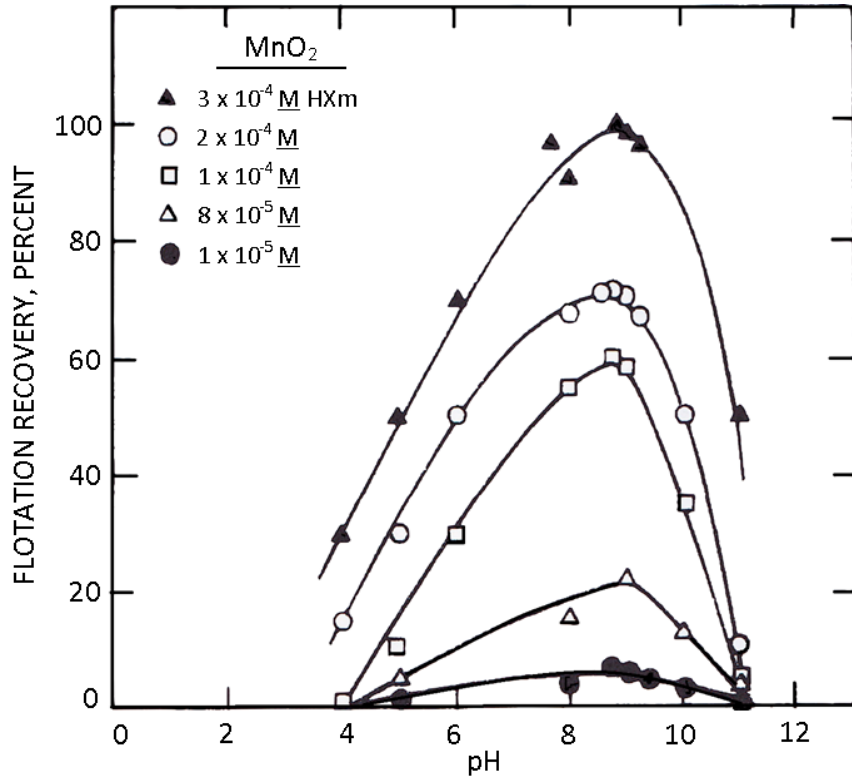


Figure 12: Flotation recovery of $\gamma\text{-MnO}_2$ as a function of pH using potassium octyl hydroxamate. Adapted from Natarajan and Fuerstenau [46]

In the case of hydroxamate, peak flotation response occurs at pH 9, which also correlates with peak adsorption. The PZC of the γ - MnO_2 was pH 5.6. In the case of anionic SDS, recovery only occurs below pH 6, when γ - MnO_2 has a positive surface charge, meaning adsorption must be electrostatic or physical in nature. Hydroxamate is also an anionic collector; however, recovery only occurs above the PZC for γ - MnO_2 , meaning adsorption must be chemical in nature. IR studies indicate a manganous hydroxamate complex at the γ - MnO_2 surface [46]. The peak in flotation response correlates to the pKa of hydroxamic acid, below which molecular hydroxamic acid is predominant, and above which hydroxamate anions are predominate.

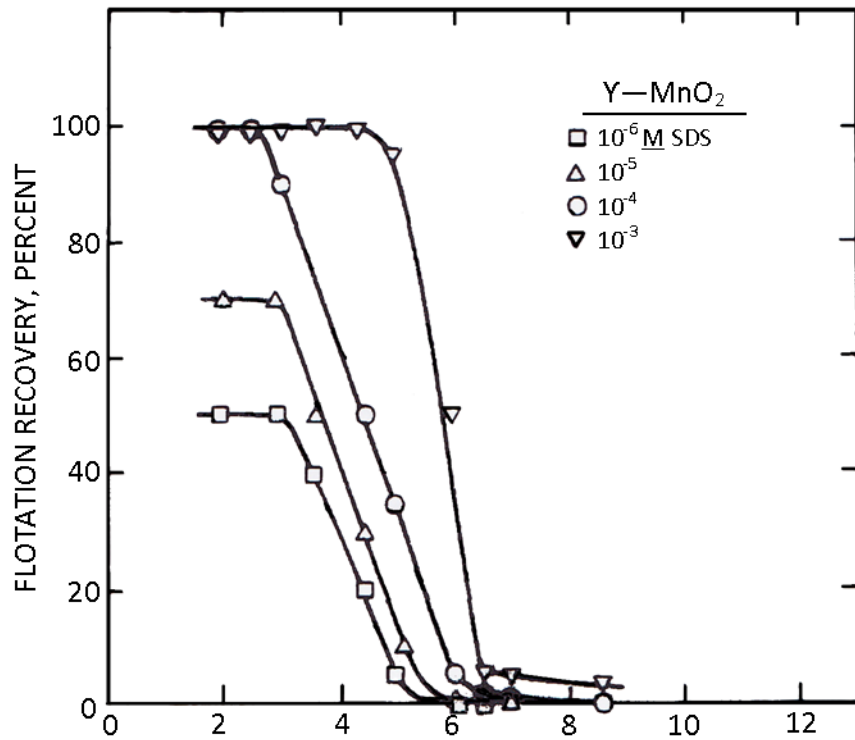


Figure 13: Flotation recovery of γ - MnO_2 as a function of pH using sodium dodecyl sulfonate. Adapted from Natarajan and Fuerstenau [46]

Several studies have been done to investigate the flotation behaviour of manganese dioxides in the presence of oleic acid or oleates [7, 8, 45, 49]. The

flotation of pyrolusite using oleate is unique from amine, sulfonate, or hydroxamate flotation as it exhibits regions of both physical adsorption and chemical adsorption [7]. Figure 14 shows recovery as a function of pH for a high grade pyrolusite using potassium oleate [7]. The pyrolusite sample used has a PZC of pH 7.4 [7]. Recovery is divided into two distinct regions. The first region, occurring from pH 2 to 6, having a peak in recovery at approximately pH 4 is attributed to physical adsorption of oleate, as in this region pyrolusite is positively charged and oleate is negatively charged [7]. The second region, having much stronger maximum recovery than the first, occurs from pH 7 to 11, with a peak in recovery at approximately pH 8.5. Since both pyrolusite and oleate are negatively charged in this region adsorption is considered to be chemical in nature [7].

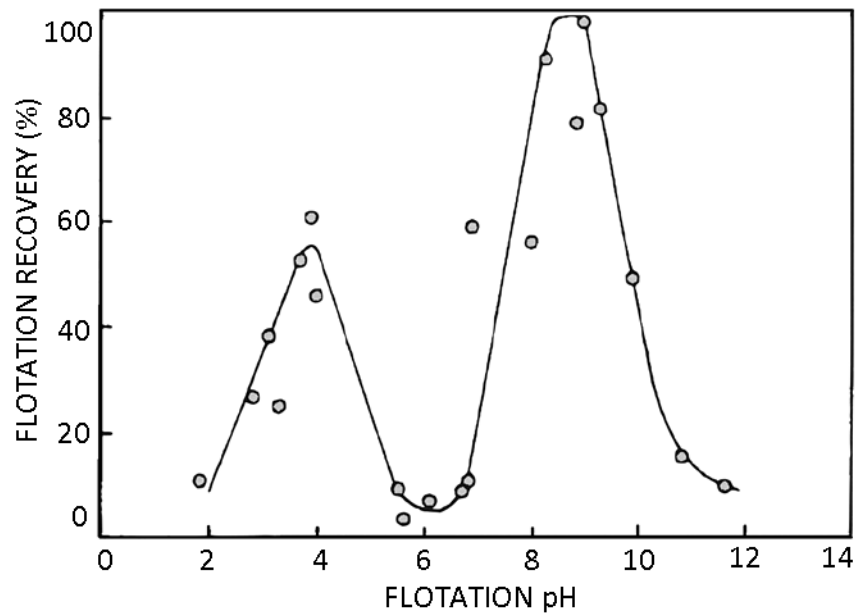


Figure 14: Flotation recovery of pyrolusite using 1×10^{-4} mol/L potassium oleate as a function of pH at 23°C. Adapted from Fuerstenau and Rice [7]

Figure 15 shows the effect of temperature on the recovery of pyrolusite when using oleate as a collector [7]. Increasing the temperature from 23°C to 60°C had the effect of increasing the maximum recovery from 40% to nearly 100%, and

also moved the peak recovery from ~pH 10 to 8.5. Increased flotation recovery with increasing temperature was also observed by Arafa [50], who studied the flotation of pyrolusite with sodium dodecyl benzene sulphonate. Not only did Arafa observe that increasing temperatures resulted in increased flotation recovery, but noted that a decreased amount of collector was required to achieve a given amount of recovery [50].

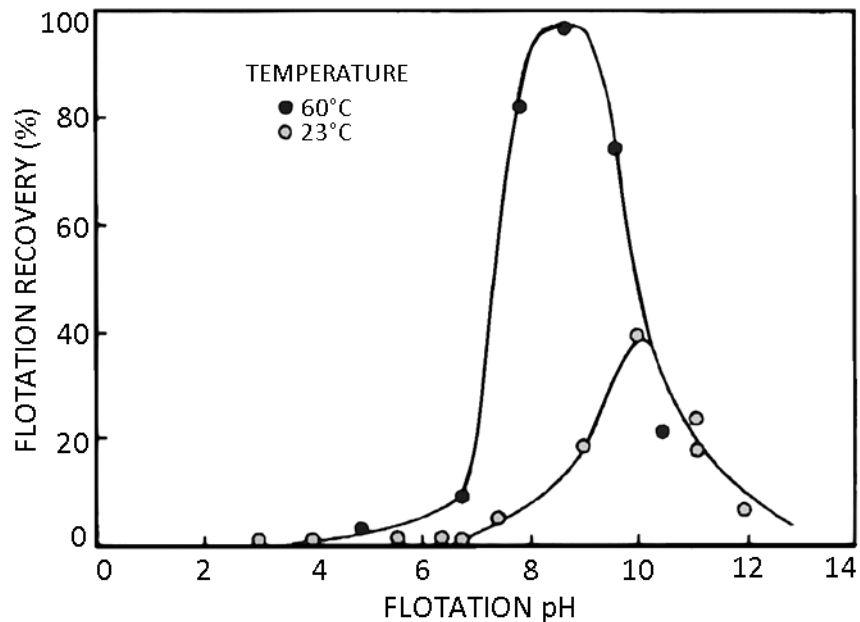


Figure 15: Flotation recovery of pyrolusite using 1×10^{-4} mol/L potassium oleate as a function of pH at 23°C and 60°C. Adapted from Fuerstenau and Rice [7]

The sample of pyrolusite used for the results shown in Figure 15 was impure compared to that used in Figure 14, and contained 0.21 wt% Zn and 4.32 wt% Fe with a PZC of pH 5.6 [7]. The lack of a physical adsorption peak in the region of pH 4, and the poor recovery at pH 10 at room temperature are attributed to the impure nature of the sample [7]. The source and purity of pyrolusite would appear to significantly affect its behaviour when using oleate as a collector. Just as the results from Fuerstenau vary depending on the pyrolusite sample, the results of Bogdanov [51] also differ. Using sodium oleate as a collector a broad

recovery peak was observed from pH 5 to 8, corresponding to the maximum adsorption of oleate from pH 6.5-8 [51]. This observation of a single broad recovery curve may have been due to the oleate dosage being high enough to blend the physical and chemical adsorption regions, the sensitivity of the flotation technique, or the nature of the pyrolusite sample itself which could have a different PZC than that used for Figure 14.

2.3.4 Cations in Pyrolusite Flotation

Several fundamental studies have been carried out to investigate the effect of cations on the flotation of manganese dioxides using both cationic and anionic collectors. The effect of Fe^{3+} , Cu^{2+} , and Mn^{2+} cations on pyrolusite flotation was investigated by Abeidu, with the resulting effect of their additions on the zeta potential of pyrolusite shown in Figure 16 [8]. The pyrolusite sample used by Abeidu had an IEP of pH 3.8 [8]. Looking first at the case of Fe^{3+} addition, below pH 2.5 the addition of Fe^{3+} had only a minor effect on the zeta potential of pyrolusite, while above pH 2.5 it had a negligible effect [8]. This is attributed to the fact that Fe^{3+} will be present predominantly as the species $\text{Fe}(\text{OH})^{2+}$ and $\text{Fe}(\text{OH})_2^+$ in the range of pH 2.2 - 3.7 [8]. In this pH range pyrolusite will predominately carry a positive surface charge as it is below the IEP, resulting in little interaction with the iron species. Above pH 3.7, Fe^{3+} will be present as neutral $\text{Fe}(\text{OH})_3$, and will have no interaction with the pyrolusite surface.

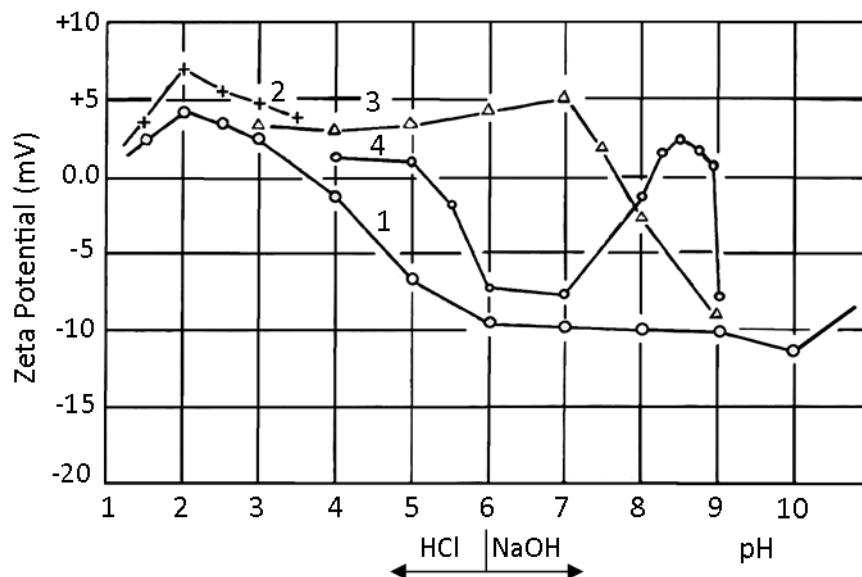


Figure 16: Zeta potential of pyrolusite as a function of pH: (1) no additions; (2) 50 mg/L FeCl₃; (3) 50 mg/L CuSO₄; (4) 50 mg/L MnSO₄. Adapted from Abeidu [8]

As shown in Figure 16, the addition of Cu²⁺ cations has a large effect on the zeta potential of pyrolusite from pH 3 – 9 [8]. The zeta potential of pyrolusite is made positive from pH 3 – 7, at which point it gradually becomes negative until pH 9, when the effect of Cu²⁺ becomes negligible. This behaviour is attributed to the hydrolysis of Cu²⁺ cations [8]. Above pH 8, Cu²⁺ will be hydrolyzed into neutral Cu(OH)₂, accounting for the decline in interaction with pyrolusite from pH 8 – 9 [8]. Below pH 8, Cu²⁺ will be present either as Cu(OH)⁺ or Cu²⁺, and will readily interact with the negatively charged pyrolusite surface [8].

The role of Mn²⁺ cations in the flotation of pyrolusite has been investigated by Fuerstenau, Yousef, Abeidu, and Arafa [7, 8, 11, 12]. Mn²⁺ has the effect of both altering the zeta potential and the flotation behaviour of pyrolusite. The effect of Mn²⁺ on the zeta potential of pyrolusite, as found by Abeidu, is shown in Figure 16 [8]. Zeta potential is reversed in two regions, with maxima at pH 5 and 8.5. Abeidu postulated that in the region of pH 3-5, Mn²⁺ interacts with Mn(OH) surface sites to produce a positive zeta potential, while in the region of pH 8-9,

$\text{Mn}(\text{OH})^+$ interacts with MnO^- surface sites to produce a positive zeta potential [8]. The effect of Mn^{2+} addition on the flotation of pyrolusite with oleic acid seems to depend on the nature of the particular ore used; however, in the cases of both Abeidu [8] and Fuerstenau [7], peak recovery was increased and shifted to pH 8.5. In the case of Fuerstenau [7], peak recovery was shifted from pH 10 to pH 8.5, and Abeidu [8] found the peak to shift from a broad range of pH 6-8 to a narrow pH 8.5.

Manganese oxides in solution will naturally release Mn^{2+} , so regardless of its addition, Mn^{2+} will always play a role in pyrolusite flotation [47]. Aside from the effect on zeta potential, Mn^{2+} also affects the adsorption of collectors. Yousef observed that the addition of MnCl_2 increased the adsorption density of oleate compared to adsorption without its addition [45]. In the case of a cationic collector, cetyl trimethyl ammonium bromide (CTAB), Arafa found that at low enough collector dosages, the Mn^{2+} cation will competitively adsorb onto the pyrolusite surface, but increasing the collector dosage to a sufficient level will cause the collector to be preferentially adsorbed [47]. This phenomena is shown in Figure 17 [47].

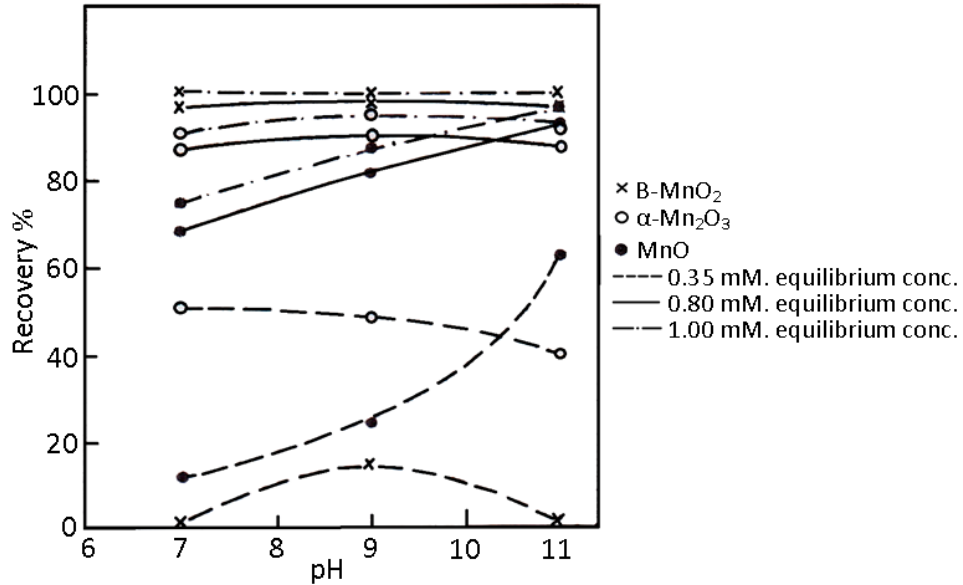


Figure 17: Flotation of manganese oxides as a function of pH and cetyl trimethyl ammonium bromide (CTAB) concentration. Adapted from Arafa, El-Nozahi, and Yousef [47]

2.3.5 Depressants and Modifiers in Pyrolusite Flotation

There has been little fundamental research on the effects of depressants and or modifiers on the flotation of pure manganese dioxides, with most literature focusing on the role of depressants and modifiers in industrial manganese ore flotation. The exceptions are sodium sulphite and sodium silicates.

Bogdanov, Gomelaui, and Abeidu investigated the effect of sodium silicate (Na_2SiO_3) on the flotation of pyrolusite using oleic acid as a collector [8, 16, 17]. Gomelaui found waterglass (sodium silicate) to be ineffective in the separation of pyrolusite from quartz and feldspar [52]. Abeidu used a mixture of waterglass and aluminum sulphate ($\text{Al}_2(\text{SO}_4)_3$) as a depressant, finding barite, gypsum, and calcite to be effectively depressed while the flotation of pyrolusite was unaffected [8]. It was suggested that the active anion was $\text{Al}_2\text{SiO}_3(\text{OH})_6^-$, which selectively depressed the gangue minerals due to their positive zeta potential, leaving pyrolusite unaffected due to its negative zeta potential in the pH range tested [8].

Yousef studied the effect of sodium sulphite addition on the flotation of β -MnO₂ using sodium oleate as a collector [45]. As shown in Figure 18, the adsorption of oleate by β -MnO₂ was found to increase due to the addition of sulphite, while the presence of oleate decreased the adsorption of sulphite. The increased adsorption of oleate can be explained by the release of Mn²⁺ cations by β -MnO₂ due to the addition of sulphite [45]. When sulphite is added to solution, sulphurous acid (SO₃²⁻) reacts with β -MnO₂ to form either manganese (II) sulphate or dithionate, either of which will dissociate releasing Mn²⁺ cations [45]. Mn²⁺ adsorbed on the surface of β -MnO₂ will act as an adsorption site for oleate anions [45]. The relationship between the release of Mn²⁺ cations by β -MnO₂ and sulphite addition is shown in Figure 19.

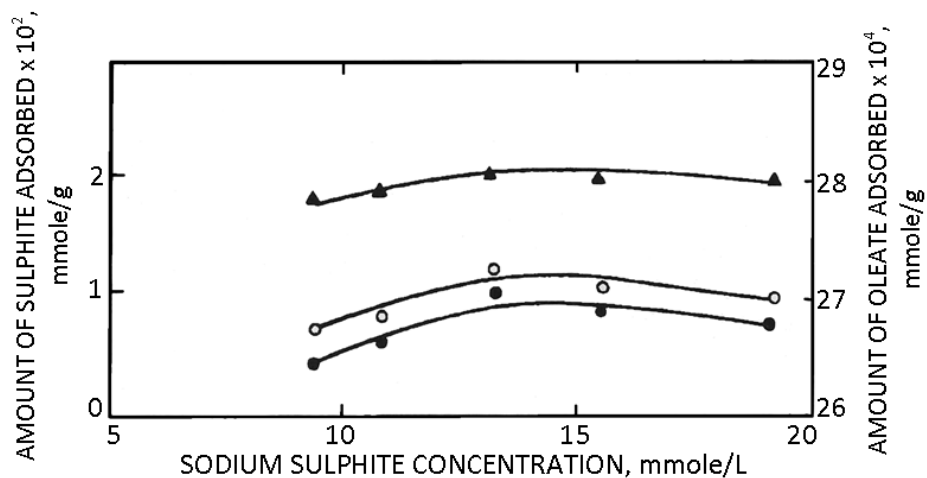


Figure 18: Co-adsorption of sulphite and oleate on β -MnO₂ at pH 7 and room temperature. Open circles: adsorption of sulphite in absence of oleate; Solid circles: adsorption of sulphite from 0.57×10^{-3} mol/L sodium oleate solution; Triangles: adsorption of oleate from sodium sulphite solutions. Adapted from Yousef, Arafa, and Malati [45]

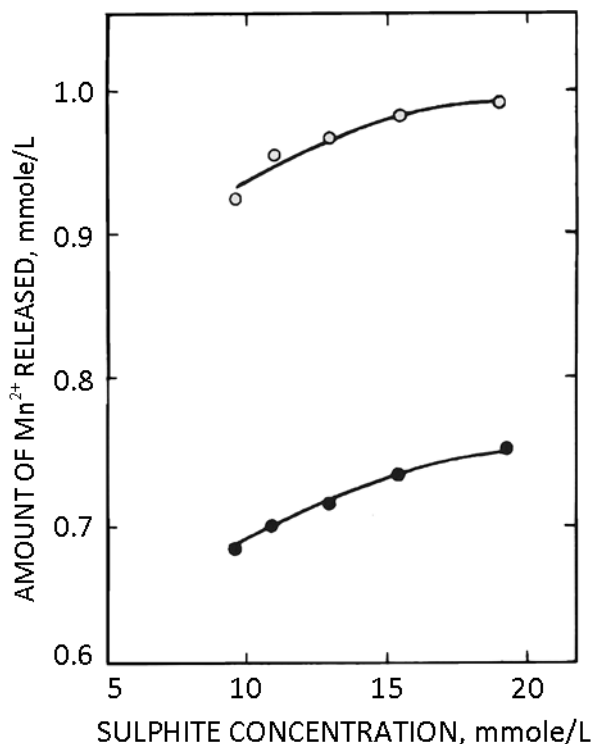


Figure 19: Amount of Mn^{2+} ions formed on conditioning β - MnO_2 in sulphite solution at pH 7 and 35°C. Open circles: in absence of sodium oleate; Solid circles: in 0.57×10^{-3} mol/L sodium oleate solution. Adapted from Yousef, Arafa, and Malati [45]

2.3.6 Flotation of Manganese Oxide Ores

While no previous examples could be found for flotation of iron ores bearing manganese, the case of manganese ore flotation is completely opposite. In virtually all the studies found describing the flotation of manganese ores, iron was a significant component. With this in mind, the review of manganese ore flotation can be found in Section 2.4: Manganese and Iron bearing mineral flotation.

2.4 Manganese and Iron Bearing Mineral Flotation

A number of studies have been carried out investigating the flotation of manganese bearing ores, a summary of which is shown below in Table 2. All the ores listed in Table 2 contain a significant amount of Fe.

Table 2: Summary of manganese ore flotation

Ore Type	Collector	Flotation pH	Feed Grade (wt% Mn)	Conc. Grade (wt% Mn)	Recovery (wt% Mn)	Reference
Pyrolusite	Oleic acid	NA	25.3	56.0	91.0	Devany [53]
Wad	Oleic acid	NA	28.3	39.5	72.6	Shelton [54]
Psilomelane	Oleic acid	NA	8.7	12.8	76.6	Fine [55]
Pyrolusite- Psilomelane	Oleic acid	NA	14.0	37.4	73.5	Johnston [56]
Pyrolusite- Psilomelane	Oleic acid	NA	8.4	28.2	82.3	Shelton [57]
Wad	Soap	NA	25.6	42.3	83.1	McCarroll [58]
Cryptomelane	Sodium oleate	8	25.9	48.0	89.6	Sun [59]
Pyrolusite	Tall oil	5	16.2	36.6	90.8	Stickney [60]

Some of the earliest investigations into manganese mineral flotation were carried out in the late 1920's by the United States Bureau of Mines [53]. Faced with the challenge of producing enough ferromanganese domestically to adequately supply domestic steel production, the United States Bureau of Mines began a program of manganese ore dressing studies[53]. While some of these studies were focused on pyro- and hydrometallurgical processing, the remainder consisted of mineralogical studies followed by applications of gravity, magnetic, and anionic and cationic flotation separation. The first such study was reported by DeVaney and Clemmer in 1929 [53]. Manganese ore bearing primarily pyrolusite was floated using pine oil, oleic acid, sodium silicate and sodium carbonate. This produced a concentrate of 56 wt% Mn with 91% Mn recovery from an ore containing 25.3 wt% Mn. The iron content of the ore was not

significant enough for reporting; however it was noted that ores containing large amounts of iron posed great difficulty with flotation.

By the early 1940's the United States Bureau of Mines began a large scale research program on upgrading domestic manganese ores [61]. The first paper in this series was Report 3606 by Zimmerley, Vincent, and Schack, 1942, and serves as a blueprint for the subsequent reports in the series [61].

Of the investigations done by the United States Bureau of Mines testing anionic flotation, the testing of ore from the Interstate Manganese Company from Johnston County, Tennessee is quite characteristic [56]. The manganese bearing minerals in the ore were soft pyrolusite, hard nodular psilomelane [(Ba, H₂O)₂Mn₅O₁₀], and wad, all being associated with clay. Iron oxides were also present, and were intimately associated with the manganese oxides. Gangue minerals consisted of quartzite, barite, kaolin, and clay. Chemical analysis of the ore gave 14 wt% manganese, 15.9 wt% iron, 27.5 wt% silica, and 11.8 wt% alumina. Batch flotation tests were conducted with ore ground to -200 mesh, and used sodium silicate and oleic acid. This resulted in a recovery of 73.5% of the manganese at a grade of 37.4 wt% Mn. Iron was not selectively floated as 30% of the iron was floated in a concentrate bearing 34 wt% of the feed. A similar flotation scheme using oleic acid and sodium silicate was used on other iron bearing manganese ores, also resulting in non-selective iron recovery. As with most of the investigations in the series, no mention of flotation pH was made.

Virtually identical flotation conditions were used in the flotation of manganese bearing ore from the Stange Mine [57]. Flotation tests were conducted using oleic acid and sodium silicate with ore ground to -200 mesh. In this case the ore was a mixture of manganese oxides, iron oxides, sandstone and clay. Manganese

occurred as pyrolusite and psilomelane, while the type of iron oxide present was not identified. Analysis of the ore was 8.4 wt% Mn, 10.2 wt% Fe, 61.5 wt% SiO₂, 3.9 wt% Al₂O₃, and 1.6 wt% Ba. While flotation conditions appear identical to those used for the Interstate Mining Company ore, in this case iron was selectively recovered with manganese. A concentrate was produced grading 28.2 wt% Mn and 24.0 wt% Fe bearing 27.5 wt% of the initial feed. Recovery of Mn into the concentrate was 82.3% while Fe was 69.5%. The reason for selective iron recovery in this ore and not with Interstate Mining Company ore cannot be inferred from the given data.

In report 3842, flotation of ore from the Davis Claim was investigated, which primarily bears manganese as pyrolusite, with small amounts of other manganese oxides present [62]. Iron was present as an ocherous form and was too intimately associated with manganese oxides to be liberated by fine grinding. Calcite was the primary gangue mineral. Flotation using sodium silicate, sodium hydroxide, and oleic acid was found to be effective for the removal of calcereous gangue, while no selective separation between manganese and iron was observed. It was noted that “several flotation procedures were investigated, but no significant separation of manganese and iron was obtained”. No description of the “several flotation procedures” was given.

Sun and Morris studied flotation of manganese ore from the Sherman Valley area, Pennsylvania [59]. Using sodium oleate, sodium silicate, sodium dihydro-orthophosphate (NaH₂PO₄), and hexanol at pH 8.0, a concentrate of 48.0 wt% Mn and 2.23 wt% Fe with 89.6% Mn recovery was produced from an ore bearing 25.9 wt% Mn and 4.02 wt% Fe. This is a case of manganese minerals being selectively concentrated while iron minerals were depressed. The main manganese mineral present was cryptomelane (KMn₆⁴⁺Mn₂²⁺O₁₆) with some pyrolusite and psilomelane, with gangue minerals being clay, quartz, goethite,

limonite, calcite, orthoclase, and carbonates. Sodium oleate was found to be more effective than amines and could be substituted with oleic acid or tall oil. With sodium silicate, sodium dihydro-orthophosphate was a more effective conditioner/depressant than sodium hexametaphosphate, tannic acid, or quebraco. The optimum pH for rougher flotation was 8.0, while cleaner flotation pH ranged from 8.3 to 9.0, increasing with iron content.

Low grade ore from the Nette Mine, and waste tailings from Domestic Manganese & Development Company, of Butte, Montana were successfully concentrated on both lab and pilot plant scales using a fuel oil-tall oil emulsion as collector at pH 5.0 [60]. Manganese minerals were selectively flocculated and separated from siliceous gangue. Iron was slightly concentrated with the manganese minerals during flotation. In the case of the Nette Mine ore, 90.8% of the manganese was recovered in a concentrate grading 36.6 wt% Mn and 5.5 wt% Fe. The feed ore graded 16.2 wt% Mn and 4.25 wt% Fe, Manganese in the Nette mine ore was identified as pyrolusite, while that of the Domestic Manganese and Development Company was only identified as manganese oxide.

A unique form of soap flotation was used at the Three Kids Mine of Henderson, Nevada [58, 63, 64]. The chief manganese mineral of the ore is psilomelane, with other manganese minerals present including pyrolusite. Gangue minerals include quartz, opal, kaolinite, montmorillonite, calcite, gypsum, celestite, and barite [64]. Iron is present in minor amounts [58]. A process was used called "Emulsion Flotation", which uses high dosages of flotation reagents (around 90 kg/tonne of ore) [63]. Soap, fuel oil, and sulphonate wetting agent are emulsified, and added to a pulp after the addition of sulphur dioxide [64]. Sulphur dioxide is used to produce manganese ions and activate the manganese mineral surfaces, although manganese sulphate can also be used [63]. The pulp has a solids density of 18 to 23 wt% [64]. Aside from reagent dosage, emulsion flotation can be differentiated

from froth flotation by the intensive conditioning used prior to flotation. Intensive conditioning, consuming up to 42 kWh per tonne of ore, produces agglomerates of manganese minerals [64]. Fine particles that would be difficult to deal with in froth flotation can be successfully recovered using emulsion flotation due to agglomeration, albeit with increased reagent consumption [63]. Recovery of Mn has been reported in the 80-90% range [63], with early test work showed concentrates grading 45.5 wt% Mn with 84.0% recovery produced from a feed bearing 21.3 wt% Mn [58].

An example of the separation of pure manganese and iron bearing minerals was carried out by Nayak and Kuloor, who studied the flotation of quartz, pyrolusite, and hematite using n-heptadecyl amine hydrochloride [48]. Using small-scale single-mineral flotation, favourable conditions for the collection of hematite and depression of pyrolusite were observed. Hematite could be selectively floated using 20 mg/L ferric chloride at pH 7.6 – 8.7, or using 4 mg/L ceric sulphate at pH 1.3 – 2.0 [48]. Separation windows were very small and highly dependent on both pH and ferric chloride or ceric sulphate dosage. Flotation of an artificial mixture of pyrolusite and hematite was conducted using a Leaf and Knoll cell with ferric chloride as a depressant. Although optimum conditions for flotation were given, no details concerning the grade of the flotation products were provided other than the statement “manganese concentrates fall short of specifications” [48].

2.5 Oxide Mineral Hydrolysis and Flotation

The adsorption of anionic collectors on oxide minerals was investigated by Palmer, Gutierrez, and Fuerstenau [49]. It was observed that collector adsorption was affected by the presence of hydroxy complexes formed from the divalent metal ions of the oxide mineral [49]. In the case of chromite ($\text{FeO}\cdot\text{Cr}_2\text{O}_3$) flotation recovery with oleic acid, and consequently adsorption, are maximized

at approximately pH 8.3 as shown in Figure 20, where the species $\text{Fe}(\text{OH})^+$ is at its maximum concentration, as shown in Figure 21 [49]. The flotation recovery of hematite with potassium oleate, as shown in Figure 7, exhibits maximum recovery in the same pH range as chromite. In the case of chromite, while $\text{Fe}(\text{OH})^+$ was found to play a significant role in the adsorption of oleic acid, $\text{Cr}(\text{OH})^{2+}$ and $\text{Al}(\text{OH})_2^+$ were found to play no role [49]. Both chromium and aluminum ions are trivalent and coordinate octahedrally with oxygen, while divalent iron forms a tetrahedral structure with oxygen [49].

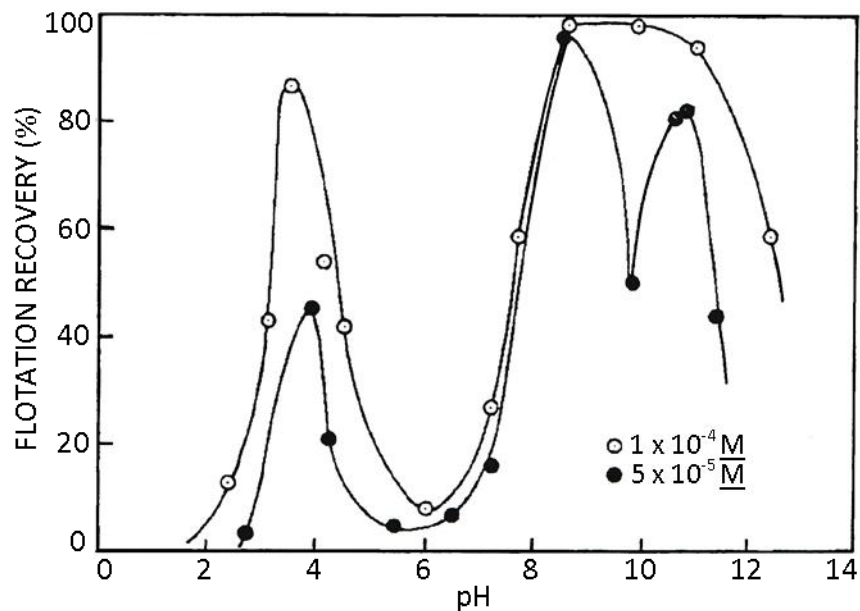


Figure 20: Flotation recovery of chromite with oleic acid as a function of pH. Adapted from Palmer, Gutierrez, and Fuerstenau [49]

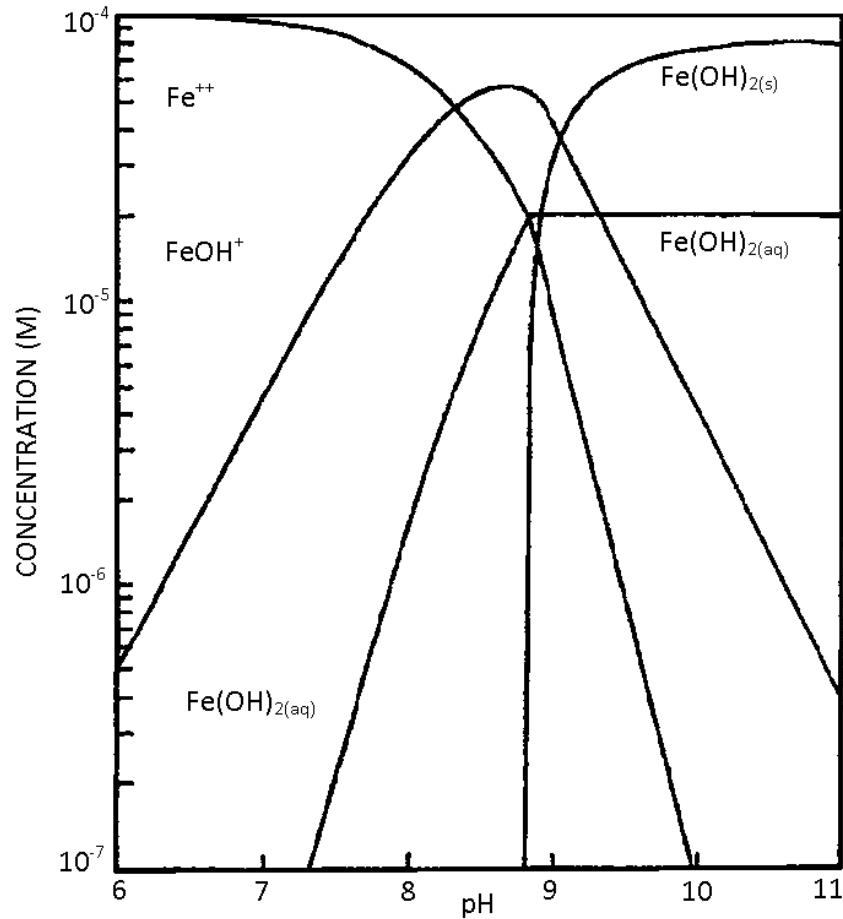


Figure 21: The logarithmic concentration diagram for 1×10^{-4} mol/L Fe^{2+} . Adapted from Palmer, Gutierrez, and Fuerstenau [49]

Palmer, Gutierrez and Fuerstenau also studied the role of ion hydrolysis in the flotation of rhodonite (MnSiO_3) with hydroxamate [49]. Flotation behaviour of rhodonite with hydroxamate was found to correlate with the hydrolysis of Mn^{2+} to Mn(OH)^+ [49]. Figure 22A shows the flotation recovery of rhodonite using potassium octyl hydroxamate [49]. Figure 22B shows that the addition of Mn^{2+} reverses the zeta potential of rhodonite starting at pH 7.6, and peaking at \sim pH 8.5. This is the same pH at which the peak in recovery occurs in the flotation of rhodonite with hydroxamate, Figure 22A. As shown in Figure 22C, pH 8.5 is in the region where Mn^{2+} begins to hydrolyze into Mn(OH)^+ .

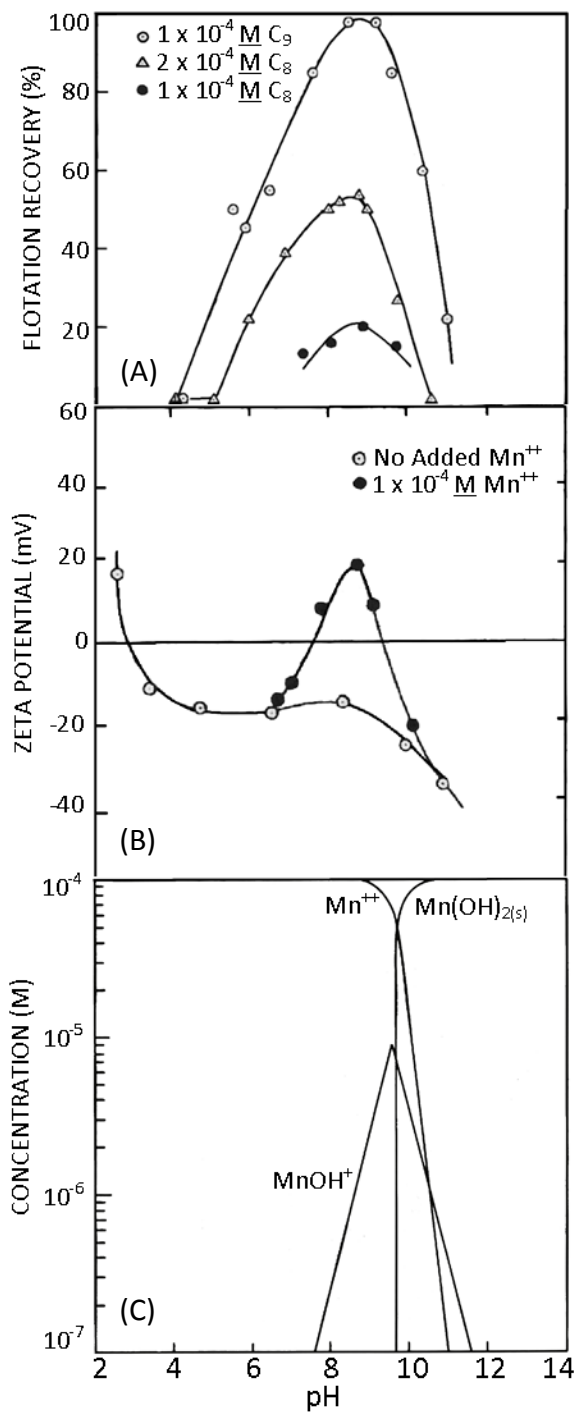


Figure 22: (A) Flotation recovery of rhodonite with potassium octyl and nonyl hydroxamate as a function of pH. (B) The effect of Mn^{2+} addition on the zeta potential of rhodonite as a function of pH, and (C), the concentration diagram for $1 \times 10^{-4} \text{ mol/L } Mn^{2+}$. Adapted from Palmer, Gutierrez, and Fuerstenau [49]

Palmer et al postulated that there are three key steps in the adsorption of hydroxamate on rhodonite [49]. The first step is the adsorption of Mn(OH)^+ on the mineral surface, producing a Mn^+ site [49]. The second is the physical adsorption of hydroxamate to this Mn^+ site [49]. The third requires the formation of a collector precipitate, manganous hydroxamate, the hydrocarbon tail of which associates with the physically adsorbed hydroxamate, therefore increasing the hydrophobicity of rhodonite [49]. Infrared spectroscopic studies confirmed the formation of manganous hydroxamate when rhodonite was exposed to potassium octyl hydroxamate [49]. The hydrolysis of manganese ions is likely to have a similar role in the flotation of pyrolusite with potassium oleate since, as shown in Figure 14, the peak in recovery due to chemical adsorption is at about pH 8.5, where Mn^{2+} hydrolyzes to Mn(OH)^+ .

2.6 Fatty Acid Adsorption

Characterization of carboxyl bonding with metal ions has been studied in great detail. Fourier transform infrared spectroscopy (FTIR) is a commonly used tool in identifying the coordination of carboxyl-metal bonding. While there are seemingly no contemporary studies investigating the adsorption of fatty acids on manganese dioxides, several exist concerning adsorption on iron oxides.

The latest study in this field was done by Chernyshova et al., who studied the adsorption of sodium laurate on hematite using FTIR and XPS [65]. The potential bonding modes of the carboxyl group of sodium laurate with hematite, as presented in their paper, are shown in Table 3.

Table 3: Modes of carboxyl-iron bonding

Structure	Bonding Type
$\text{R-CH}_2\text{-C} \begin{array}{l} \text{// O} \\ \backslash \text{OFe} \end{array}$	Inner-Sphere Monodentate Mononuclear (ISMM) or Unidentate
$\text{R-CH}_2\text{-C} \begin{array}{l} \text{/ OFe} \\ \backslash \text{OFe} \end{array}$	Inner-Sphere Bidentate Binuclear (ISBB) or Bridging
$\text{R-CH}_2\text{-C} \begin{array}{l} \text{/ O} \\ \backslash \text{O} \end{array} \text{Fe}$	Chelating or Bidentate
$\text{R-CH}_2\text{-C} \begin{array}{l} \text{/ O} \text{--- HOFe} \\ \backslash \text{O} \text{--- HOFe} \end{array}$	Open Sphere (OS) Surface Hydration - Shared
$\text{R-CH}_2\text{-C} \begin{array}{l} \text{/ O} \text{--- H} \text{--- O} \text{--- HOFe} \\ \backslash \text{O} \text{--- H} \text{--- O} \text{--- HOFe} \end{array}$	Open Sphere (OS) Surface Hydration - Separated

Chemical bonding of carboxyl groups is typically identified using FTIR by observation of the vibration frequencies of the CO_2^- group. The symmetric, $\nu_s\text{CO}_2^-$, and asymmetric, $\nu_{as}\text{CO}_2^-$, modes appear as a pair of peaks. The frequency splitting, $\Delta\nu\text{CO}_2^-$, has been used as a means of identifying bonding mode, whether unidentate, chelating, or otherwise in studies by Chernyshova et al. [65], Roonasi et al. [66], and others. Some contention exists in characterizing bonding modes strictly on $\Delta\nu\text{CO}_2^-$ values alone [67]; however, it is a useful indication of the presence of the bonds, and potentially the number of different bonding modes. Table 4 is a summary of important bonding frequencies identified in the literature for fatty acid adsorption on iron oxides.

Table 4: FTIR frequencies for fatty acid bonding on iron oxides

Peak Assignment	Frequency (cm ⁻¹)	Reference
vC=O v _{as} CO ₂ ⁻ , v _s CO ₂ ⁻ (ISMM) v _{as} CO ₂ ⁻ , v _s CO ₂ ⁻ (OS-Shared) δCH ₂ , scissor bending ωCH ₂ , wagging	1707 1540, 1410 1530, 1425 1466, 1458 1300-1200	Chernyshova, Ponnurangam, Somasundaran, 2011 [65]
v _{as} CH ₂ , v _s CH ₂ vC=O v _{as} CO ₂ ⁻ , v _s CO ₂ ⁻ δCH ₂ , scissor bending	2926, 2855 1722 1568, 1427 1456	Potapova, Carabante, Grahn, Holmgren, Hedlund, 2010 [68]
vC=O v _{as} CO ₂ ⁻ , v _s CO ₂ ⁻	1711 1550, 1420	Roonasi, Yang, Holmgren, 2010 [66]
C=CH stretch vC=O v _{as} CO ₂ ⁻ , v _s CO ₂ ⁻ δCH ₂ , scissor bending	3006 1711 1529, 1430 1465, 1458	Roonasi, Holmgren, 2009 [69]
v _{as} CH ₃ , v _s CH ₃ v _{as} CH ₂ , v _s CH ₂ vC=O v _{as} CO ₂ ⁻ v _s CO ₂ ⁻ δCH ₂ , bending δCH ₃ , asym bending δCH ₃ , sym bending	2970-2950/2880-2860 2935-2915/2865-2845 1725-1700 1610-1550 1420-1300 1485-1445 1470-1430 1380-1370	Coates, 2000 [70]
C=CH stretch v _{as} CH ₃ , v _s CH ₃ v _{as} CH ₂ , v _s CH ₂ vC=O v _{as} CO ₂ ⁻ , bridged v _{as} CO ₂ ⁻ , chelating δCH ₂ , scissor bending	3007 2959, 2890 2924, 2853 1713 1580 1518 1466	Gong, Parentich, Little, Warren, 1991 [71]
vC=O v _{as} CO ₂ ⁻ , v _s CO ₂ ⁻	1717 1520, 1425	Rocchiccioli-Deltcheff, Franck, Cabuil, Massart, 1987 [72]
v _{as} CH ₃ , v _s CH ₃ v _{as} CH ₂ , v _s CH ₂ vC=O v _{as} CO ₂ ⁻ v _s CO ₂ ⁻ δCH ₂ , scissor bending	2975-2950/2885-2865 2940-2915/2870-2840 1725-1700 1610-1550 1420-1335 1480-1440	Socrates, 1980 [73]

3. Objectives

The primary purpose of this investigation is to determine the feasibility of separating pyrolusite and hematite using froth flotation for application to iron ore at the Wabush Mine. To the Author's knowledge, this will also be the first fundamental investigation of hematite and pyrolusite separation using froth flotation. After reviewing the available information presented in the literature, sodium oleate was chosen as the base collector as its chemistry has been investigated in the flotation of both iron and manganese oxides. It is also known to be chemically adsorbing on both minerals under certain conditions. Due to the similarity of pyrolusite and hematite, a chemically adsorbing collector in combination with depressants under fixed pH conditions may lead to greater selectivity than a physically adsorbing collector.

Faced with the challenges outlined above, the goals of this study are as follows:

- 1) Characterize the iron and manganese bearing minerals present in the Wabush iron ore.
- 2) Using pure pyrolusite and hematite, conduct small-scale single mineral flotation tests to find selective separation conditions of specific pH, depressants and reagent dosage.
- 3) Test the effectiveness of the identified reagent schemes on real ore using bench-scale flotation, with a target of reaching 90% mass pull with no more than 60% manganese recovery.
- 4) Identify the reagent-mineral interaction mechanisms.

In order to meet the objectives outlined above, the following studies have been conducted:

- 1) Mineralogical analysis: The nature of the iron and manganese minerals present in the Wabush iron ore was studied using inductively coupled plasma (ICP) mass spectrometry for compositional analysis, and scanning

electron microscopy (SEM), energy-dispersive X-ray spectroscopy (EDX), electron probe micro-analysis (EPMA), and X-ray diffraction (XRD) for mineralogical characterization.

- 2) Zeta potential measurements: The zeta potential of pure pyrolusite and iron ore concentrate was measured at different values of pH and sodium oleate dosage.
- 3) Micro-flotation tests: Single mineral micro-flotation tests were conducted using pure minerals. The effect of sodium oleate, depressants, modifiers, pH, and reagent dosages were studied in order to identify potential selective separation conditions.
- 4) Bench-flotation tests: The effectiveness of the most promising results from micro-flotation experiments was tested on Wabush Spiral Concentrate in order to simulate flotation on a plant scale. Flotation conditions were subsequently refined to obtain selective separation of pyrolusite.
- 5) Mechanism studies: To identify the mechanism of reagent selectivity between hematite and pyrolusite, Fourier transform infrared spectroscopy (FTIR) was used to identify the nature of chemical bonding between collector, depressant, and the mineral surface under selective flotation conditions.

4. Materials and Methods

4.1 Iron Ore Concentrate

4.1.1 Sample Description and Preparation

The iron ore concentrate sample was received from the Wabush mine in a 200 liter drum. The received ore was referred to as “spiral concentrate”, as it had undergone crushing, grinding, and spiral concentration at the Wabush mine. The spiral concentrate as received was moist, so it was air dried at room temperature before coning and splitting into 500 g samples for bench flotation tests. As shown in Figure 23, the 80% passing size of the as-received spiral concentrate was 365 μm .

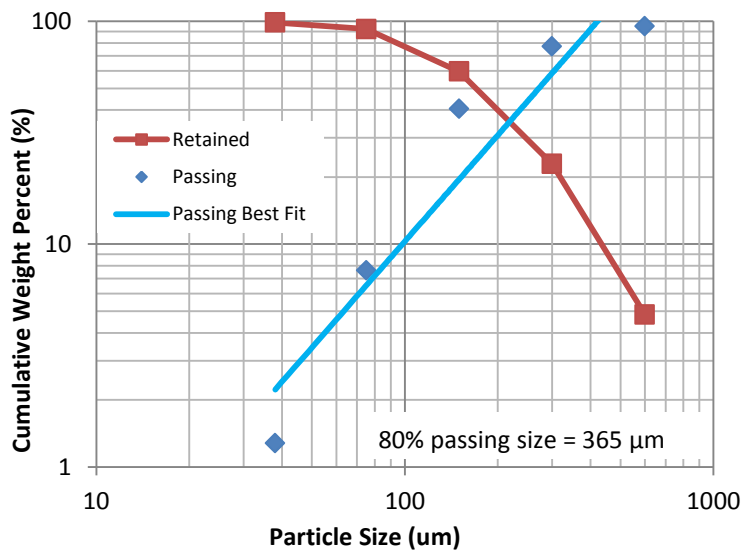


Figure 23: Size analysis of as-received Wabush spiral concentrate

The chemical analysis of the spiral concentrate is shown in Table 5. A mineralogical study had previously been carried out by the COREM organization studying a Wabush spiral iron concentrate containing about 1.5 wt% Mn [74]. Measuring by area, pyrolusite (MnO_2) was found to account for 90% of the manganese present, while the remaining 10% was present in iron-manganese

solutions [74]. In the bulk sample, 48% of the manganese bearing minerals were fully liberated, while in the -212 μm fraction 60-70% of the pyrolusite was liberated, and 20-30% was associated with oxides and hydroxides of iron and quartz [74].

Table 5: Chemical analysis of iron ore samples

Mineral Sample	Fe ₂ O ₃ (wt%)	MnO (wt%)	SiO ₂ (wt%)
Spiral Concentrate	93.38	2.71	2.63
Iron Ore Concentrate	93.49	2.56	2.77

For the purpose of producing an “iron ore concentrate” for micro-scale flotation tests, 500 g of spiral concentrate was subjected to wet high intensity magnetic separation (WHIMS). An Outokumpu Carpc separator set at 6 amperes of current was used. With the current applied, the spiral concentrate was added to the separation cell in 50 g batches and washed with 1 L of distilled water. When the initial wash was completed, the current was turned off and the magnetic concentrate was collected. This process was repeated until 500 g of the spiral concentrate was processed. The magnetic concentrate product was called iron ore concentrate (IOC) with the chemical analysis is shown in Table 5. The IOC was not ground for micro-scale flotation tests, and maintained the same 80% passing size as the spiral concentrate of 365 μm .

4.1.2 SEM, EDX, and EPMA Analysis

Backscattered electron imaging and energy-dispersive x-ray analysis (EDX) were carried out on Wabush spiral concentrate in the Chemical and Materials engineering department at the University of Alberta. A sample of un-ground spiral concentrate, and a sample of concentrate from bench-scale flotation test BI06 were mounted on 12 mm diameter spectro tabs (carbon conductive double coated), and evaporatively coated with carbon. The BI06 concentrate assayed

80.9 wt% Fe₂O₃, 5.9 wt% MnO, and 8.1 wt% SiO₂. Analysis was carried out using a Hitachi S-2700 scanning electron microscope equipped with a Princeton Gamma-Tech IMIX digital imaging system. A PGT PRISM IG (intrinsic germanium) detector was used for EDX measurements, and a GW Electronics 47, four quadrant, solid state back scattered electron detector was used for back scattered electron (BSE) imaging. Vacuum pressure was in the range of 2.6 x 10⁻⁹ to 7.9 x 10⁻⁹ atm, and the electron source was a pre-centered hairpin tungsten wire filament.

Additional analysis was carried out by Dr. Allen Pratt at CANMET on the spiral concentrate, as well as a tails sample from test B113. The B113 tails sample assayed 49.9 wt% Fe₂O₃, 23.6 wt% MnO, and 17.4 wt% SiO₂. Wavelength dispersive spectrometry was carried out on the samples using a JEOL JXA 899 electron probe micro-analyzer (EPMA). Accelerating voltage was 20 kV, with a probe current of 20 nA. The characteristic X-ray lines and standards are shown in Table 6. XRD analysis of the spiral concentrate and B113 tails was also carried out.

Table 6: Characteristic X-ray lines and standards for EPMA

Element	X-ray Line	Mineral Standard
Mn	K _α	Rhodochrosite
Fe	K _β	Hematite
K	K _α	Orthoclase
Ba	L _α	Barite

Further analysis was carried out by Jeff Harris of Harris Exploration Services, and Peter Le Couteur of Micron Geological Ltd. A sample of concentrate collected from bench-scale flotation test B106, which assayed 80.9 wt% Fe₂O₃, 5.9 wt% MnO, and 8.1 wt% SiO₂, was mounted in epoxy and polished. An AMRAY 1810 scanning electron microscope equipped with a Genesis EDX analyzer was used for BSE imaging and X-ray mapping. During analysis the mineral surfaces were

uncoated and no standards were used for the EDX analysis, so the results are semi-quantitative.

4.2 Pyrolusite Mineral Sample

For the purpose of micro-scale flotation testing and mechanism studies, pure pyrolusite crystals originating from a deposit in New Mexico, USA, were obtained from Arkenstone Inc. Chemical analysis of the pyrolusite is shown in Table 7. While the manganese content is balanced to MnO, 80.28 wt% MnO equates to 98.38 wt% MnO₂ for the same amount of Mn.

Table 7: Chemical analysis of pyrolusite concentrate

Mineral Sample	Fe ₂ O ₃ (wt%)	MnO (wt%)	SiO ₂ (wt%)	K ₂ O (wt%)
Pyrolusite	5.32	80.28	0.55	2.02

The crystals were confirmed as pyrolusite using XRD, with the XRD pattern shown in Figure 24. As shown, the pattern is well matched to that of synthetic pyrolusite, indicating a high purity of the pyrolusite sample. Based on spectra fitting using MDI JADE, the sample is predominately pyrolusite based on the matching of the highest intensity peaks. The presence of minor peaks matching the pattern for a manganese dioxide sample of lower crystallinity and purity indicates the presence of polymorphs in the sample.

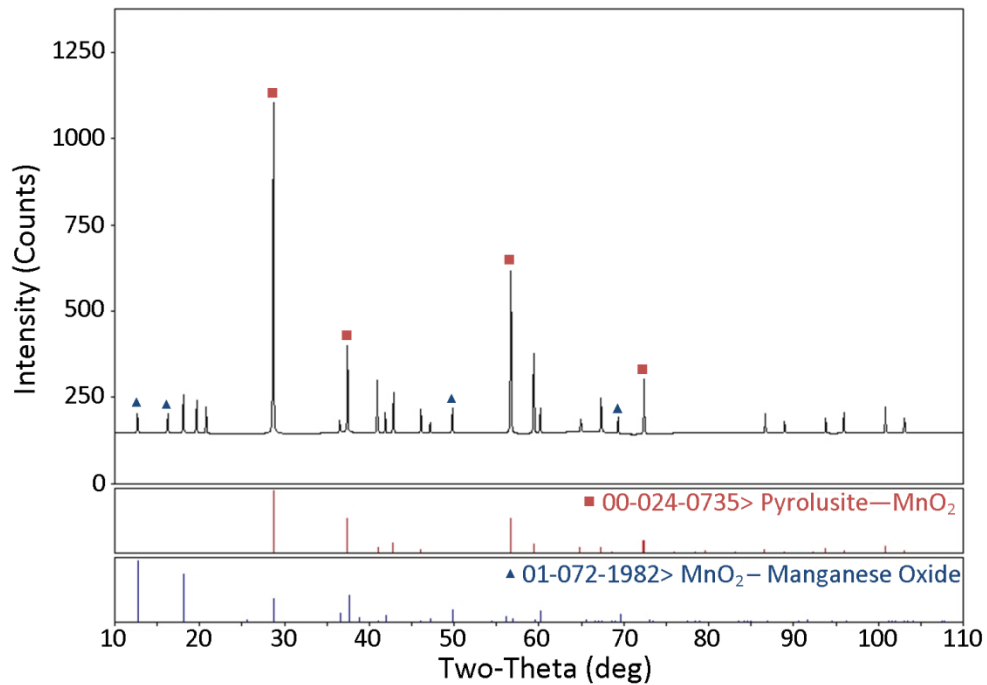


Figure 24 : XRD pattern for pyrolusite

Preparation of the pyrolusite for micro-scale flotation included crushing with a hammer followed by grinding with a Fritsch Pulverisette automatic mortar and pestle grinder. Following grinding the pyrolusite was separated into -38 μm , -106+38 μm , and +106 μm size fractions by dry sieving with a Ro-Tap machine. The -106+38 μm fraction was used for micro-scale flotation.

4.3 Chemical Assays

Chemical assays of the spiral concentrate, IOC, and pyrolusite were performed by Inspectorate America Analytical Division, of Richmond, BC. Whole rock analysis was carried out by LiBO₂ fusion, followed by inductively coupled plasma mass spectrometry. Bench-scale flotation products were sent to COREM for chemical analysis.

4.4 Reagents

All inorganic reagents were obtained from Fisher Scientific, and were of American Chemical Society (ACS) reagent grade. Sodium oleate was supplied by Sigma Aldrich, and was of purum grade assaying a minimum of 82 wt% fatty acids. Armeen 18D was used as an amine collector and is a product of AKZO Nobel. Sodium silicate pentahydrate was supplied by Fisher and was of technical grade. Kerosene was tested in certain bench-scale flotation tests and was of commercial grade. KBr powder used for FTIR experiments was of spectroscopic grade and supplied by Pike Technologies.

For experiments using sodium oleate, a stock solution was prepared by adding 0.1 g of sodium oleate to a 100 mL volumetric flask and diluting with distilled water. Ultrasonic agitation was used to fully dissolve the oleate. Solutions were prepared fresh daily as needed.

Potato starch was prepared as a 1 wt% solution using the digestion method for corn starch utilized by Peres and Correa [34]. The procedure used is as follows:

1. Add 1.25 g potato starch to 11.25 mL distilled water in a 250 mL beaker.
2. Add 7.8 mL of 1M NaOH, stir for 20 minutes.
3. Dilute to 1 wt% starch (125 g of solution total), stir for 10 minutes.

Armeen 18D was prepared as a 0.1 wt% solution and acetic acid was used in a molar ratio of 1:1 for dissolution in water. Solutions were prepared fresh as needed.

For use in bench-scale flotation tests kerosene was emulsified with distilled water. A water and kerosene mixture of approximately 5 wt% kerosene was used for emulsification, which was carried out with a high speed blender.

4.5 Micro-Scale Flotation: Single Minerals

The micro-scale flotation tests were conducted using a modified "Siwek" tube as shown in Figure 25 [75]. Prepared solution is added through the small funnel at the top of the main tube. Nitrogen gas enters at the base, and bubbles through a porous frit, which also serves as a base for a magnetic stir bar. Mineral particles that attach to bubbles are carried upwards to the neck between the main tube and the collection bulb. Once passed the neck, bubbles will reach the liquid surface in the concentrate bulb, and break, releasing the collected minerals.



Figure 25: "Siwek" type micro-scale flotation tube

Pyrolusite used for the small-scale flotation had a particle size of $-106+38 \mu\text{m}$. The iron ore concentrate used for the small-scale flotation tests had a particle size of 80% passing $365 \mu\text{m}$.

The test procedure for the micro-scale flotation was as follows:

1. Add 1.5 g of mineral and a magnetic stir bar to a 250 mL beaker.
2. Add 125 mL distilled water and begin stirring.

3. Add the desired amount of depressant, adjust pH, and condition for three minutes. Skip if no depressant is desired.
4. Add the desired amount of collector, adjust pH, and condition for three minutes.
5. Transfer the conditioned solution to the flotation tube, and add distilled water until flotation height is achieved (165 mL total solution).
6. Begin stirring, and open nitrogen gas valve, slowly pressurizing the gas feed system. When the first bubbles appear in the tube, turn off feed valve (gas pressure in the gas feed is sufficient to consistently produce bubbles for one minute).
7. After 1 minute of collection time, remove the gas feed hose and collect the concentrate.

4.6 Bench-Scale Flotation: Wabush Spiral Concentrate

4.6.1 Bench-Scale Flotation Procedure

Bench-scale flotation tests were carried out using a JK Tech bottom drive flotation machine, and a 1.5 L flotation cell, which are shown in Figure 26. Wabush spiral concentrate was used as the feed stock in 500 g batches. Flotation was carried out at a pulp density of ~30 wt% solids using distilled water. Compressed air was used to produce bubbles.



Figure 26: JK Tech bottom drive flotation machine and 1.5 L cell

The general procedure for bench-scale flotation tests is shown below. Details for each specific bench-scale test are provided in Appendix I.

1. (Optional) Grind 500 g of spiral concentrate with 350 mL of distilled water for the desired time using mild steel balls.
2. Transfer the slurry to the flotation cell and dilute to 1.5 L using distilled water. Agitate the slurry at 1200 RPM and record pH.
3. Add depressant, record pH, and condition for three minutes (optional).
4. Add collector and adjust pH to the desired value, and condition for three minutes.
5. Open air valve to desired airflow, add frother if necessary, and collect froth for specified time. Turn off air flow when complete. Record pH.
6. Step 5 may be repeated for the collection of the next concentrate. If the addition of more collector or depressant is necessary, repeat steps 3-5.
7. Record final pH and record the weights of the wet concentrates and tails.
8. Following drying in an oven at 80°C, record the weights of the dry concentrates and tails.

4.6.2 *Spiral Concentrate Grinding and Particle Size*

The size distribution of the spiral concentrate was determined by dry sieving 500 g of sample in a Ro-Tap using 600, 300, 150 and 75 μm sieves. The -75 μm fraction was then wet screened with a 38 μm sieve. A size distribution plot was then made to determine the 80% passing size, and is shown in Figure 23.

This same procedure was used to determine the particle size distribution after grinding the spiral concentrate. The spiral concentrate was ground in a ball mill using mild steel balls in 500 g batches. Both dry grinding and wet grinding at 60 wt% solids were tested. Dry grinding for 20 minutes resulted in an 80% passing size of 188 μm , and 25 minutes produced 149 μm . Wet grinding for 25 minutes produced an 80% passing size of 117 μm , and 86 μm for 35 minutes of grinding. Size analysis charts and passing size calculations are shown in Appendix II.

4.7 **Mineral-Reagent Interaction Mechanism Study**

4.7.1 *Zeta Potential*

Zeta potential measurements were conducted on pyrolusite and the IOC using a Brookhaven Instruments ZetaPALS Zeta Potential Analyzer, shown in Figure 27. The Smoluchowski model was used to calculate zeta potentials from the measured electrophoretic mobilities. Each reported zeta potential value is the mean of 10 runs, with 20 measurement cycles per run. The highest and lowest runs were removed for the calculation of mean zeta potential. The sample preparation for zeta potential was as follows:

1. Prepare a stock mineral suspension by adding 1.0 g of -38 μm mineral to 1 L of 1.0×10^{-3} mol/L KCl solution. Allow the suspension to stand for 24 hours.
2. Vigorously agitate the mineral suspension and withdraw 100 mL into an empty 250 mL beaker. Add 100 mL 1.0×10^{-3} mol/L KCl to the 100 mL of mineral suspension, making a total suspension volume of 200 mL.

3. Add the desired amount of collector if necessary.
4. Condition the 200 mL suspension for 20 minutes at each value of pH chosen. Separate suspensions should be used for acidic pH range tests and basic pH range tests, using natural pH as a starting point. To avoid dilution of KCl, adjust pH with KOH or HCl solutions prepared using 1.0×10^{-3} mol/L KCl solution.
5. After conditioning transfer ~ 1.6 mL of conditioned solution to a disposable sample cuvette for measurement.



Figure 27: Brookhaven Instruments ZetaPALS Zeta Potential Analyzer

4.7.2 FTIR Sample Preparation

To study the mechanism of collector adsorption on pure pyrolusite and hematite (IOC), samples of these minerals were reacted with fixed dosages of sodium oleate under controlled pH values. These samples were then analysed using Fourier Transform Infrared Spectroscopy (FTIR). Preparation of the mechanism study samples was carried out as follows:

1. Weigh 2 g of $-38 \mu\text{m}$ pure mineral (pyrolusite or IOC) and transfer to a 250 mL beaker with 100 mL distilled water.
2. Add the needed amount of 1.0 wt% sodium oleate solution to the mineral solution to achieve 0, 0.5, or 1.0×10^{-3} mol/L concentration.
3. Add the balance of distilled water to the mineral solution needed for a total volume of 200 mL water.
4. Adjust pH to the required value (7 or 11) using dilute HCl or NaOH.
5. Condition using a magnetic stirrer for 30 minutes.

6. After conditioning, vacuum filter the mineral suspension and dry the filter cake in a vacuum desiccator overnight.

4.7.3 *Pure Mineral Experiment: FTIR*

Fourier Transform Infrared Spectroscopy (FTIR) was used for detection and characterization of chemical bonds formed between sodium oleate and pure mineral samples. A Nicolet 8700 spectrometer outfitted with a Thermo Smart Collector was used for Diffuse Reflectance Infrared Fourier Transform Spectroscopy (DRIFTS) measurements, and is shown in Figure 28. Thermo OMNIC software was used for data processing.



Figure 28: Nicolet 8700 spectrometer

For each sample 64 scans were made, using a scanning range of $400 - 4000 \text{ cm}^{-1}$, and a resolution of 2 cm^{-1} . KBr was used as a background material. For each measurement, 0.025 g of mineral was added to 0.5 g of KBr, for a concentration of approximately 5 wt% mineral. The mineral sample was ground using a mortar and pestle for 1 minute prior to mixing with KBr. For the analysis of pure sodium oleate, 0.05 g was added to 0.5 g KBr, for a concentration of approximately 10 wt% sodium oleate powder.

5. Mineralogical Analysis

5.1 SEM and EDX Analysis

A back-scattered electron SEM image of Wabush spiral concentrate is shown below in Figure 29A. An EDX line scan was carried out between points 1 and 2, with the composition profile shown in Figure 29B.

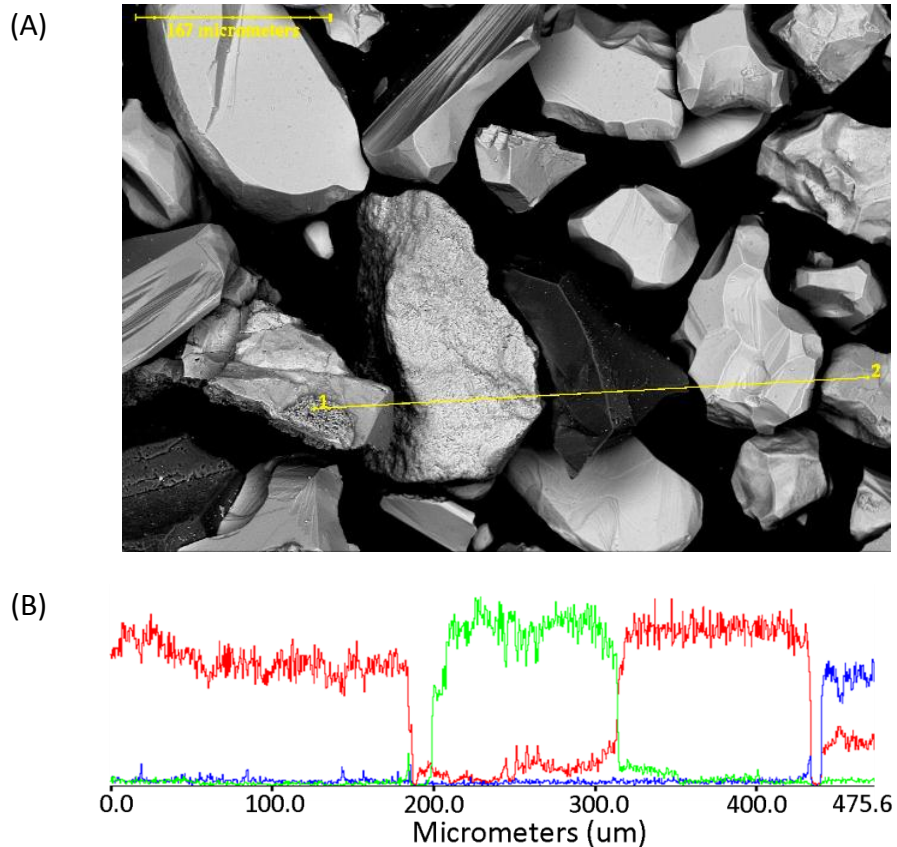


Figure 29: (A) Back-scattered electron SEM Image of Wabush spiral concentrate. The line segment between points 1 and 2 indicates the path of the EDX scan. (B) EDX profile between points 1 and 2: blue = Mn, red = Fe, green = Si

The EDX profile in Figure 29B shows the compositional profile of Fe, Mn, and Si in the particles. Starting at point 1, the first two particles are predominately Fe, the third primarily Si, the fourth primarily Fe, and the fifth is primarily Mn with a significant amount of Fe. As the atomic weight of Si is about half of those of Mn

and Fe, it produces fewer back-scattered electrons, and thus the Si bearing minerals appear dark (black) compared to the Mn and Fe bearing minerals. Comparing the first and second particles to the fourth, it is apparent that the surface texture of the Fe bearing minerals is variable. Also, the Mn-bearing fifth particle is visibly indistinguishable from the Fe-bearing particles. This is partly due to Mn and Fe having nearly identical atomic weights, which results in the amount of back-scattered electrons, and subsequently brightness, being virtually the same for each element. This effect is compounded for the fifth particle as it contains both Mn and Fe. A close up image and EDX profile of the fifth particle is shown in Figure 30.

Figure 30 is an example of the Mn bearing oxide particle in the spiral concentrate. The EDX line scan carried out between points 1 and 2 in Figure 30A shows both Mn and Fe are present throughout the particle, shown in Figure 30B. Throughout the particle Fe is present at about $\frac{1}{4}$ the intensity of Mn. The consistency of Mn and Fe intensities throughout the profile indicates that these elements are in an oxide solution together, as opposed to combined non-liberated oxides of each element.

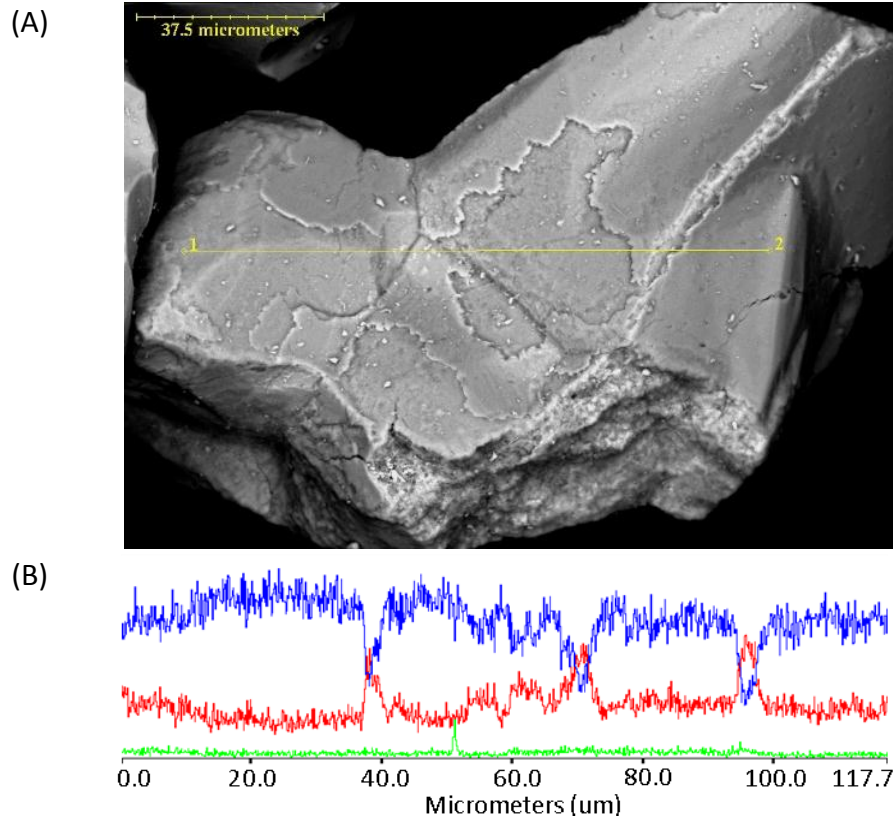


Figure 30: (A) Back-scattered electron SEM Image of Mn bearing particle in Wabush spiral concentrate. The line segment between points 1 and 2 indicates the path of the EDX scan. (B) EDX profile between points 1 and 2: blue = Mn, red = Fe, green = Si

5.2 SEM and X-Ray Mapping by Harris Exploration

Further analysis of the BI06 concentrate was carried out by Harris Exploration and Micron Geological Ltd using BSE imaging and X-ray mapping. Their full report can be found in Appendix IV. X-ray mapping indicated that by area the sample was composed of approximately 2-5% Mn minerals, 15-20% Si minerals, with the remainder being Fe bearing minerals. As these values are approximate and qualitative in nature, they can be considered to be in general agreement with the assay values of 81.90 wt% Fe_2O_3 , 5.93 wt% MnO , and 8.06 wt% SiO_2 for this sample. An example of an X-ray mapped BSE image is shown in Figure 31.

There were two important conclusions drawn by this study. The first is that the Mn observed in the sample occurred mainly as Mn oxide minerals with high MnO contents. Some of the Mn bearing minerals contained only Mn and O while others contained some Si, Fe and K. Determining the composition of the Mn bearing minerals would require XRD analysis. The second main finding is that the Mn observed was predominately limited to the Mn oxides minerals. The bulk of the Fe oxide particles observed contain only Fe and O. The Mn and Fe bearing minerals that were collected in this flotation concentrate were fully liberated from each other.

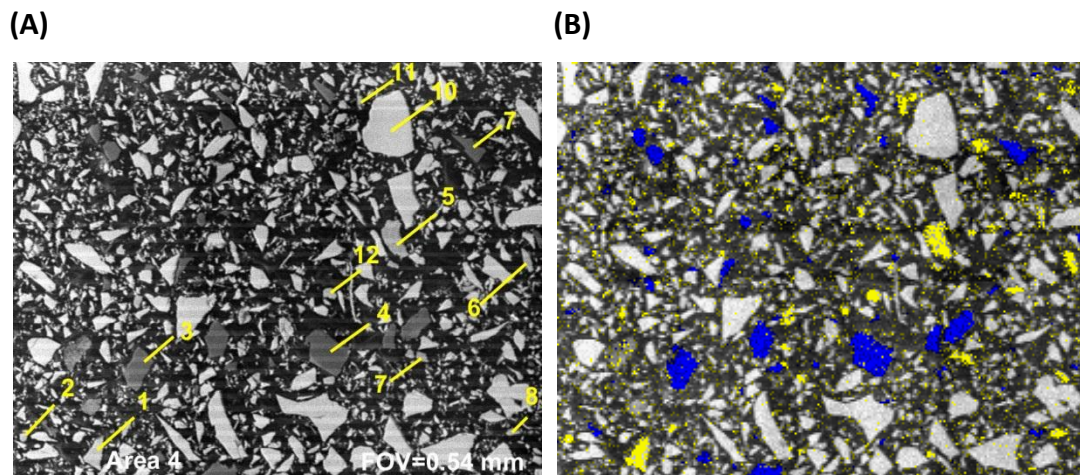


Figure 31: BI06 Concentrate. (A): BSE image with numbers 1 through 12 indicating EDX line scans. (B): X-ray map of area in (A). White = Fe, Blue = Si, and Yellow = Mn.

5.3 SEM and Wavelength Dispersive Spectrometry by CANMET

Analysis of the Wabush spiral concentrate and bench-scale test BI13 tails was carried out by Dr. Allen Pratt of CANMET using XRD and EPMA. The full set of data provided by Dr. Pratt is attached in Appendix III. XRD analysis of the Wabush spiral concentrate is shown below in Figure 32. XRD analysis confirms that the primary minerals present are hematite (Fe_2O_3), quartz (SiO_2), and pyrolusite (MnO_2).

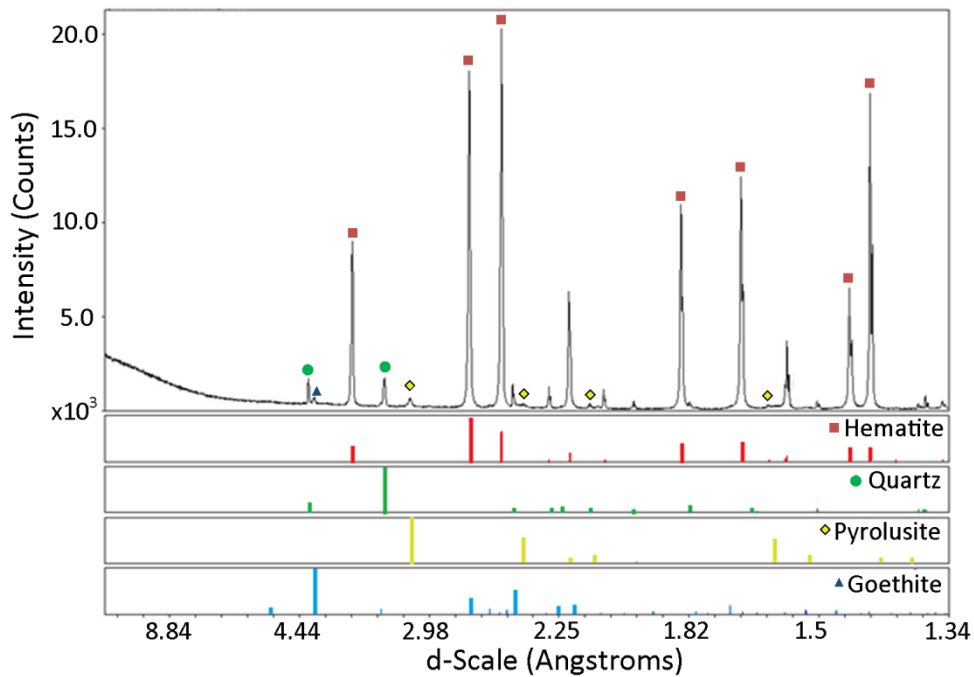
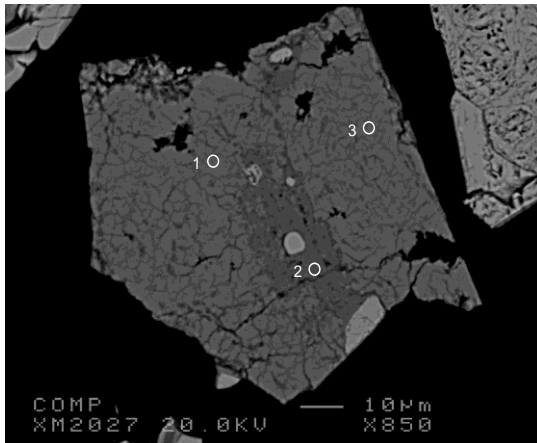


Figure 32: XRD Analysis of Wabush spiral concentrate. Analysis provided by CANMET

The BSE image and EPMA analysis results for a pyrolusite particle in the spiral concentrate are shown in Figure 33. This figure is representative of the variability in composition of the pyrolusite particles. All the particles observed contained traces of Fe, with values typically below 5 wt%. As illustrated in Figure 33, the composition can vary significantly throughout individual particles. K and Ba are also found in the bulk of the pyrolusite particles. Although typically present in trace amounts, as in Figure 33, K was observed in concentrations up to ~5 wt%, and up to ~14 wt% Ba was observed.

While the chemical composition of the pyrolusite observed in the spiral concentrate appears to be variable in Fe, K, and Ba content, XRD analysis ultimately confirms that the predominant morphology of the Mn bearing minerals is pyrolusite. A factor that must be considered is the fact that the pyrolusite particles of varied composition are more easily distinguished from the

bulk hematite samples. With this in mind, the EPMA analysis may have been in bias of the pyrolusite of varied composition, giving the perception that the overall composition of pyrolusite in the spiral concentrate is much more varied than it really is.



Wt%	1	2	3
MnO ₂	100.09	2.61	99.59
Fe ₂ O ₃	0.87	76.93	0.87
K ₂ O	0.13	0.00	0.09
BaO	0.06	0.02	0.00
Total	101.15	79.55	100.55

Figure 33: BSE image of Wabush Spiral Concentrate and EPMA analysis of points 1-3. Image and analysis data provided by CANMET

BSE imaging and EPMA analysis of the BIO6 tails shows no significant change in pyrolusite composition. XRD analysis shows the primary minerals are still hematite, quartz, and pyrolusite, although the intensity of quartz and pyrolusite increased compared to the spiral concentrate. Particle size of the pyrolusite observed in the BIO6 tails is significantly reduced from the spiral concentrate, which is as expected as the flotation feed had been ground.

6. Flotation and Mineral-Reagent Interaction Mechanism Studies

6.1 Zeta Potential

Zeta potential values for IOC as a function of pH and sodium oleate dosage are shown in Figure 34.

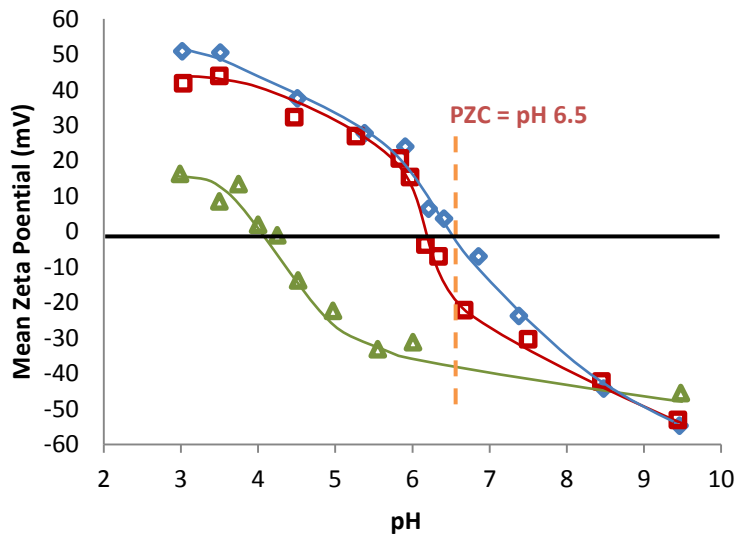


Figure 34: Zeta Potential of IOC as a function of pH and sodium oleate dosage. KCl concentration is 1.0×10^{-3} mol/L. Blue = 0 mol/L, red = 5×10^{-7} mol/L, and green = 2.5×10^{-6} mol/L sodium oleate.

The point of zero charge (PZC) for the IOC was pH 6.5 in the absence of sodium oleate. This is in agreement with PZC values of hematite found in the literature, which ranged from pH 5.3 – 8.6 [11–15]. The addition of 5×10^{-7} mol/L sodium oleate has minimal effect on zeta potential values; however, 2.5×10^{-6} mol/L sodium oleate significantly shifts zeta potential values to more negative values. The PZC value is shifted from pH 6.5 to approximately pH 4.0. This behaviour is in agreement with the model of a chemisorbed collector described by Han et al [10], and shown in Figure 3. Chemisorption of an anionic surfactant is characterised by a shift to a negative potential at the PZC (pH 6.5), and a shift of

the PZC to lower pH values. If sodium oleate was physically adsorbed, the PZC would not shift.

The effect of sodium oleate on the zeta potential of pyrolusite is shown in Figure 35. The PZC observed in the absence of sodium oleate was pH 4.6, which is in the range of pH 4.2 – 7.4 cited for pyrolusite in the literature [7, 11, 44–47]. As discussed in the literature review, Healy et al [44] found pyrolusite to have a PZC of pH 7.3, and Mn dioxides of increasing oxygen deficiency have decreasing PZC values. Since XRD analysis confirmed the pyrolusite sample as having the β -MnO₂ crystal structure, the PZC is likely lowered due to the presence of impurities. As shown in Table 5, the pyrolusite concentrate contains Fe, Si, and K. In the study done by Fuerstenau and Rice [7], a pyrolusite sample bearing 4.32 wt% Fe had a PZC of pH 5.6, while a pure pyrolusite sample with no impurities had a PZC of pH 7.4. Another phenomena observed by Fuerstenau and Rice [7] was that of grain structure. They found that for a pure pyrolusite sample which had elongated crystals the PZC was pH 4.2. The pyrolusite sample used for this project was also fractured into elongated crystals.

At the dosages of sodium oleate tested, no significant effect on the zeta potential of pyrolusite can be inferred. With this in mind, it seems likely that sodium oleate has a lower activation concentration for interaction with IOC over pyrolusite. Further tests at increased sodium oleate dosages would reveal the type of adsorption behaviour with pyrolusite, whether chemical or physical. Further zeta potential measurements at higher sodium oleate dosages was not carried out as at higher dosages the mineral particles are collected from solution and floated to the surface of the conditioning beaker, for both IOC and pyrolusite.

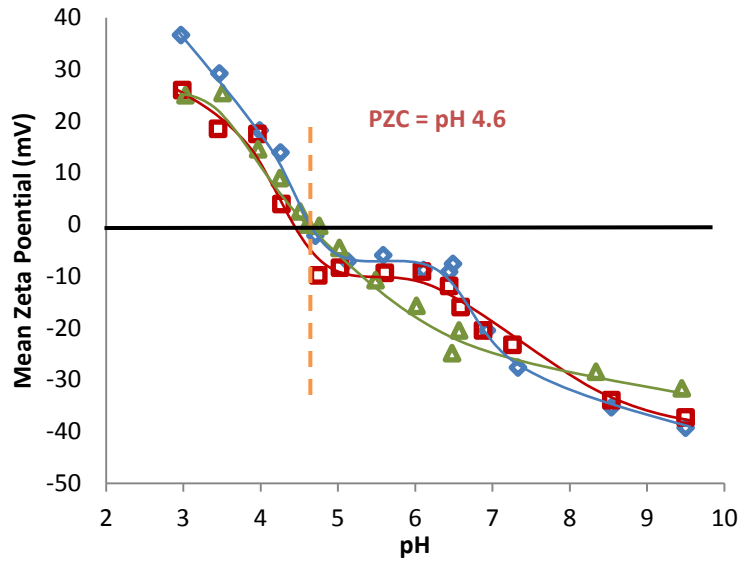


Figure 35: Zeta potential of pyrolusite as a function of pH and sodium oleate dosage. KCl concentration is 1.0×10^{-3} mol/L. Blue = 0 mol/L, red = 5×10^{-3} mol/L, and green = 2.5×10^{-6} mol/L sodium oleate

6.2 Micro-Scale Flotation

Micro-scale single mineral flotation tests were conducted using pyrolusite and iron ore concentrates (IOC) according to the procedure outlined in Section 4.5. Flotation was conducted from pH 7-12 since this is the region in which chemical adsorption of oleate is considered to occur on pyrolusite and hematite [7, 22, 45, 49]. Sodium oleate was used as the collector for all tests. Based on findings of the literature review, the modifying reagents tested in micro-scale flotation tests were sodium silicate pentahydrate ($\text{Na}_2\text{SiO}_3 \cdot 5\text{H}_2\text{O}$), potato starch, sodium dihydrogen phosphate (NaH_2PO_4), tannic acid, manganese (II) sulphate, and copper (II) sulphate. To set a recovery baseline for the micro-scale flotation tests IOC and pyrolusite were first floated with only sodium oleate as a collector and no modifying reagents; the results are presented in Figure 36.

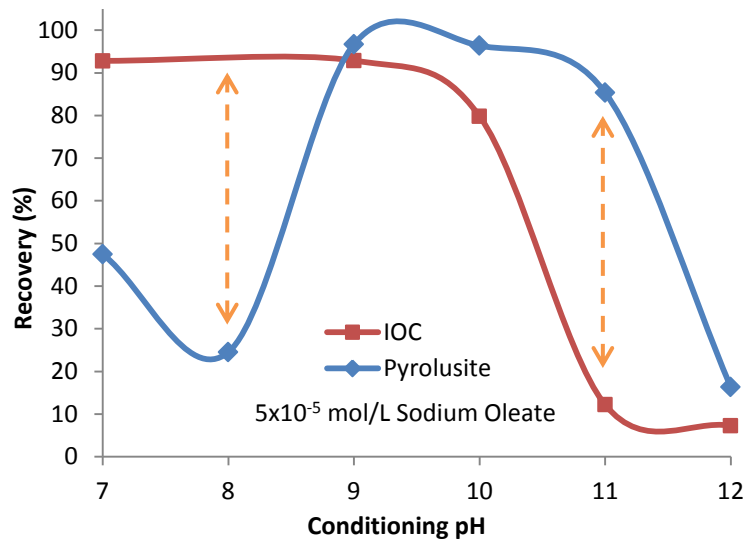


Figure 36: Micro-scale flotation recovery of IOC and pyrolusite as a function of pH at a sodium oleate dosage of 5×10^{-5} mol/L

Two regions of selectivity can be seen in Figure 36. The first region is at pH 8, where IOC recovery is over 90%, while pyrolusite recovery is ~20%. The second region is at pH 11, where pyrolusite recovery approaches 90%, while IOC recovery is ~10%.

The IOC recovery curve approaches 90% from pH 7-10, at which point recovery drops drastically. While Fuerstenau, Harper, and Miller [22] observed a sharp recovery peak with a maximum of about pH 8.5, Figure 7, the recovery curve shown in Figure 36 is similar to that observed in Figure 9 by Laskowski and Nyamekye [26], and others [12, 18, 24, 27]. The peak in IOC recovery correlates to the peak in $\text{Fe}(\text{OH})^+$ species shown in Figure 21.

The recovery of pyrolusite in Figure 36 is similar to that observed by Fuerstenau and Rice [7], which is shown in Figure 14. There is some deviation however, as pyrolusite recovery in this case decreases from pH 7-8, at which point it increases to a broad maximum from pH 9-11. Fuerstenau and Rice observed a

much narrower peak in recovery at about pH 8.5 [7]. Potassium oleate was used rather than sodium oleate at twice the dosage (1×10^{-4} mol/L) used in this study. The peak in pyrolusite recovery begins at about pH 9, which correlates to the peak in MnOH^+ concentration of Mn^{2+} ions in solution shown in Figure 22 [49]. Palmer et al found that the presence of MnOH^+ was directly related to oleic acid adsorption [49].

To test the significance of pyrolusite recovery at pH 8, flotation was conducted with varying dosages of sodium oleate; the results are shown in Figure 37. The decrease in recovery of pyrolusite from pH 9 to pH 8 can be considered significant since lowering the dosage of sodium oleate results in lower recovery, and increasing the dosage results in increased recovery.

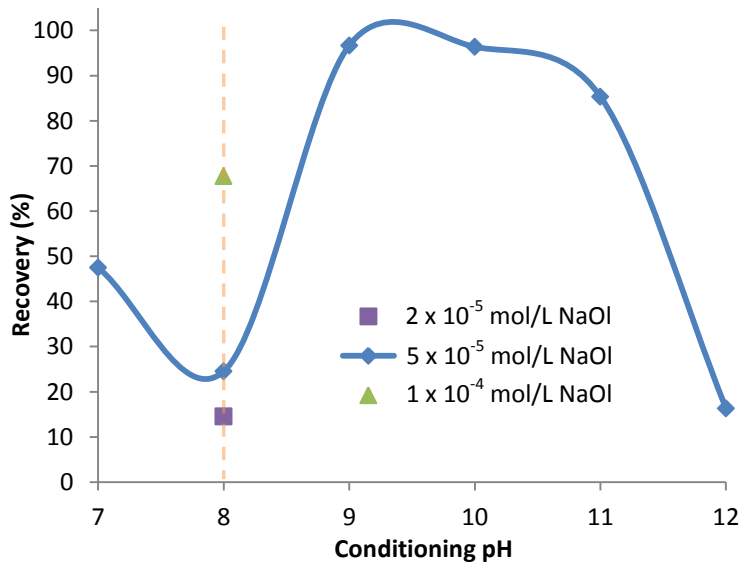


Figure 37: Micro-scale flotation recovery of pyrolusite as a function of pH at sodium oleate dosages of 2×10^{-5} mol/L, 5×10^{-5} mol/L, and 1×10^{-4} mol/L

The results of flotation tests using sodium silicate and sodium dihydrogen phosphate are shown in Figure 38A and B respectively.

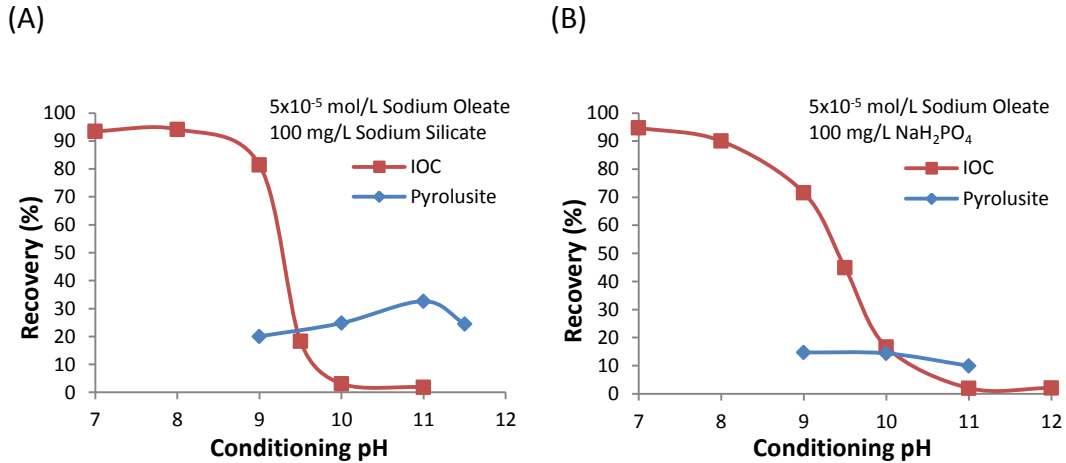


Figure 38: Micro-scale flotation recovery of pyrolusite and IOC as a function of pH at a sodium oleate dosage of 5×10^{-5} mol/L. (A) sodium silicate dosage of 100 mg/L, and (B) sodium dihydrogen phosphate dosage of 100 mg/L

The addition of sodium silicate had little effect on the recovery of IOC from pH 7–9, but significantly depressed pyrolusite from pH 9–10. Pyrolusite recovery decreased from >90% to ~30% from pH 9–11. Selective separation of pyrolusite and IOC may be possible below pH 9 for the flotation of IOC and depression of pyrolusite, or possibly above pH 10 to float pyrolusite while depressing IOC.

The sodium silicate used had the composition $\text{Na}_2\text{SiO}_3 \cdot 5\text{H}_2\text{O}$, which has a $\text{SiO}_2:\text{Na}_2\text{O}$ modulus of 1:1. Dissolution of Na_2SiO_3 in water produces many different species in both colloidal and ionic form [76]. With a modulus of 1:1, no colloidal silica should be present [76], and the active silicate species should be monosilicic acid ($\text{Si}(\text{OH})_4$) below pH 9, and monosilicate ($\text{SiO}(\text{OH})_3^-$) from pH 9–12 [77].

As shown in Figure 38B, recovery of IOC using sodium dihydrogen phosphate exhibits similar behaviour to flotation using sodium silicate; however, pyrolusite recovery is largely depressed. As is the case with sodium silicate, IOC could potentially be floated from pyrolusite below pH 9. Further flotation tests using

decreased dosages of NaH_2PO_4 , the results of which are shown in Appendix V, showed that even at 10 mg/L, pyrolusite was significantly depressed.

Recovery curves for the flotation of IOC and pyrolusite with the addition of potato starch and tannic acid are shown in Figure 39A and B, respectively. At a dosage of 50 mg/L, potato starch completely depressed pyrolusite from pH 7-9, while IOC maintained a peak recovery of ~85% at pH 8. At pH 8 IOC could potentially be selectively floated from pyrolusite.

While no previous research has been found studying the effects of starch in the flotation of manganese oxides, starch is used extensively as a depressant of iron oxides in the reverse cationic flotation of iron ores. In these cases corn starch is typically used in conjunction with an amine collector. The adsorption of dextrin on hematite has been investigated by Liu and Laskowski [32], who found the adsorption to be chemical in nature. As dextrin is a component of starch, similar adsorption behaviour of potato starch on hematite could be expected. Considering the strong recovery of IOC at pH 8, it seems that potato starch adsorption at pH 8 is unable to compete with the adsorption of oleate at this pH.

Of all the reagent schemes tested in this study on a micro-scale, tannic acid produced the most unique results, as shown in Figure 39B. Tannic acid is the only reagent tested in conjunction with sodium oleate that depresses IOC while under the same conditions floated pyrolusite. Pyrolusite recovery is depressed from pH 7-8, and then peaks at 70-90% from pH 9-11. IOC recovery fluctuates between pH 7 and 11, however it is generally depressed as recovery does not exceed 40%.

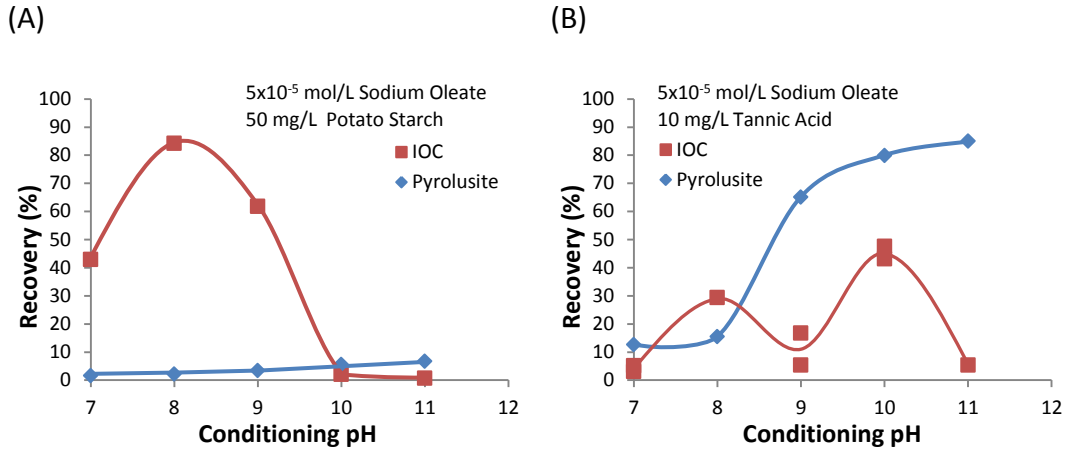


Figure 39: Micro-scale flotation recovery of pyrolusite and IOC as a function of pH at a sodium oleate dosage of 5×10^{-5} mol/L. (A) potato starch dosage of 50 mg/L, and (B) tannic acid dosage of 10 mg/L

Flotation of a cryptomelane bearing manganese ore containing goethite and limonite was studied by Sun and Morris using sodium oleate as a collector [59]. They found that in the presence of sodium silicate, tannic acid was less effective as an iron mineral depressant than sodium dihydrogen phosphate. Sun and Morris conducted their flotation tests between pH 8 and 9 [59]. This seems contradictory to the results of this study, as at pH 9 both sodium silicate and sodium dihydrogen phosphate seem to depress pyrolusite and float IOC. However the flotation system studied by Sun and Morris was much more complex, having several types of minerals and multiple depressants. Regardless, the findings shown in Figure 35B indicate that the combination of tannic acid and sodium oleate may selectively float pyrolusite from IOC between pH 9 and 11.

The effect of Mn^{2+} and Cu^{2+} ions on the micro-scale flotation of IOC and pyrolusite is shown in Figure 40. The addition of Cu^{2+} ions (Figure 40A), has the effect of completely depressing pyrolusite from pH 7 to 11. This behaviour is contrary to findings of Abeidu, who observed $CuSO_4$ to enhance pyrolusite flotation, with a peak recovery at pH 6-7.5 [8]. Recovery of IOC with Cu^{2+} is the opposite of flotation with only sodium oleate, as IOC is completely depressed

from pH 7-10, and nearly completely floated at pH 11. These results indicate that IOC could be selectively floated from pyrolusite at pH 11 using additions of CuSO_4 .

The effect of MnSO_4 addition on the flotation of IOC and pyrolusite is shown in Figure 40B. Recovery of IOC is strong from pH 7-10, and insignificant from pH 11-12. Pyrolusite recovery is half that of IOC at pH 9-10, but remains at ~50% at pH 11. Abeidu found that the recovery of pyrolusite was not significantly depressed by the addition of MnSO_4 , although peak recovery was shifted from pH 8 to 9, and the recovery peak became about 2 pH units narrower [8]. While the margins are not large, flotation of IOC is favored at pH 9 and 10, while pyrolusite flotation is favored at pH 11.

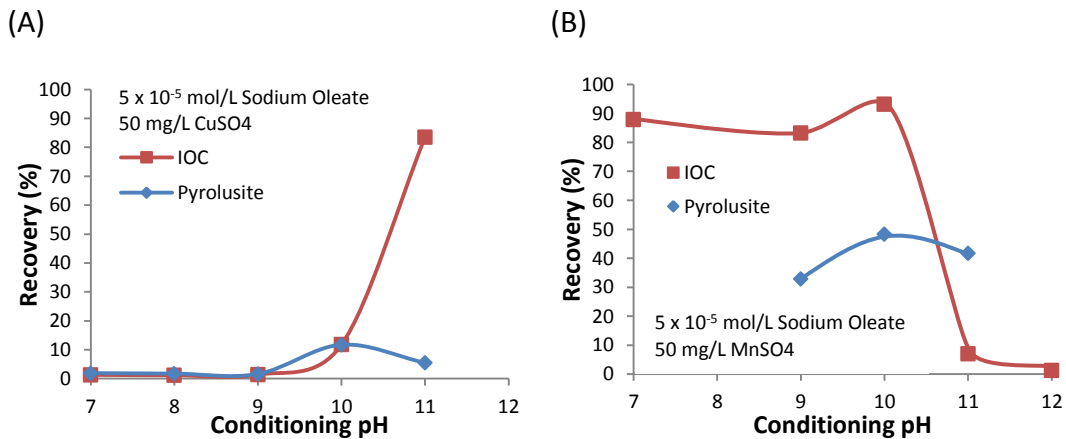


Figure 40: Micro-scale flotation recovery of pyrolusite and IOC as a function of pH at a sodium oleate dosage of 5×10^{-5} mol/L. (A) CuSO_4 dosage of 50 mg/L, and (B) MnSO_4 dosage of 50 mg/L

A summary of the promising conditions found for potential differential flotation of pyrolusite from IOC are shown below in Table 8. Reverse flotation conditions, where pyrolusite would be floated and IOC depressed, would be preferable since pyrolusite is a small component of the Wabush ore. Direct flotation conditions would float the iron oxide, while pyrolusite would be depressed.

Table 8: Potential conditions for differential flotation of pyrolusite and hematite

Reverse Flotation (Pyrolusite Flotation)	Direct Flotation (Pyrolusite Depression)
<ul style="list-style-type: none"> • sodium oleate, pH 11 • sodium oleate + sodium silicate, pH 10-11 • sodium oleate + tannic acid, pH 9-11 • sodium oleate + $MnSO_4$, pH 11 	<ul style="list-style-type: none"> • sodium oleate, pH 8 • sodium oleate + sodium silicate, pH 7-9 • sodium oleate + NaH_2PO_4, pH 7-9 • sodium oleate + potato starch, pH 7-9 • sodium oleate + $MnSO_4$, pH 7-10 • sodium oleate + $CuSO_4$, pH 11

6.3 Bench-Scale Flotation

Bench-scale flotation tests were conducted using Wabush spiral concentrate and a JK Tech 1.5 L bottom-drive flotation cell according to the procedure outlined in section 4.6. The promising conditions, shown in Table 8, for selective separation of pyrolusite and IOC found in micro-scale testing were used as starting points for bench-scale testing. As mentioned in the objectives section, the target of the bench-scale flotation tests is to achieve 90% mass pull with no more than 60% Mn recovery. Test parameters and metallurgical balances for each bench-scale flotation test are provided in Appendix I.

When presenting the bench-scale flotation data, Mn recovery is plotted as a function of mass pull into the rougher concentrate. This format provides a visual method for determining selectivity of the flotation test for Mn bearing minerals, or in this case pyrolusite. The entrainment line represents non-selectivity of the flotation test; every gram of material floated has the same composition as the feed. If pyrolusite is being selectively floated, or recovered, the trendline will be above the entrainment line. In the case of pyrolusite depression, or selective iron oxide flotation, the test trendline will be below the entrainment line.

6.3.1 Reverse Flotation

While favorable differential flotation conditions found from micro-scale flotation can be easily divided into reverse and direct flotation categories, flotation behaviour on a bench-scale with real ore turned out to be more complicated. Results of bench-scale flotation tests following the reverse flotation conditions shown in Table 8 are shown in Figure 41.

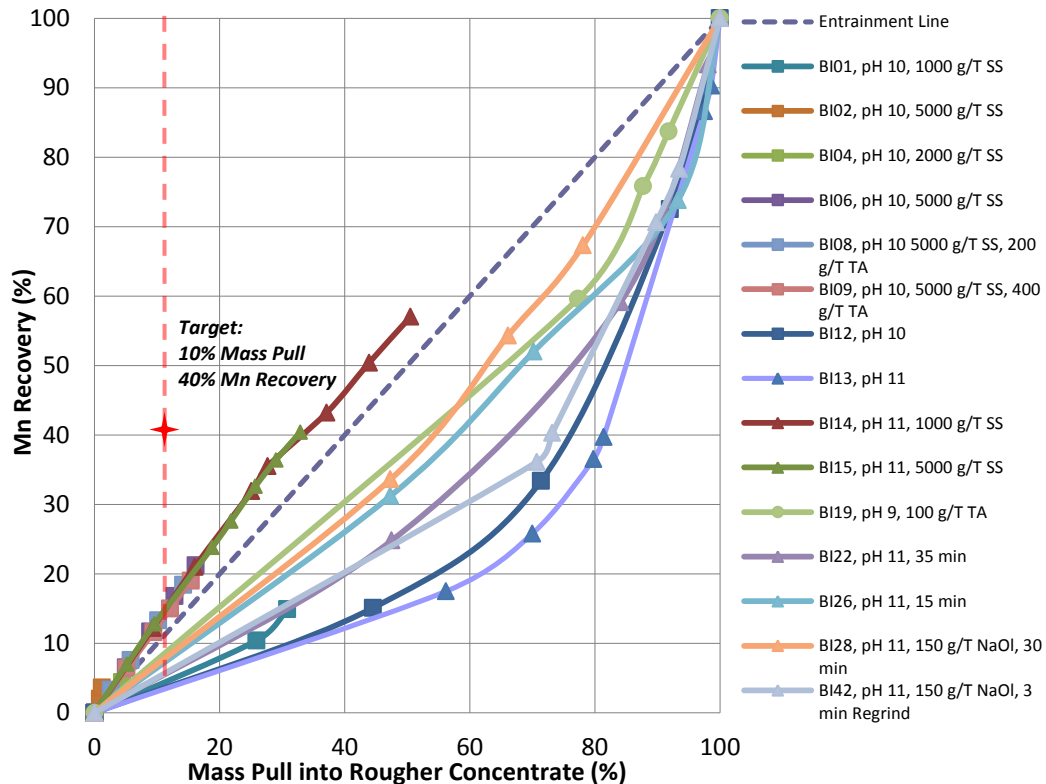


Figure 41: Mn Recovery vs. Mass pull for bench-scale flotation of Wabush spiral concentrate. Sodium oleate dosage (NaOI) is 200 g/T unless otherwise specified. Frother was DF-250, except for BI42 which used MIBC. BI01-BI05 were conducted with no grinding, while 25 minutes grinding was used in other tests unless otherwise specified. SS = sodium oleate, TA = tannic acid

Under reverse flotation conditions pyrolusite is selectively floated, so the Mn recovery curve will trend above the entrainment line when plotted as a function of mass pull. As shown in Figure 41, all test conditions which showed promise on

a micro-scale for selective reverse flotation of pyrolusite fell significantly short of the target, which in the case for reverse flotation is 10% mass pull and 40% Mn recovery. In fact many of the tests produced Mn recovery curves that trended well below the entrainment line, meaning hematite was being selectively collected. Due to the poor results for reverse flotation of the Wabush spiral concentrate on a bench-scale, direct flotation of the hematite became the focus. The bench-scale results will now be discussed in detail with an emphasis on achieving separation of pyrolusite via the direct flotation of hematite.

6.3.2 Effect of Grind Size

The first set of flotation experiments to be discussed in detail was conducted using various particle sizes and sodium oleate at pH 11. Results from these tests are shown in Figure 42.

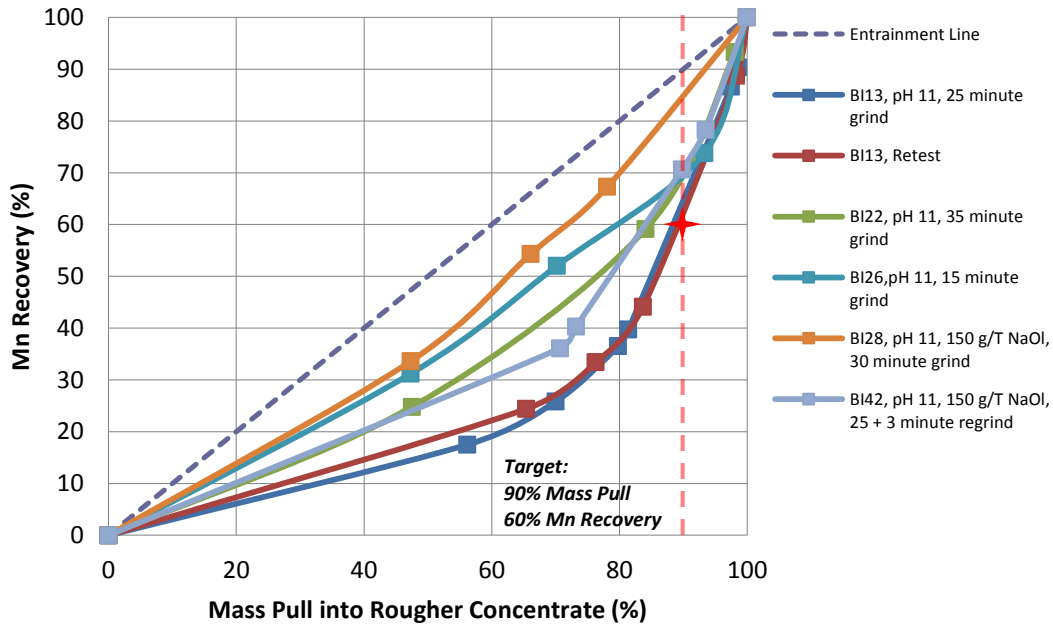


Figure 42: Mn Recovery vs. Mass pull for bench-scale flotation of Wabush spiral concentrate. Sodium oleate dosage (NaOl) is 200 g/T unless otherwise specified. Frother was DF-250, except for BI42 which used MIBC

Figure 42 shows Mn recovery as a function of grinding size for bench-scale flotation of the Wabush spiral concentrate at pH 11 using sodium oleate as a collector. All tests trend below the entrainment line, meaning pyrolusite is not being selectively floated in the concentrate, and tends to remain in the tails. This is opposite of what was predicted from the micro-scale flotation tests. Regardless, test BI13 comes close to the target of 90% mass pull, and 60% Mn recovery; achieving this target, but not exceeding it. The metallurgical balance for BI13 is shown in Table 9. Under these reagent conditions the optimum grinding time was 25 minutes of wet grinding, which produces an 80% passing size of 117 μm as shown in section 4.6.2. Test BI42 should have produced the same amount and grade of concentrate as BI13 up until the point of regrinding, but did not. With all other factors being the same, it seems that MIBC frother used for test BI42 was responsible for the decrease in selectivity, as BI13 and the other tests shown used DF250.

Table 9: Metallurgical balance for bench-scale flotation test BI13, the flotation of Wabush spiral concentrate at pH 11 using sodium oleate, at a grind size of 80% passing 117 μm .

Product	Solid Weight		Water Weight (g)	Assay (wt%)			Distribution (%)		
	(g)	(wt%)		Fe ₂ O ₃	MnO	SiO ₂	Fe ₂ O ₃	MnO	SiO ₂
Concentrate 1	323.3	65.4	296.2	96.90	1.35	1.27	70.2	24.4	17.5
Concentrate 2	53.6	10.8	109.9	92.20	3.02	3.91	11.1	9.0	8.9
Conc. 1+2	376.9	76.3	406.1	96.23	1.59	1.65	81.2	33.4	26.5
Concentrate 3	36.8	7.4	281.3	83.80	5.16	8.77	6.9	10.6	13.8
Conc. 1+2+3	413.7	83.7	687.4	95.13	1.91	2.28	88.1	44.1	40.2
Concentrate 4	71.9	14.5	1195.3	67.70	11.10	17.40	10.9	44.6	53.4
Conc. 1+2+3+4	485.6	98.3	1882.7	91.06	3.27	4.52	99.0	88.7	93.6
Tails	8.6	1.7	968.8	49.90	23.60	17.40	1.0	11.3	6.4
Total	494.2	100.0	2851.5	90.35	3.62	4.74	100.0	100.0	100.0

6.3.3 Effect of Sodium Silicate

The next set of flotation conditions discussed was conducted at pH 10-11 using sodium silicate, which according to the micro-scale flotation tests should selectively float pyrolusite. Results are shown in Figure 43. With the exception of test BI01 the addition of sodium silicate selectively floats pyrolusite, which is in agreement with the micro-scale flotation tests. Overall mass pull for tests BI01-BI05 was limited as without grinding a large fraction of the particles are too large for effective flotation. When sodium silicate is used, the degree of selectivity is fixed, regardless of sodium oleate dosage, sodium silicate dosage, and particle size. Although pyrolusite is selectively floated, the selectivity is not high enough to achieve the target. If pyrolusite is being floated rather than depressed, the target is 10% mass pull and 40% Mn recovery. Direct flotation of iron oxides, tests BI12 and BI13, is much more effective.

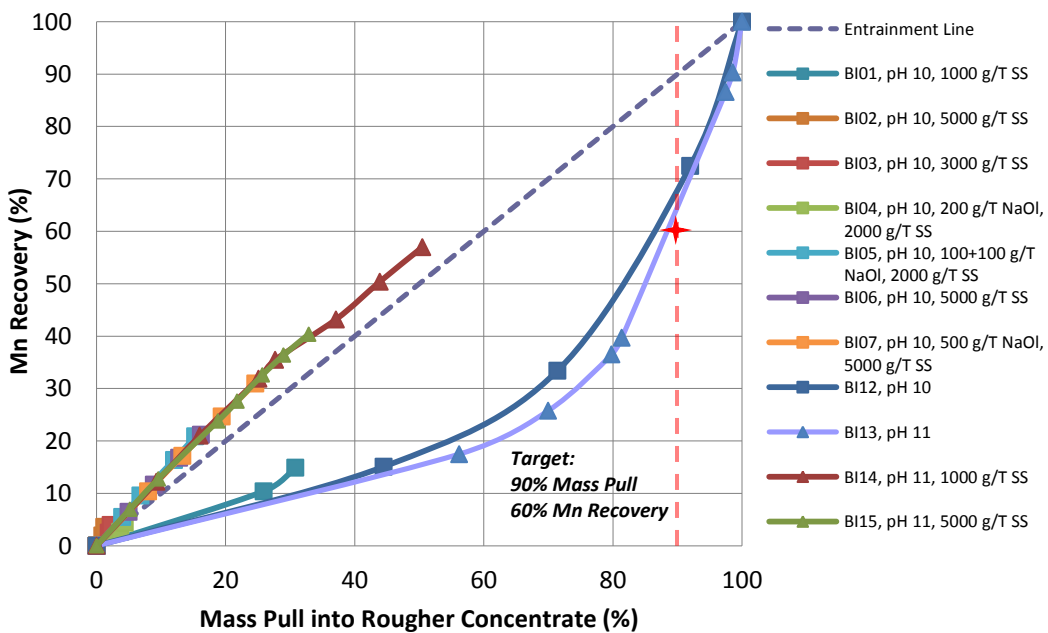


Figure 43: Mn Recovery vs. Mass pull for bench-scale flotation of Wabush spiral concentrate. Sodium oleate dosage (NaOI) is 200 g/T unless otherwise specified. BI01-BI05: no grinding, BI06-BI15: 25 minutes wet grinding, SS = sodium silicate

6.3.4 Complexing Agents and Cations

Figure 44 shows the results of additional tests conducted at pH 10 and 11. Citric acid was tested in conjunction with sodium silicate, as citric acid is known to be a surface cleaning agent [78]. Citric acid can form complexes with hydrolysable metal ions [78]. If hydrolysable metal ions are present on the pyrolusite surface and are interfering with sodium silicate and sodium oleate adsorption during flotation, citric acid may clean the surface enhancing selectivity. As shown in tests BI10 and BI11, citric acid had no effect on the recovery of pyrolusite in the presence of sodium silicate. Under similar conditions, BI08 and BI09, tannic acid was also tested with no apparent effect. According to micro-scale flotation results, the use of tannic acid at pH 11 without sodium silicate should result in the depression of iron oxides, and the flotation of pyrolusite. On a bench-scale, however, as shown by test BI16, iron oxides are selectively floated, albeit at a rate significantly lower than without tannic acid, BI13.

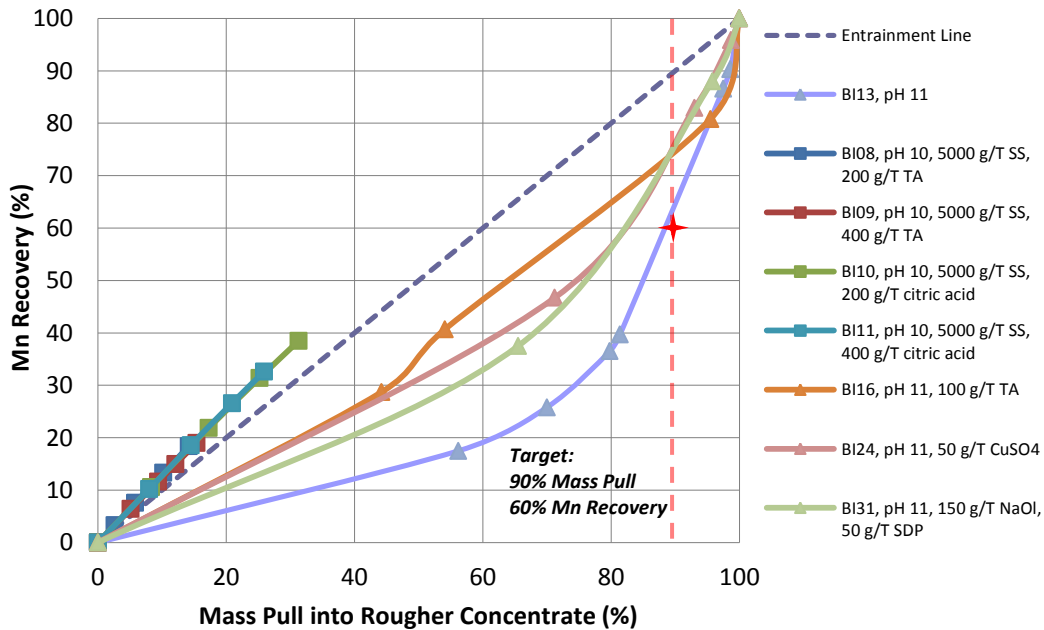


Figure 44: Mn Recovery vs. Mass pull for bench-scale flotation of Wabush spiral concentrate. Sodium oleate dosage (NaOI) is 200 g/T and wet grinding time was 25 minutes unless otherwise specified. SS = sodium silicate, SDP = sodium dihydrogen phosphate, TA = tannic acid

Also shown in Figure 44 are the effects of CuSO_4 and NaH_2PO_4 additions on bench-scale flotation at pH 11. In the case of CuSO_4 addition, as shown by test BI24, iron oxides are selectively floated which is in agreement with the micro-scale flotation results shown in Figure 40A. However, pyrolusite is not depressed to the degree suggested by the micro-scale results, since overall selectivity is decreased from the base condition of BI13. The addition of NaH_2PO_4 however, test BI31, has the effect of decreasing selectivity which is in agreement with the micro-scale flotation results, Figure 38B.

6.3.5 Effect of Potato Starch

The effects of potato starch on the flotation of Wabush ore are shown in Figure 45. Tests BI18 and BI21 are the baselines for flotation without potato starch at pH 9 and 8, respectively. Overall, the test that trended closest to the target was BI23, which was conducted at pH 9 with 250 g/T potato starch, 200 g/T sodium oleate, and used a 25 minute grinding time. BI41 used similar conditions as BI23, with a revised collection procedure and a regrind stage. The initial concentrates produced in test BI41 were of higher Fe grade than BI23; however, the addition of sodium oleate after regrinding decreased selectivity.

The metallurgical balance for BI23 is shown in Table 10. Note that the first concentrate contains only 0.87 wt% MnO and 0.80 wt% SiO_2 . After collection of the first concentrate, which accounts for nearly 60% of the initial mass, the Fe grade gradually decreases, while Mn content of the concentrate increases.

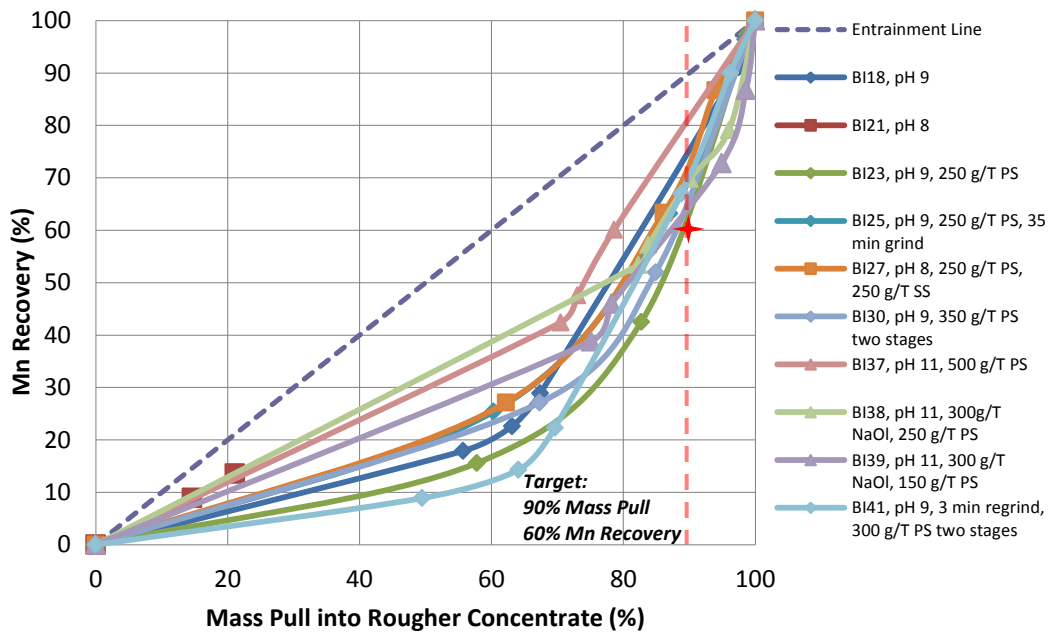


Figure 45: Mn Recovery vs. Mass pull for bench-scale flotation of Wabush spiral concentrate. Sodium oleate dosage (NaOl) is 200 g/T and wet grinding time was 25 minutes unless otherwise specified. PS = potato starch, SS = sodium silicate. Frother was DF-250, except for BI41 which used MIBC

Table 10: Metallurgical balance for bench-scale flotation test BI23, the flotation of Wabush spiral concentrate at pH 9 using sodium oleate and potato starch, at a grind size of 80% passing 117 μm .

Product	Solid Weight		Water Weight (g)	Assay (wt%)			Distribution (%)		
	(g)	(wt%)		Fe ₂ O ₃	MnO	SiO ₂	Fe ₂ O ₃	MnO	SiO ₂
Concentrate 1	288.3	57.8	234.8	97.80	0.87	0.80	62.1	15.6	11.4
Concentrate 2	124.4	24.9	380.8	91.10	3.44	3.35	25.0	26.8	20.6
Conc. 1+2	412.7	82.7	615.6	95.78	1.64	1.57	87.1	42.5	32.1
Concentrate 3	80.3	16.1	638.2	67.50	10.90	16.40	11.9	54.9	65.2
Conc. 1+2+3	493.0	98.8	1253.8	91.17	3.15	3.98	99.0	97.4	97.3
Tails	5.8	1.2	821.2	75.10	7.17	9.35	1.0	2.6	2.7
Total	498.8	100.0	2075.0	90.99	3.20	4.05	100.0	100.0	100.0

6.3.6 Silicate Flotation

An observation made of the assays of the bench-scale flotation results using sodium oleate as a collector was that Si bearing minerals seemed to be floating at the same rates as the Mn bearing minerals. This could mean that the Si bearing minerals were somehow physically associated with the Mn bearing minerals, or their flotation behaviour is similar simply due to the flotation chemistry using sodium oleate as a collector. To determine which case is true, three bench-scale flotation tests were conducted using typical parameters for quartz flotation from iron ores, as described in section 2.2.5. Test BI32 was conducted at pH 11, using sodium oleate as a collector, potato starch for hematite depression, and Ca^{2+} for quartz activation. BI33 was conducted at pH 7 using amine as a collector, and test BI35 was conducted at pH 10 using amine as a collector for quartz, and potato starch as a hematite depressant. Figure 46 shows Si mineral recovery as a function of Mn mineral recovery for tests BI32, BI33, and BI35 and compares the results to tests BI13 and BI23, which produced concentrates closest to the bench-scale flotation target.

As shown in Figure 46, the recovery curves for BI13 and BI23 trend closely to the entrainment line, meaning Si and Mn bearing minerals are being floated at nearly the same rates. Tests BI32 and BI33 also follow this trend. BI35, however, has a high selectivity for Si mineral flotation, achieving approximately 85% Si recovery overall, for a Mn recovery of only about 15%. Figure 47 shows the Si recovery as a function of mass pull to the rougher concentrate, which indicates that test BI35 effectively floated the Si minerals.

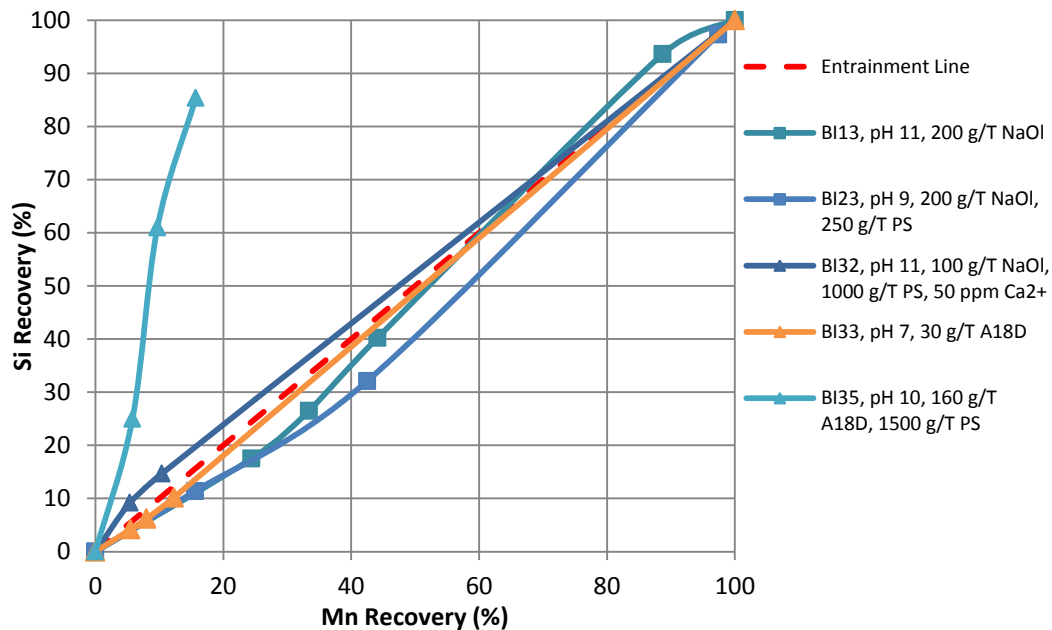


Figure 46: Si mineral recovery as a function of Mn mineral recovery for bench-scale flotation of Wabush spiral concentrate. Wet grinding for 25 minutes was used for all tests. NaOl = sodium oleate, A18D = Armeen 18D amine collector, PS = potato starch, and Ca^{2+} was added in the form of CaCl_2

Two important pieces of information can be drawn from Figure 47. The first is the fact that the Si and Mn bearing minerals in the Wabush spiral concentrate can be floated separately from each other, given the right flotation conditions. The second important conclusion is that the Si bearing minerals in the Wabush ore can be successfully removed using conventional flotation methods; in this case flotation at pH 10 using amine as a collector and potato starch as a hematite depressant. The metallurgical balance for BI35 is shown in Table 11. The tails of BI35, which is the iron concentrate, retains 87.0% of the original mass, and grades 94.2 wt% Fe_2O_3 , 3.26 wt% MnO, and 0.73 wt% SiO_2 compared to a feed composition of 90.33 wt% Fe_2O_3 , 3.36 wt% MnO, and 4.37 wt% SiO_2 . The Mn content changed minimally while 85% of the Si content was removed.

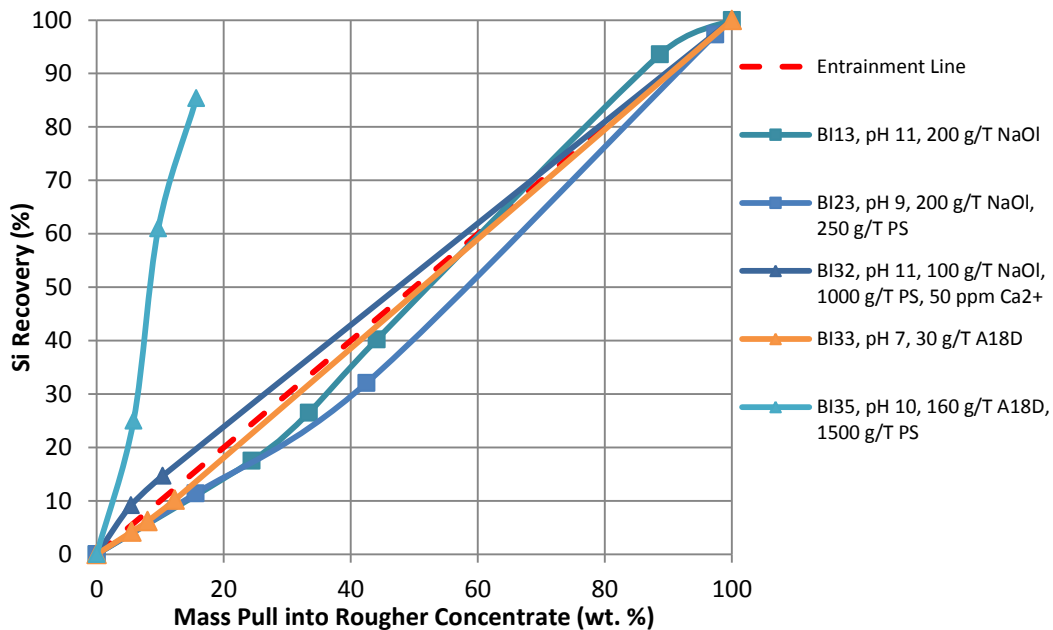


Figure 47: Si mineral recovery as a function of total rougher concentrate mass pull for bench-scale flotation of Wabush spiral concentrate. Wet grinding for 25 minutes was used for all tests. NaOl = sodium oleate, A18D = Armeen 18D amine collector, PS = potato starch, and Ca²⁺ was added in the form of CaCl₂

Table 11: Metallurgical balance for bench-scale flotation test BI35, the amine flotation of Si minerals from Wabush spiral concentrate, at a grind size of 80% passing 117 µm. Potato starch was used to depress iron oxide.

Product	Solid Weight		Water Weight (g)	Assay (wt%)			Distribution (%)		
	(g)	(wt%)		Fe ₂ O ₃	MnO	SiO ₂	Fe ₂ O ₃	MnO	SiO ₂
Concentrate 1	22.6	4.6	317.0	68.80	4.28	23.80	3.5	5.8	25.0
Concentrate 2	19.3	3.9	229.9	54.80	3.34	40.00	2.4	3.9	35.9
Conc. 1+2	41.9	8.5	546.9	62.35	3.85	31.26	5.9	9.7	61.0
Concentrate 3	22.0	4.5	202.5	68.40	4.46	23.90	3.4	5.9	24.5
Conc. 1+2+3	63.9	13.0	749.4	64.43	4.06	28.73	9.3	15.7	85.4
Tails	428.2	87.0	827.0	94.20	3.26	0.73	90.7	84.3	14.6
Total	492.1	100.0	1576.4	90.33	3.36	4.37	100.0	100.0	100.0

6.3.7 *Micro and Bench-Scale Flotation Correlation*

The two bench-scale flotation tests that came closest to achieving the target of 90% mass pull with maximum 60% Mn recovery were tests BI13 and BI23. The results of test BI23 agree with the predictions made from micro-scale experiments; at pH 9 using sodium oleate and potato starch pyrolusite should be depressed and hematite should be floated, as shown in Figure 39A. Test BI13, however, does not agree with the initial predictions made from the micro-scale flotation results, which are shown in Figure 36. At pH 11 using only sodium oleate, pyrolusite should float strongly while hematite should be depressed, yet the results of BI13 show strong hematite recovery and pyrolusite depression. One reason for this discrepancy was found in the micro-scale flotation procedure.

In micro-scale flotation tests, the pyrolusite sample had a particle size of -106+38 μm , while the IOC had not undergone grinding and had a size distribution of 80% passing 365 μm , much coarser than the pyrolusite sample. Additional flotation tests were conducted at pH 11 using ground IOC having a size range of -106+38 μm , with the results shown in Figure 48.

The result of decreasing the particle size range of the IOC was increased recovery at pH 11. While the magnitude of the recovery for the finer IOC is still only half that of the pyrolusite, the fact that it is 50% as opposed to 10% for the coarse IOC indicates that flotation of hematite at this pH is largely dependent on particle size. This explains why hematite is floatable on a bench-scale at pH 11. The question of why the pyrolusite is poor floating on a bench-scale at pH 11 will be investigated further through the mineral-reagent interaction mechanism study.

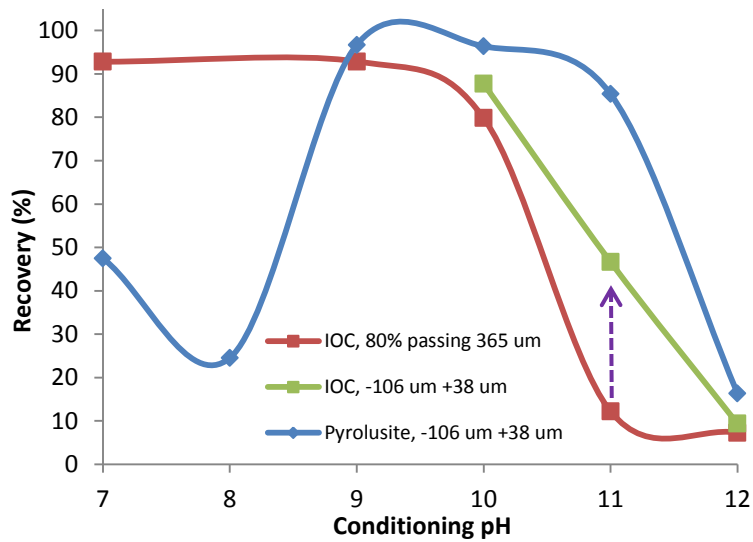


Figure 48: Recovery as a function of pH and grind size for the micro-scale flotation of IOC and pyrolusite at a sodium oleate dosage of 5×10^{-5} mol/L

6.4 Mineral-Reagent Interaction Mechanism Study: FTIR

In order to determine the mechanism of oleate adsorption on hematite (IOC) and pyrolusite, FTIR was used on pure mineral samples as described in Sections 4.7.2 and 4.7.3. The IOC or pyrolusite sample was conditioned in a 1.0×10^{-3} mol/L solution of sodium oleate at pH 7 and 11. The pH values of 7 and 11 were chosen because the most selective bench-scale flotation test using only sodium oleate, BI13, was conducted at pH 11. An in-depth investigation of the adsorption of sodium laurate on hematite was conducted at pH 7 by Chernyshova et al [65], using FTIR and XPS; pH 7 was, therefore, used as a baseline for comparison. No comparative studies had been found investigating the adsorption of fatty acids on Mn oxides.

FTIR (DRIFTS) spectrometry was carried out on samples of pure hematite and pyrolusite, as described in section 4.7.2. Figure 49 shows the FTIR spectra of solid sodium oleate in comparison to hematite and pyrolusite conditioned at pH 7 with 1.0×10^{-3} mol/L sodium oleate. Absorption spectra from two primary groups

will be present due to the adsorption of sodium oleate; $-\text{CH}_2-$ groups of the hydrocarbon tail, and $-\text{COO}$ from the carboxylic acid head group. As discussed by Socrates, due to the much higher concentration of $-\text{CH}_2-$ groups in the saturated C_{18} chain of sodium oleate, their signals are expected to be dominant in the range of $1400 - 1500 \text{ cm}^{-1}$ in comparison to the $-\text{CH}_3$ and $-\text{CH}=\text{CH}-$ groups [73]. Bands from the carboxyl groups are generally of medium to strong intensity, with the carbonyl group, $\text{C}=\text{O}$, appearing in the $1700\text{-}1725 \text{ cm}^{-1}$ region, while asymmetric and symmetric vibrations of carboxylic acid salts appear in the $1520\text{-}1610 \text{ cm}^{-1}$ and $1335\text{-}1435 \text{ cm}^{-1}$ regions, respectively [65–70, 72–74, 80].

In Figure 49A there are two primary regions of spectral features; $1800\text{-}1200 \text{ cm}^{-1}$, and $3000\text{-}2800 \text{ cm}^{-1}$. Bands in the $3000\text{-}2800 \text{ cm}^{-1}$ region are due to the stretching vibrations of the CH_2 and CH_3 groups. The primary peaks at 2920 and 2850 cm^{-1} are assigned to $\nu_{\text{as}}\text{CH}_2$ and $\nu_{\text{s}}\text{CH}_2$, respectively, while the much weaker peaks at 2955 and 2880 cm^{-1} are assigned to $\nu_{\text{as}}\text{CH}_3$ and $\nu_{\text{s}}\text{CH}_3$, respectively. The νCH_3 features are somewhat shrouded in the sodium oleate and hematite spectra due to the strong intensity of the νCH_2 peaks. The observance of these peaks is in agreement with values found in Table 3. While the observance of these peaks on the pyrolusite and hematite indicates the presence of adsorbed sodium oleate, it does not provide any information as to the nature of the adsorption. In order to glean information about the adsorption of the carboxyl group of the sodium oleate, the region of $1800\text{-}1200 \text{ cm}^{-1}$ was analysed in greater detail, as shown in Figure 49B.

Important features indicated in Figure 49B can be classified into three primary groups: bands due to physically bound carboxylic acid, bands due to chemically bound carboxylic acid, and bands due to deformation of the hydrocarbon tail.

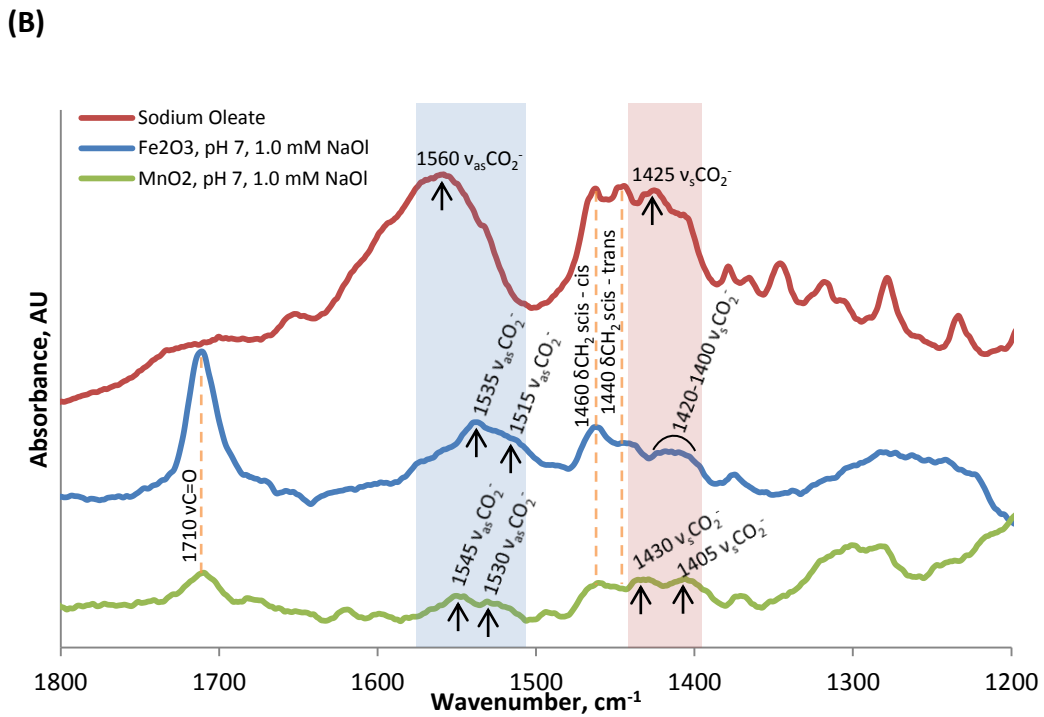
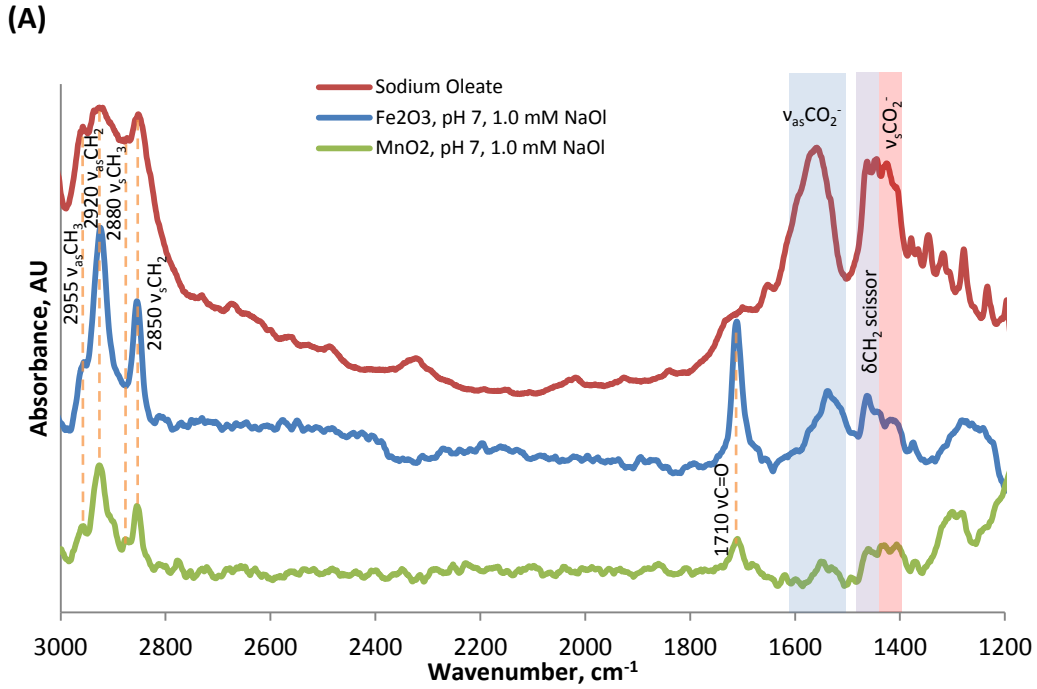


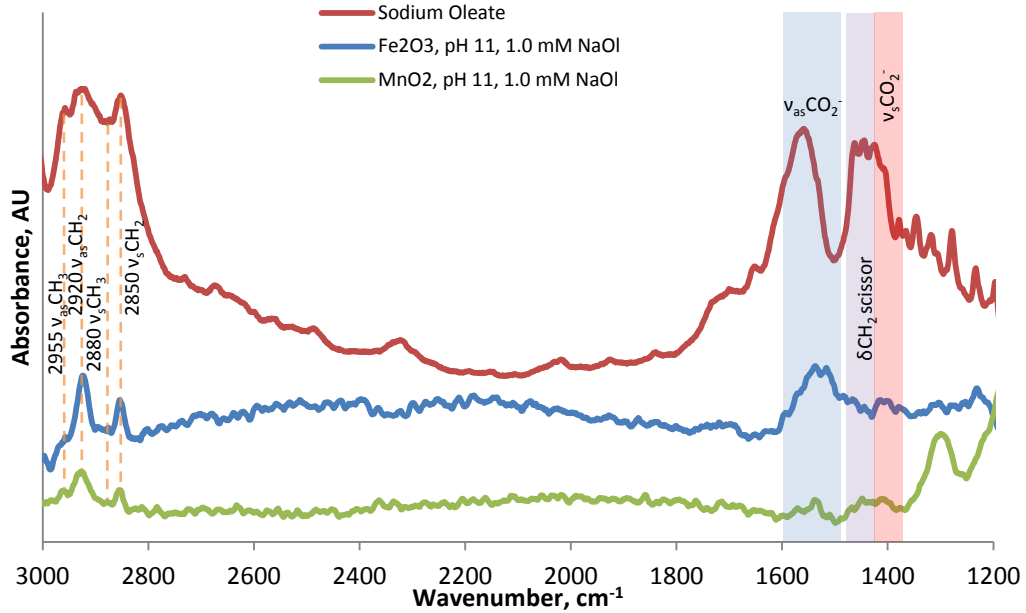
Figure 49: (A) FTIR (DRIFTS) spectra of solid sodium oleate in comparison to Fe_2O_3 (IOC) and MnO_2 (pyrolusite) conditioned in 1.0×10^{-3} mol/L sodium oleate solution at pH 7 over a range of 1200 – 3000 cm^{-1} ; (B) the same conditions as (A) with a spectral range of 1200 – 1800 cm^{-1}

The band at 1710 cm^{-1} on the hematite and pyrolusite spectra indicates the presence of the carbonyl mode (C=O) of oleic acid ($\text{C}_{17}\text{H}_{33}\text{COOH}$), and is generally considered to indicate physically adsorbed species [66, 71, 72]. For the presence of this band, the carboxyl group must be protonated, or in its $-\text{COOH}$ form. This feature is not present in the spectra of solid sodium oleate ($\text{C}_{17}\text{H}_{33}\text{COO}^-\text{Na}^+$), as the carboxyl group is in a salt form and observed as νCO_2^- vibrations; this has been shown true in the case of sodium laurate and lauric acid by Chernyshova et al [65]. As pH 7 is above the PZC for hematite (pH 6.5) and pyrolusite (pH 5.0), both minerals will carry a negative charge in solution, with pyrolusite being slightly more negative than hematite as indicated in Figure 34 and Figure 35. Since sodium oleate will either be present as neutral oleic acid or as a negatively charged acid soap complex at pH 7 [25], and both minerals exhibit negative zeta potentials, it could be argued that physical adsorption should not occur.

Evidence for this bond to be physically adsorbed can be found by comparing Figure 49 to Figure 50, which is the FTIR spectra of hematite and pyrolusite conditioned with 1.0×10^{-3} mol/L sodium oleate at pH 11. The prominent difference between the spectra of both hematite and pyrolusite conditioned at pH 7 and 11 is the absence of the carbonyl peak at 1710 cm^{-1} . The dissociation of oleic acid, $\text{HOI}_{(\text{aq})} = \text{H}^+ + \text{OI}^-$, has a pKa of 4.95 [25]. Given the same initial oleate concentration, at pH 11 the fraction of oleate present as neutral oleic acid will be drastically lower than at pH 7, and most of the oleate will be present as negatively charged species. At pH 7 the combination of relatively high neutral oleic acid concentration and low magnitude negative surface charge of the minerals allows for the physical adsorption of neutral oleic acid to the remaining positively charged surface sites on the mineral surfaces. At pH 11 the concentration of neutral oleic acid is drastically reduced, and the magnitude of the negative surface charge on both hematite and pyrolusite is greatly increased,

effectively preventing the physical adsorption of any oleic acid as shown by the absence of the carbonyl peak at 1710 cm^{-1} on either mineral at pH 11.

(A)



(B)

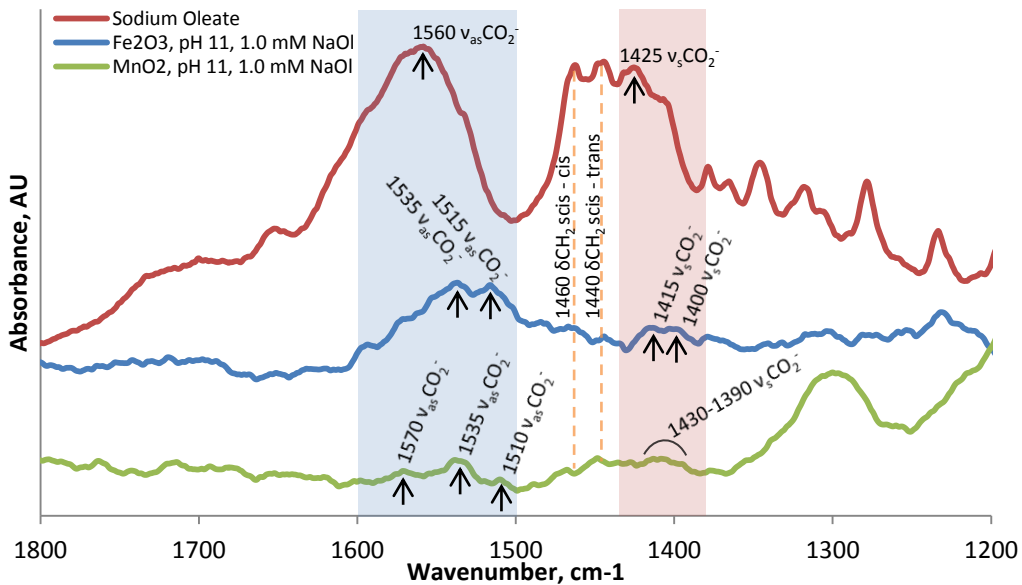


Figure 50: (A) FTIR (DRIFTS) spectra of solid sodium oleate in comparison to Fe_2O_3 (IOC) and MnO_2 (pyrolusite) conditioned in 1.0×10^{-3} mol/L sodium oleate solution at pH 11 over a range of $1200 - 3000\text{ cm}^{-1}$; (B) the same conditions as (A) with a spectral range of $1200 - 1800\text{ cm}^{-1}$

Two peaks common to each spectrum shown in Figure 49 and Figure 50 are the δCH_2 scissor bending modes at 1460 and 1440 cm^{-1} . These values are in agreement with reference values for methylene bending [73, 74]. Hayashi showed that fatty acids can exhibit both cis and trans configurations of the $\text{C}_\beta\text{-C}_\alpha\text{-C=O}$ group, and that for C18 compounds the trans configuration is the lower energy form [79]. With this in mind the higher energy peak at 1460 cm^{-1} was assigned to the δCH_2 scissor – cis mode, while the lower energy 1440 cm^{-1} peak was assigned to the δCH_2 scissor – trans mode.

Additional charts used for FTIR spectra comparison can be found in Appendix VI. A summary of the bands identified in Figure 49 and Figure 50 is shown in Table 12. It can be noted that bands due to methyl and methylene groups of the oleate hydrocarbon chain have a constant wavelength under all conditions. However, variation can be seen in wavelengths for bands due to the CO_2^- carboxylate mode of carboxylic acid. In previous studies of fatty acid adsorption on iron oxides, these bands have been used as evidence for chemical adsorption, as well as bonding mode [65–67, 69].

Considering first hematite at pH 7, CO_2^- bands are observed at 1535, 1515, and 1410 cm^{-1} . The peak at 1410 cm^{-1} is broad, and by comparing Figure 49B to Figure 50B, it is apparent that it is composed of two components. The peaks at 1535 and 1515 cm^{-1} are assigned to $\nu_{\text{as}}\text{CO}_2^-$ modes, while the peaks in the 1400–1425 range are assigned to the $\nu_{\text{s}}\text{CO}_2^-$ mode. While the degree of band splitting (Δ) between the asymmetric and symmetric νCO_2^- modes can be used as an indicator for bonding mode [67], it can also be invalidated by vibrational couplings of the carboxylate groups [65]. In the study of laurate adsorption on hematite, Cheryshova et al observed $\nu_{\text{as}}\text{CO}_2^-/\nu_{\text{s}}\text{CO}_2^-$ pairs at 1545/1410 cm^{-1} , and at 1530/1425 cm^{-1} [65]. The 1545/1420 cm^{-1} pair was assigned to inner-sphere monodentate mononuclear (ISMM) bonding, while the 1530/1425 pair was assigned to open-sphere (OS) surface hydration-shared bonding [65].

Table 12: Summary of FTIR band assignments for solid sodium oleate as well as hematite (Fe₂O₃) and pyrolusite (MnO₂) conditioned in 1.0 x 10⁻³ mol/L sodium oleate solution at pH 7 and 11

Sample	Band Assignment	Wavelength (cm ⁻¹)	
		pH 7	pH 11
Fe ₂ O ₃	$\nu_{as}CH_3, \nu_sCH_3$	2955, 2880	2955, 2880
	$\nu_{as}CH_2, \nu_sCH_2$	2920, 2850	2920, 2850
	$\nu C=O$	1710	NA
	$\nu_{as}CO_2^-$	1535, 1515	1535, 1515
	δCH_2 , scissor bending cis & trans	1460, 1440	1460, 1440
	$\nu_sCO_2^-$	1420-1400	1415, 1400
MnO ₂	$\nu_{as}CH_3, \nu_sCH_3$	2955, 2880	2955, 2880
	$\nu_{as}CH_2, \nu_sCH_2$	2920, 2850	2920, 2850
	$\nu C=O$	1710	NA
	$\nu_{as}CO_2^-$	NA	1570
	$\nu_{as}CO_2^-$	1545,	1535, 1510
	δCH_2 , scissor bending cis & trans	1530,	1460, 1440
	$\nu_sCO_2^-$	1460, 1440 1430, 1405	1430-1390
Sodium Oleate	$\nu_{as}CH_3, \nu_sCH_3$	2955, 2880	
	$\nu_{as}CH_2, \nu_sCH_2$	2920, 2850	
	$\nu C=O$	NA	
	$\nu_{as}CO_2^-$	1560	
	δCH_2 , scissor bending cis & trans	1460, 1440	
	$\nu_sCO_2^-$	1425	

In the absence of more detailed analysis, the mode of the oleate CO₂⁻ group bonding to hematite cannot be confirmed on $\nu_{as}CO_2^-/\nu_sCO_2^-$ wavenumbers alone. However, by comparison to previous works [65], it seems likely that the $\nu_{as}CO_2^-/\nu_sCO_2^-$ pairs in this study are 1535/1400 cm⁻¹ and 1515/1415 cm⁻¹ for adsorption on hematite. While the symmetric vibration wavelength may have changed slightly from pH 7 to 11, the asymmetric vibrations appear constant. By comparison these pairs can be assigned to ISMM and OS surface hydration-shared bonding modes, respectively. But while the frequency of the asymmetric vibrations did not change with increasing pH, the intensity of each band did, with

the 1515 cm^{-1} band increasing to equal intensity of the 1535 cm^{-1} band. With this in mind, chemical adsorption of oleate on hematite shifts from predominately ISMM at pH 7, to a mixture of ISMM and OS surface hydration-shared at pH 11.

Similar to the hematite spectra, at pH 7 pyrolusite spectra exhibits two unique vCO_2^- bands. For hematite the $\text{v}_{\text{as}}\text{CO}_2^-$ bands were constant at 1535 and 1515 cm^{-1} at both pH 7 and 11, while in the case of pyrolusite these bands change with an increase in pH. At pH 7 $\text{v}_{\text{as}}\text{CO}_2^-$ bands appear at 1545 and 1530 cm^{-1} , while at pH 11 three bands are apparent at 1570, 1535, and 1510 cm^{-1} . The band at 1570 cm^{-1} is apparent when analyzing the pyrolusite spectra in greater detail using Figure 51. Changes to the v_sCO_2^- are somewhat more ambiguous as at pH 7 there are two strong peaks at 1430 and 1405 cm^{-1} , but at pH 11 there is a single broad feature from 1390-1420 cm^{-1} , with minor features at 1430 cm^{-1} . This is likely due to contributions from each different bonding mode.

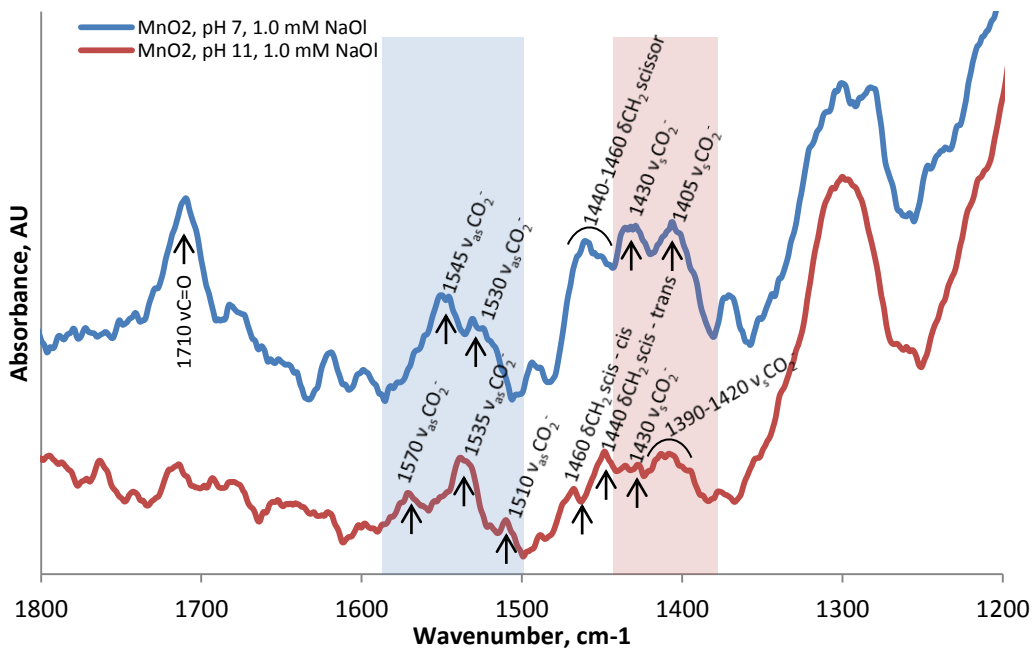


Figure 51: FTIR (DRIFTS) spectra of MnO_2 (pyrolusite) conditioned in 1.0×10^{-3} mol/L sodium oleate solution at pH 7 and 11 over a range of 1200 – 1800 cm^{-1}

By analysis of Figure 51 the $\nu_{\text{as}}\text{CO}_2^-/\nu_{\text{s}}\text{CO}_2^-$ pairs for pyrolusite at pH 7 are likely 1545/1430 cm^{-1} and 1530/1405 cm^{-1} . The pair of 1530/1405 cm^{-1} is comparable to the 1535/1400 cm^{-1} $\nu_{\text{as}}\text{CO}_2^-/\nu_{\text{s}}\text{CO}_2^-$ pair for the ISMM mode of oleate adsorption on hematite. The bonding mode of the 1545/1430 cm^{-1} pair is uncertain without further investigation, as there are no direct comparisons.

ISMM bonding appears to become dominant on pyrolusite when the pH is increased to 11, as the dominant $\nu_{\text{as}}\text{CO}_2^-$ peak is 1535 cm^{-1} , as opposed to 1545 cm^{-1} at pH 7. Also with the increase in pH to 11, the 1545/1430 cm^{-1} pair diminishes and gives rise to $\nu_{\text{as}}\text{CO}_2^-$ peaks at 1570 and 1510 cm^{-1} . The broadening of the 1390-1420 cm^{-1} peak implies multiple peak contributions. At pH 11 the $\nu_{\text{as}}\text{CO}_2^-/\nu_{\text{s}}\text{CO}_2^-$ pairs appear to be 1570/1430, 1535/~1405, 1510/~1415 cm^{-1} . The 1510/1415 pair is similar to the 1515/1415 pair observed on hematite and can be assigned to the OS surface hydration–shared complex. The 1570 cm^{-1} feature may be the shifted 1545 $\nu_{\text{as}}\text{CO}_2^-$ band observed at pH 7, or an entirely new bonding mode. In the FTIR study of oleate adsorption on hematite, Gong et al observed $\nu_{\text{as}}\text{CO}_2^-$ peaks at 1580 and 1518 cm^{-1} , and assigned them to ISBB and chelating bidentate bonding, respectively [71]. With this in mind the $\nu_{\text{as}}\text{CO}_2^-$ band at 1570 cm^{-1} is assigned to an ISBB structure.

The selectivity of hematite over pyrolusite in bench flotation using sodium oleate at pH 11 may be a result of the differences in bonding modes observed with FTIR. In the case of hematite at pH 11, oleate is adsorbed in a mixture of ISMM and OS surface hydration-shared modes. In the case of pyrolusite at pH 11, ISMM is the primary mode, with contributions of OS surface hydration-shared and ISBB modes. Neither mineral showed signs of physically adsorbed oleate at pH 11. Monodentate bonding modes are generally more common than bidentate modes in the case of smaller molecules (oleate would be considered small in relation to most proteins) [81]. As discussed by Dudev and Lim, the mode of carboxylate to metal bonding depends on (i) the immediate neighbors of the

carboxylate group (the hydrocarbon chain in the case of oleate), (ii) the type of metal and its coordination, (iii) the total charge of the metal complex, and (iv) the relative exposure of the metal binding site to solvent [81].

Considering solution chemistry as constant for the testing of pyrolusite and hematite, metal coordination and charge must be the determining factors of bonding mode. For bidentate bonding to occur rather than monodentate, interaction of the second oxygen of the carboxylate group with the metal cation must be preferred over interaction with the surrounding ligands [81]. The presence of ISBB bonding of oleate on pyrolusite and not hematite indicates that Mn^{4+} in pyrolusite is better able to accept charge from the second carboxylate oxygen than Fe^{3+} in hematite [81]. Pyrolusite and hematite both have unique crystal structures, with pyrolusite being composed of tetragonal coordinated Mn^{4+} [44], and hematite being composed of Fe^{3+} coordinated in a trigonal rhombohedral system [82]. Although both Fe^{3+} and Mn^{4+} share a coordination number of 6 in hematite and pyrolusite, respectively, the difference in crystal structure between the two minerals likely leads to differences in ligand cation interactions, and the ability of either cation to attract the second carboxylate oxygen.

While bonding mode does not inherently explain differences in the overall selectivity of oleate between hematite and pyrolusite, selectivity can be explained by relative adsorption density. At both pH 7 and 11, the intensity of adsorbed oleate bands are consistently weaker on pyrolusite than on hematite. This can imply that sodium oleate has a higher affinity for adsorption on hematite than pyrolusite. If this is indeed the case, then for a mixture of hematite and pyrolusite in a sodium oleate solution of limited concentration, the oleate may preferentially adsorb on the hematite first, or at higher density. Additional oleate added to the system will eventually result in complete coverage of both minerals.

This concept is similar to the results for test BI13. The initial limited amount of sodium oleate added to the flotation pulp is preferentially adsorbed on the hematite, which is also present in a much greater quantity than the pyrolusite, 90% vs. 4%. As the initial quantity of sodium oleate is adsorbed primarily on the hematite, the initial concentrates are high grade hematite. With the bulk of the hematite removed in the initial concentrates, subsequent additions of sodium oleate are adsorbed on all the remaining minerals and selectivity is drastically reduced or reversed.

7. Conclusions and Recommendations

7.1 General Findings

Due to the challenges faced by the Wabush mine, the feasibility of separating pyrolusite from hematite using froth flotation was investigated. Following an extensive literature review, pure single mineral micro-scale flotation testing was carried out using sodium oleate as a collector in conjunction with various reagents identified in the literature as potentially producing conditions for selective flotation of pyrolusite and hematite. These reagents included sodium silicate, sodium dihydrogen phosphate, potato starch, tannic acid, copper (II) sulphate, and manganese (II) sulphate. Several potential separation windows were identified, and are listed below:

Pyrolusite Flotation (Reverse Flotation):

- Sodium oleate, pH 11
- Sodium oleate + sodium silicate, pH 10-11
- Sodium oleate + tannic acid, pH 9-11
- Sodium oleate + MnSO_4 , pH 11

Hematite Flotation (Direct Flotation):

- Sodium oleate, pH 8
- Sodium oleate + sodium silicate, pH 7-9
- Sodium oleate + NaH_2PO_4 , pH 7-9
- Sodium oleate + potato starch, pH 7-9
- Sodium oleate + MnSO_4 , pH 7-10
- Sodium oleate + CuSO_4 , pH 11

The effectiveness of the conditions listed above was tested on a bench-scale using Wabush spiral concentrate, which graded 93.38 wt% Fe_2O_3 , 2.71 wt% MnO, and 2.63 wt% SiO_2 , and primarily consisted of the minerals hematite, pyrolusite, and quartz. With pyrolusite being a minor component of the spiral concentrate, reverse flotation, or flotation of the pyrolusite, was the initial focus. While micro-scale testing showed promise for reverse flotation of pyrolusite, on a bench-scale

adequate reverse flotation could not be produced. Direct flotation conditions, however, were able to produce concentrates which reached the target values of 60% Mn recovery at 90% mass pull. Two test conditions were able to reach the target; the first being test BI13, which was conducted at pH 11 using 200 g/T sodium oleate at an 80% passing size of 117 μm . The second test to meet the target was BI23, which was conducted at pH 9, using 200 g/t sodium oleate and 250 g/T potato starch, and also having an 80% passing size of 117 μm .

Mineralogical studies conducted on the Wabush spiral concentrate and bench flotation products found that pyrolusite particles were ~50% liberated from hematite particles in the spiral concentrate bulk sample. Considering the reduction in particle size from 80% passing 365 μm to 117 μm for tests BI13 and BI23, liberation is not a limiting factor in pyrolusite separation. However, the nature of the pyrolusite composition as observed by the mineralogical studies may play a role. While hematite particles were consistently found to be liberated and composed of only Fe and O, pyrolusite particles were found to be of more varied composition, often containing significant amounts of Fe, K, and Ba in solution. While the varied composition may have had an effect on flotation selectivity, the morphology of the manganese bearing minerals was confirmed as being pyrolusite using XRD.

The mechanism of sodium oleate adsorption on pyrolusite and hematite was investigated using zeta potential and FTIR measurements. Pyrolusite and hematite were found to have PZC values of pH 4.6 and 6.5, respectively, which is consistent with values cited in the literature. FTIR measurements showed sodium oleate to be both physically and chemically adsorbed to both pyrolusite and hematite at pH 7, while at pH 11 only chemical adsorption was observed on either mineral. One of the factors responsible for selective flotation of hematite on a bench-scale at pH 11 was the difference in bonding mode of oleate. At pH

11, oleate was found to adsorb on hematite in a mixture of ISMM and OS surface hydration-shared modes, while on pyrolusite adsorption was found to be primarily ISMM, with contributions of OS surface hydration-shared and ISBB modes. Differences in bonding mode were attributed to the different crystal structures of hematite and pyrolusite, which affects the ability of the metal cations to bond with both oxygen atoms of the carboxylate group.

Another important observation was the intensity of oleate adsorption on hematite and pyrolusite in general. Adsorption bands of sodium oleate species were found to be of higher intensity in the FTIR spectra of hematite at both pH 7 and 11 when compared to pyrolusite. With this in mind it appears oleate has a higher affinity for adsorption on hematite over pyrolusite. This is supported by zeta potential measurements, which show that at a sodium oleate concentration of 2.5×10^{-6} mol/L, significant shifting occurs in the PZC of hematite, while the PZC of pyrolusite is unchanged.

7.2 Recommendations for Future Work

With the advances and innovation occurring in the field of mineral flotation, it is inevitable that new collectors and modifying reagents will be discovered that will be effective in the separation of pyrolusite and hematite. However, building on current research, the following two key areas would be logical routes of investigation

- 1) Studies of adsorption and bonding mode of oleate on hematite and pyrolusite with and without the addition of supplementary reagents such as potato starch.
- 2) Optimization of the bench-scale flotation procedures in the areas of grind size, pulp density, air flow, and reagent dosages.

8. References

- [1] C. N. Resources, "STEEL STARTS HERE," *America*. Cliffs Natural Resources, Cleveland, 2011.
- [2] G. Farquharson and H. Thalenhorst, "WABUSH MINES REVIEW OF SCULLY MINE RESERVES," Toronto, 2006.
- [3] B. Damjanovic and J. R. Goode, "Cleveland Cliffs-Wabush Mines," *Canadian Milling Practice*, no. Special Volume 49, 2000.
- [4] R. J. S. Lewis, "Pyrolusite," *Hawley's Condensed Chemical Dictionary*. John Wiley & Sons, p. 1063, 2007.
- [5] R. J. S. Lewis, "Hematite, red," *Hawley's Condensed Chemical Dictionary*. John Wiley & Sons, p. 636, 2007.
- [6] T. A. Bibawy and A. A. Yousef, "Flotation Behaviour of Hematite," *Tenside Detergents*, vol. 19, no. 1, pp. 18-22, 1982.
- [7] M. C. Fuerstenau and D. A. Rice, "Flotation Characteristics of Pyrolusite," *Society of Mining Engineers of AIME, Transactions*, vol. 241, no. 4, pp. 453-457, 1968.
- [8] E. Abeidu, A.M.(Laboratory of Metallurgy, National Research Center, "The Feasibility of Activation of Manganese Minerals Flotation," *Transactions of the Japan Institute of Metals*, vol. 14, no. 1, pp. 45-49, 1973.
- [9] B. A. Wills, "Froth Flotation," in *Mineral Processing Technology*, Sixth., Butterworth-Heinemann, 1997, pp. 258-341.
- [10] K. N. Han, T. W. Healy, and D. W. Fuerstenau, "The Mechanism of Adsorption of Fatty Acids and Other Surfactants at the Oxide-Water Interface," *Journal of Colloid and Interface Science*, vol. 44, no. 3, pp. 407-414, Sep. 1973.
- [11] G. A. Parks, "The Isoelectric Points of Solid Oxides, Solid Hydroxides, and Aqueous Hydroxo Complex Systems," *Chemical Reviews*, vol. 65, no. 2, pp. 177-198, 1965.
- [12] R. D. Kulkarni and P. Somasundaran, "Flotation Chemistry of Hematite/Oleate System," *Colloids and Surfaces*, vol. 1, no. 3-4, pp. 387-405, 1980.
- [13] K. B. Quast, "A Review of Hematite Flotation Using 12-Carbon Chain Collectors," *Minerals Engineering*, vol. 13, no. 13, pp. 1361-1376, Nov. 2000.
- [14] M. Kosmulski, *Chemical Properties of Mineral Surfaces*. New York: Marcel Dekker, 2001.
- [15] I. dos Santos and J. Oliveira, "Utilization of Humic Acid as a Depressant for Hematite in the Reverse Flotation of Iron Ore," *Minerals Engineering*, vol. 20, pp. 1003-1007, Aug. 2007.
- [16] A. C. Partridge and G. W. Smith, "Flotation and Adsorption Characteristics of the Hematite-Dodecylamine-Starch System," *Canadian Metallurgical Quarterly*, vol. 10, no. 3, pp. 229-234, 1971.
- [17] J. S. Laskowski, R. M. Vurdela, and Q. Liu, "The Colloid Chemistry of Weak-Electrolyte Collector Flotation," in *XVI International Mineral Processing Congress*, 1988, pp. 703-715.
- [18] I. Iwasaki, R. B. Cooke, and H. S. Choi, "Flotation Characteristics of Hematite, Goethite, and Activated Quartz with 18-Carbon Aliphatic Acids and Related Compounds," *Transactions of the American Institute of Mining, Metallurgical and Petroleum Engineers*, vol. 217, pp. 237-244, 1960.

- [19] A. D. McNaught and A. Wilkinson, "Hydrophobic Interaction," *Compendium of Chemical Terminology, the "Gold Book,"* vol. 1077. Blackwell Scientific Publications, Oxford, 1997.
- [20] S. Takeda and I. Matsuoka, "The Effect of the Structure of n-Hexylamine on the Flotation of Quartz from an Artificial Mixture with Hematite," *Colloids and Surfaces*, vol. 47, pp. 105-115, 1990.
- [21] K. B. Quast, "Flotation of Hematite Using Hydroxamates as Collectors," *AusIMM Proceedings*, vol. 304, no. 1, pp. 7-13, 1999.
- [22] M. C. Fuerstenau, R. W. Harper, and J. D. Miller, "Hydroxamate vs. Fatty Acid Flotation of Iron Oxide," *Society of Mining Engineers of AIME, Transactions*, vol. 247, no. 1, pp. 69-73, 1970.
- [23] K. B. Quast, "Flotation of Hematite Using Oleates as Collectors," *AusIMM Proceedings*, vol. 304, no. 1, pp. 15-22, 1999.
- [24] C. Gutierrez and J. Iskra, "The Action of Neutral Oleic Acid in the Flotation of Hematite," *International Journal of Mineral Processing*, vol. 4, pp. 163-171, 1977.
- [25] L. J. Morgan, K. P. Ananthapadmanabhan, and P. Somasundaran, "Oleate Adsorption on Hematite: Problems and Methods," *International Journal of Mineral Processing*, vol. 18, no. 1-2, pp. 139-152, 1986.
- [26] J. S. Laskowski and G. A. Nyamekye, "Colloid Chemistry of Weak Electrolyte Collectors : The Effect of Conditioning on Flotation with Fatty Acids," *International Journal of Mineral Processing*, vol. 40, no. 3-4, pp. 245-256, Feb. 1994.
- [27] J. Iskra, G. Gutierrez, and J. A. Kitchener, "Influence of Quebracho on the Flotation of Fluorite, Calcite, Hematite, and Quartz with Oleate as Collector," *Transactions of the Institution of Mining and Metallurgy, Section C: Mineral Processing and Extractive Metallurgy*, vol. 82, no. June, p. C73-C78, 1973.
- [28] S. R. B. Cooke, I. Iwasaki, and H. S. Choi, "Effect of Temperature on Soap Flotation of Iron Ore," *Mining Engineering*, vol. 12, pp. 491-498, 1960.
- [29] S. R. B. Cooke and W. Nummela, "Fatty and Resin Acids as Collectors for Iron Oxides," *Bureau of Mines Report of Investigations*, vol. 5498, p. 24, 1959.
- [30] K. Quast, "Flotation of Hematite Using C6-C18 Saturated Fatty Acids," *Minerals Engineering*, vol. 19, no. 6-8, pp. 582-597, May 2006.
- [31] A. M. Abeidu, "Reagents Influencing the Selective Soap Flotation of Hematite & Goethite," *Indian Journal of Technology*, vol. 14, no. 5, pp. 249-253, 1976.
- [32] Q. Liu and J. S. Laskowski, "Adsorption of Polysaccharides on Minerals," *Encyclopedia of Surface and Colloid Science*. Taylor & Francis, pp. 649-668, 2006.
- [33] C. L. L. Pinto, A. C. Araujo, and A. E. C. Peres, "The Effect of Starch, Amylose and Amylopectin on the Depression of Oxi-Minerals," *Minerals Engineering*, vol. 5, no. 3-5, pp. 469-478, 1992.
- [34] A. E. C. Peres and M. I. Correa, "Depression of Iron Oxides with Corn Starches," *Minerals Engineering*, vol. 9, no. 12, pp. 1227-1234, 1996.
- [35] H. D. G. Turrer and A. E. C. Peres, "Investigation on Alternative Depressants for Iron Ore Flotation," *Minerals Engineering*, vol. 23, no. 11-13, pp. 1066-1069, Oct. 2010.
- [36] H. D. G. Turrer, A. C. Araujo, R. M. Papini, and A. E. C. Peres, "Iron Ore Flotation in the Presence of Polyacrylamides," *Mineral Processing and Extractive Metallurgy: IMM Transactions section C*, vol. 116, no. 2, pp. 81-84, Jun. 2007.

- [37] W. Q. Gong, A. Parentich, L. H. Little, and L. J. Warren, "Selective Flotation of Apatite from Iron Oxides," *International Journal of Mineral Processing*, vol. 34, no. 1–2, pp. 83-102, Jan. 1992.
- [38] W. Q. Gong, C. Klauber, and L. J. Warren, "Mechanism of Action of Sodium Silicate in the Flotation of Apatite from Hematite," *International Journal of Mineral Processing*, vol. 39, no. 3–4, pp. 251-273, 1993.
- [39] T. L. Wei and R. . Smith, "Anionic Activator Function in Cationic Flotation of Hematite," in *Reagents in the Minerals Industry*, 1984, pp. 41-45.
- [40] G. G. O. O. Uwadiale, "Flotation of Iron Oxides and Quartz—A Review," *Mineral Processing and Extractive Metallurgy Review*, vol. 11, no. 3, pp. 129-161, Jun. 1992.
- [41] D. W. Fuerstenau and M. C. Fuerstenau, "The Flotation of Oxide and Silicate Minerals," in *Principles of Flotation*, R. P. King, Ed. Johannesburg: South African Institute of Mining and Metallurgy, 1982, pp. 109-158.
- [42] A. C. Araujo, P. R. M. Viana, and A. E. C. Peres, "Reagents in Iron Ores Flotation," *Minerals Engineering*, vol. 18, no. 2, pp. 219-224, Feb. 2005.
- [43] M. C. Fuerstenau, K. N. Han, and J. D. Miller, "Chapter 17: Flotation Behaviour of Chromium and Manganese Minerals," in *Advances in Mineral Processing: A Half-Century of Progress in Application of Theory to Practice*, 1986, pp. 289-307.
- [44] T. W. Healy, A. P. Herring, and D. W. Fuerstenau, "The Effect of Crystal Structure on the Surface Properties of a Series of Manganese Dioxides," *Journal of Colloid and Interface Science*, vol. 21, no. 4, pp. 435-444, 1966.
- [45] A. A. Yousef, M. A. Arafa, and M. A. Malati, "Adsorption of Sulphite, Oleate and Manganese(II) Ions by β -Manganese Dioxide and its Activation in Flotation," *Journal of Applied Chemistry and Biotechnology*, vol. 21, no. 7, pp. 200-207, Apr. 1971.
- [46] R. Natarajan and D. W. Fuerstenau, "Adsorption and Flotation Behavior of Manganese Dioxide in the Presence of Octyl Hydroxamate," *International Journal of Mineral Processing*, vol. 11, no. 2, pp. 139-153, Sep. 1983.
- [47] M. A. Arafa, S. M. R. El-Nozahi, and A. A. Yousef, "Cationic Flotation of Some Manganese Oxides," *Neue Hütte*, vol. 37, no. 12, pp. 451-457, 1992.
- [48] U. B. Nayak and N. R. Kuloor, "Selective Flotation of Quartz, Pyrolusite, and Hematite," *Chemical Age of India*, vol. 14, no. 8, pp. 571-575, 1963.
- [49] B. R. Palmer, G. Gutierrez, and M. C. Fuerstenau, "Mechanisms Involved in the Flotation of Oxides and Silicates with Anionic Collectors: Parts 1 and 2," *Transactions of the Society of Mining Engineers of AIME*, vol. 258, no. 3, pp. 257-263, 1975.
- [50] M. A. Arafa, S. M. R. El-Nozahi, and A. A. Yousef, "Effect of Temperature on the Adsorption of Anionic Surfactant on Manganese Dioxides and its Relation to Flotation," *Modelling, Measurement & Control. C, Energetics, Chemistry, Earth, Environmental & Biomedical Problems*, vol. 42, no. 3, pp. 27-42, 1994.
- [51] O. S. Bogdanov and O. P. Bondarenko, "Some Principles of the Flotation of Manganese Minerals," *Obogashchenie Rud*, vol. 12, no. 6, pp. 8-11, 1967.
- [52] N. G. Gomelauri and S. M. Kochineva, "Effect of Different Regulator Reagents on the Flotation of Manganese Minerals," *Soobshcheniya Akademii Nauk Gruzinskoi SSR*, vol. 75, no. 3, pp. 649-652, 1974.
- [53] F. D. (U. S. B. of M. Devaney and J. B. (U. S. B. of M. Clemmer, "Floating of Carbonate and Oxide Manganese Ores-A Further Step in the Utilization of Low-

- grade Reserves," *Engineering and Mining Journal*, vol. 128, no. 13, pp. 506-508, 1929.
- [54] S. M. Shelton, M. M. Fine, and J. D. Bardill, "Beneficiation of Manganese Wad Ores from the Chinn Property, Batesville, Ark.," *Bureau of Mines Report of Investigations*, vol. 3614, p. 18, 1942.
- [55] M. M. Fine, S. M. Shelton, and J. B. Zadra, "Concentration of Manganiferous Iron Ore from the Armour No. 1 Mine, Ironton, Minn.," *Bureau of Mines Report of Investigations*, vol. 3624, p. 13, 1942.
- [56] T. L. Johnston, S. M. Shelton, M. M. Fine, and W. A. Calhoun, "Concentration of Manganese-Bearing Ore from the Interstate Manganese Co., Johnson County, Tenn.," *Bureau of Mines Report of Investigations*, vol. 3623, p. 13, 1942.
- [57] S. M. Shelton, M. M. Fine, J. B. Zadra, and R. B. Fisher, "Concentration of Manganese-Bearing Ore from the Stange Mine, Bland County, Va.," *Bureau of Mines Report of Investigations*, vol. 3633, p. 14, 1942.
- [58] S. J. McCarroll, "Upgrading Manganese Ore," *Mining Engineering*, vol. 6, no. 3, pp. 289-293, 1954.
- [59] S. C. Sun and P. E. Morris, "These Tests Offer a Reagent Combination To Float Low-Grade Manganese Ore," *Engineering and Mining Journal*, vol. 157, no. 5, pp. 99, 115, 1956.
- [60] W. A. Stickney and W. E. Anable, "Utilizing Offgrade Manganese Materials From Montana," *Bureau of Mines Report of Investigations*, vol. 5255, p. 21, 1956.
- [61] S. R. Zimmerley, J. D. Vincent, and C. H. Schack, "Concentration of Manganese Ores from the Drum Mountain District, Utah," *Bureau of Mines Report of Investigations*, vol. 3606, p. 12, 1942.
- [62] G. M. Potter, A. O. Ipsen, and R. R. Wells, "Concentration of Manganese Ores from Gila, Greenlee, and Graham Counties, Ariz.," *Bureau of Mines Report of Investigations*, vol. 3842, p. 12, 1946.
- [63] A. W. Fahrenwald, "Emulsion Flotation," *Mining Congress Journal*, vol. 43, no. 8, pp. 72-74, 1957.
- [64] E. H. Gates, "Agglomeration Flotation of Manganese Ore," *Mining Engineering*, vol. 9, no. 12, pp. 1368-1372, 1957.
- [65] I. V. Chernyshova, S. Ponnurangam, and P. Somasundaran, "Adsorption of Fatty Acids on Iron (Hydr)oxides from Aqueous Solutions," *Langmuir : The ACS journal of surfaces and colloids*, vol. 27, no. 16, pp. 10007-18, Aug. 2011.
- [66] P. Roonasi, X. Yang, and A. Holmgren, "Competition Between Sodium Oleate and Sodium Silicate for a Silicate/Oleate Modified Magnetite Surface Studied by In Situ ATR-FTIR Spectroscopy," *Journal of Colloid and Interface Science*, vol. 343, no. 2, pp. 546-52, Mar. 2010.
- [67] G. . Deacon and R. J. Phillips, "Relationships Between the Carbon-Oxygen Stretching Frequencies of Carboxylate Complexes and the Type of Carboxylate Coordination," *Coordination Chemistry Reviews*, vol. 33, pp. 227-250, 1980.
- [68] E. Potapova, I. Carabante, M. Grahn, A. Holmgren, and J. Hedlund, "Studies of Collector Adsorption on Iron Oxides by In Situ ATR-FTIR Spectroscopy," *Industrial & Engineering Chemistry Research*, vol. 49, no. 4, pp. 1493-1502, Feb. 2010.
- [69] P. Roonasi and A. Holmgren, "A Fourier Transform Infrared (FTIR) and Thermogravimetric Analysis (TGA) Study of Oleate Adsorbed on Magnetite Nano-Particle Surface," *Applied Surface Science*, vol. 255, no. 11, pp. 5891-5895, Mar. 2009.

- [70] J. Coates, "Interpretation of Infrared Spectra , A Practical Approach Interpretation of Infrared Spectra , A Practical Approach," *Encyclopedia of Analytical Chemistry*. John Wiley & Sons, pp. 10815-10837, 2000.
- [71] W. Q. Gong, A. Parentich, L. H. Little, and L. J. Warren, "Diffuse Reflectance Infrared Fourier Transform Spectroscopic Study of the Adsorption Mechanism of Oleate on Haematite," *Colloids and Surfaces*, vol. 60, pp. 325-339, Nov. 1991.
- [72] C. Rocchiccioli-Deltcheff, R. Franck, V. Cabuil, and R. Massart, "Surfacted Ferrofluids: Interactions at the Surfactant-Magnetic Iron Oxide Interface," *Journal of Chemical Research, Synopses*, no. 5, pp. 126-127, 1987.
- [73] G. Socrates, *Infrared Characteristic Group Frequencies*. John Wiley & Sons, 1980.
- [74] L. (COREM) Huang, "Quoted Mineralogy Information," 2010.
- [75] B. Siwek, M. Zembala, and A. Pomianowski, "A Method for Determination of Fine-Particle Flotability," *International Journal of Mineral Processing*, vol. 8, pp. 85-88, 1981.
- [76] M. C. Fuerstenau, G. Gutierrez, and D. A. Elgillani, "The Influence of Sodium Silicate in Nonmetallic Flotation Systems," *Society of Mining Engineers of AIME, Transactions*, vol. 241, pp. 319-323, 1968.
- [77] K. I. Marinakis and H. L. Shergold, "Influence of Sodium Silicate Addition on the Adsorption of Oleic Acid by Fluorite, Calcite, and Barite," *International Journal of Mineral Processing*, vol. 14, pp. 177-193, 1985.
- [78] Y. Zhang and Q. Liu, "Effect of Surface Cleaning on Differential Flotation of Sulfide Minerals," in *Interactions in Mineral Processing: Proceedings of the Fourth UBC-McGill International Symposium on Fundamentals of Minerals Processing*, 2001, pp. 201-215.
- [79] S. Hayashi and J. Umemura, "Infrared Spectroscopic Evidence for the Coexistence of two Molecular Configurations in Crystalline Fatty Acids," *The Journal of Chemical Physics*, vol. 63, no. 5, pp. 1732-1740, 1975.
- [80] J. E. Tackett, "Characterization of Chromium (II) Acetate in Aqueous Solution," *Applied Spectroscopy*, vol. 43, no. 3, pp. 490-499, 1989.
- [81] T. Dudev and C. Lim, "Effect of Carboxylate-Binding Mode on Metal Binding/Selectivity and Function in Proteins," *Accounts of Chemical Research*, vol. 40, no. 1, pp. 85-93, Jan. 2007.
- [82] T. Lindgren, L. Vayssieres, H. Wang, and S. E. Lindquist, "Photo-Oxidation of Water at Hematite Electrodes," in *Chemical Physics of Nanostructured Semiconductors*, A. I. Kokorin and D. W. Bahnemann, Eds. Boston: VSP, 2003.

Appendix I: Bench Flotation Tests

Table 13: Test procedure and metallurgical balance for BI01

Test No: BI01

Sample: Wabush Spiral Concentrate

Project: CRDPJ379600-08

Grind size: plant condition

Date: August 3, 2010

Pulp density: 29 % solids

Operator: Marc

Objective: Scoping bench flotation test of Wabush Spiral Concentrate using Sodium Oleate and Sodium Silicate

STAGE	TIME (min)	pH	ADDITION		COMMENTS	Conc pulp weight, g
			Reagent	g/tonne		
Slurry					JKTeck flotation machine, 1600 rpm 500 g sample in 1.5 L stainless steel cell	
Condition	3	10.7	Sodium Silicate	1000	500 milligrams of Na ₂ SiO ₃ ·5H ₂ O in 50 ml water added, conditioned at natural pH	
Condition	3		Sodium Oleate	200	Adjust pH to 10, then add 100 mg of Sodium Oleate in 50 ml Water added	
		10.0				
Rougher flotation						
Rougher float 1	0.5				Air flowrate 5 No DF250 necessary	340.4
Rougher float 2	0.5				No DF250 necessary	206.1
		9.9			Record final pH	
					tailings pulp	1154.1

Product	Solid weight		Water weight (g)	Assay (%)			Distribution (%)		
	(g)	(%)		Fe2O3	MnO	SiO2	Fe2O3	MnO	SiO2
Rougher concentrate 1	128.8	25.9	211.6	96.39	0.96	1.68	26.6	10.4	18.0
Rougher concentrate 2	24.1	4.8	182.0	92.81	2.17	3.78	4.8	4.4	7.6
Rougher conc. 1+2	152.9	30.8	393.6	95.83	1.15	2.01	31.4	14.9	25.5
Float tail	344.1	69.2	810.0	92.84	2.93	2.61	68.6	85.1	74.5
Total	497.1	100.0	1203.5	93.76	2.38	2.43	100.0	100.0	100.0

Table 14: Test procedure and metallurgical balance for B102

Test No: B102

Sample: Wabush Spiral Concentrate

Project: CRDPJ379600-08

Grind size: plant condition

Date: August 4, 2010

Pulp density: 32 % solids

Operator: Marc

Objective: Scoping bench flotation test of Wabush Spiral Concentrate using Sodium Oleate and Sodium Silicate

STAGE	TIME (min)	pH	ADDITION		COMMENTS	Conc pulp weight, g
			Reagent	g/tonne		
Slurry		6.6			JKTeck flotation machine, 1600 rpm 500 g sample in 1.5 L stainless steel cell	
Condition	3	11.5	Sodium Silicate	5000	2500 milligrams of Na ₂ SiO ₃ ·5H ₂ O in 50 ml water added, conditioned at natural pH	
Condition	3	10.0	Sodium Oleate	200	Adjust pH to 10, then add 100 mg of Sodium Oleate in 50 ml water added	
Rougher flotation						
Rougher float 1	0.5				Air flowrate 5 No DF250 necessary	222.3
Rougher float 2	0.5				No DF250 necessary	164.7
		10.0			Record final pH	
					tailings pulp	1167.6

Product	Solid weight		Water weight (g)	Assay (%)			Distribution (%)		
	(g)	(%)		Fe ₂ O ₃	MnO	SiO ₂	Fe ₂ O ₃	MnO	SiO ₂
Rougher concentrate 1	4.5	0.9	217.8	80.77	6.36	7.11	0.8	2.0	2.3
Rougher concentrate 2	1.6	0.3	163.1	70.98	13.72	9.89	0.2	1.5	1.1
Rougher conc. 1+2	6.0	1.2	381.0	78.22	8.28	7.83	1.0	3.6	3.4
Float tail	490.8	98.8	676.8	92.98	2.76	2.76	99.0	96.4	96.6
Total	496.8	100.0	1057.8	92.80	2.83	2.82	100.0	100.0	100.0

Table 15: Test procedure and metallurgical balance for B103

Test No: B103

Sample: Wabush Spiral Concentrate

Project: CRDPJ379600-08

Grind size: plant condition

Date: August 5, 2010

Pulp density: 31 % solids

Operator: Marc

Objective: Scoping bench flotation test of Wabush Spiral Concentrate using Sodium Oleate and Sodium Silicate

STAGE	TIME (min)	pH	ADDITION		COMMENTS	Conc pulp weight, g
			Reagent	g/tonne		
Slurry		6.6			JKTeck flotation machine, 1600 rpm 500 g sample in 1.5 L stainless steel cell	
Condition	3	11.2	Sodium Silicate	3000	1500 milligrams of Na ₂ SiO ₃ ·5H ₂ O in 50 ml water added, conditioned at natural pH	
Condition	3	10.0	Sodium Oleate	200	Adjust pH to 10, then add 100 mg of Sodium Oleate in 50 ml water added	
Rougher flotation						
Rougher float 1	0.5				Air flowrate 5 No DF250 necessary	205.8
Rougher float 2	0.5				No DF250 necessary	179.5
		10.0			Record final pH	
					tailings pulp	1227.5

Product	Solid weight		Water weight (g)	Assay (%)			Distribution (%)		
	(g)	(%)		Fe ₂ O ₃	MnO	SiO ₂	Fe ₂ O ₃	MnO	SiO ₂
Rougher concentrate 1	9.3	1.9	196.5	88.37	3.63	4.82	1.8	2.5	2.3
Rougher concentrate 2	1.8	0.4	177.7	71.02	11.47	7.74	0.3	1.5	0.7
Rougher conc. 1+2	11.1	2.2	374.2	85.55	4.91	5.30	2.1	4.0	3.1
Float tail	484.2	97.8	743.3	91.94	2.66	3.83	97.9	96.0	96.9
Total	495.3	100.0	1117.5	91.80	2.71	3.86	100.0	100.0	100.0

Table 16: Test procedure and metallurgical balance for B104

Test No: B104

Sample: Wabush Spiral Concentrate

Project: CRDPJ379600-08

Grind size: plant condition

Date: August 5, 2010

Pulp density: 32 % solids

Operator: Marc

Objective: Scoping bench flotation test of Wabush Spiral Concentrate using Sodium Oleate and Sodium Silicate

STAGE	TIME (min)	pH	ADDITION		COMMENTS	Conc pulp weight, g
			Reagent	g/tonne		
Slurry		6.6			JKTeck flotation machine, 1600 rpm 500 g sample in 1.5 L stainless steel cell	
Condition	3	11.1	Sodium Silicate	2000	1000 milligrams of Na ₂ SiO ₃ ·5H ₂ O in 50 ml water added, conditioned at natural pH	
Condition	3	10.0	Sodium Oleate	200	Adjust pH to 10, then add 100 mg of Sodium Oleate in 50 ml water added	
Rougher flotation						
Rougher float 1	0.5				Air flowrate 5 No DF250 necessary	209.1
Rougher float 2	0.5				No DF250 necessary	180.6
		10.0			Record final pH	
					tailings pulp	1156.9

Product	Solid weight		Water weight (g)	Assay (%)			Distribution (%)		
	(g)	(%)		Fe ₂ O ₃	MnO	SiO ₂	Fe ₂ O ₃	MnO	SiO ₂
Rougher concentrate 1	18.2	3.7	190.9	92.09	2.58	3.27	3.7	2.7	3.4
Rougher concentrate 2	3.5	0.7	177.1	77.58	9.06	7.11	0.6	1.8	1.4
Rougher conc. 1+2	21.7	4.4	368.0	89.77	3.62	3.88	4.2	4.4	4.8
Float tail	476.1	95.6	680.8	92.20	3.54	3.48	95.8	95.6	95.2
Total	497.8	100.0	1048.8	92.09	3.54	3.50	100.0	100.0	100.0

Table 17: Test procedure and metallurgical balance for B105

Test No: B105

Sample: Wabush Spiral Concentrate

Project: CRDPJ379600-08

Grind size: 80% Passing 117um

Date: September 21, 2010

Pulp density: 27 % solids

Operator: Marc

Objective: Scoping bench flotation test of Wabush Spiral Concentrate using Sodium Oleate and Sodium Silicate

STAGE	TIME (min)	pH	ADDITION		COMMENTS	Conc pulp weight, g
			Reagent	g/tonne		
Slurry		8.0			JKTeck flotation machine, 1200 rpm 500 g sample in 1.5 L stainless steel cell	
Condition	3	11.1	Sodium Silicate	2000	1000 milligrams of Na ₂ SiO ₃ ·5H ₂ O in 50 ml water added, conditioned at natural pH	
Condition	3	10.0	Sodium Oleate	200 (Total)	Adjust pH to 10, then add 50 mg of Sodium Oleate in 25 ml water	
Rougher flotation						
Rougher float 1	1				Air flowrate 8, 2 drops DF250	89.9
Rougher float 2	1					130.9
Condition	3	9.9 10.0			Readjust pH to 10, then add 50mg of Sodium Oleate in 25ml water, 2 drops DF250	
Rougher float 3	1					112.7
Rougher float 4	1					97.1
		9.9			Record final pH	
					tailings pulp	1393.6

Product	Solid weight		Water weight (g)	Assay (%)			Distribution (%)		
	(g)	(%)		Fe ₂ O ₃	MnO	SiO ₂	Fe ₂ O ₃	MnO	SiO ₂
Rougher concentrate 1	11.3	2.3	78.6	77.20	7.91	4.82	2.0	4.5	2.1
Rougher concentrate 2	12.8	2.6	118.1	81.80	7.09	5.72	2.4	4.5	2.9
Rougher conc. 1+2	24.1	4.9	196.7	79.64	7.47	5.30	4.4	9.0	5.0
Rougher concentrate 3	11.6	2.4	101.1	83.40	6.43	5.86	2.2	3.7	2.6
Rougher conc. 1+2+3	35.7	7.3	297.8	80.86	7.14	5.48	6.6	12.7	7.6
Rougher concentrate 4	9.6	2.0	87.5	84.50	5.73	6.23	1.9	2.8	2.3
Rougher conc. 1+2+3+4	45.3	9.2	385.3	81.63	6.84	5.64	8.5	15.5	9.9
Float tail	445.6	90.8	948.0	89.30	3.79	5.19	91.5	84.5	90.1
Total	490.9	100.0	1333.3	88.59	4.07	5.23	100.0	100.0	100.0

Table 18: Test procedure and metallurgical balance for BI06

Test No: BI06

Sample: Wabush Spiral Concentrate

Project: CRDPJ379600-08

Grind size: 80% Passing 117um

Date: October 6, 2010

Pulp density: 27 % solids

Operator: Marc

Objective: Scoping bench flotation test of Wabush Spiral Concentrate using Sodium Oleate and Sodium Silicate. Spiral Concentrate wet ground for 25 minutes

STAGE	TIME (min)	pH	ADDITION		COMMENTS	Conc pulp weight, g
			Reagent	g/tonne		
Slurry		7.3			JKTeck flotation machine, 1200 rpm 500 g sample in 1.5 L stainless steel cell	
Condition	3	11.9	Sodium Silicate	5000	2500 milligrams of Na ₂ SiO ₃ ·5H ₂ O in 50 ml water added, conditioned at natural pH	
Condition	3	10.0	Sodium Oleate	200 (Total)	Adjust pH to 10, then add 50 mg of Sodium Oleate in 25 ml water	
Rougher flotation						
Rougher float 1	1				Air flowrate 2	225.0
Rougher float 2	1					201.5
Condition	3	10.0			Readjust pH to 10, then add 50mg of Sodium Oleate in 25ml water	
Rougher float 3	1					201.8
Rougher float 4	1					176.7
		9.9			Record final pH	
					tailings pulp	1059.3

Product	Solid weight		Water weight (g)	Assay (%)			Distribution (%)		
	(g)	(%)		Fe ₂ O ₃	MnO	SiO ₂	Fe ₂ O ₃	MnO	SiO ₂
Rougher concentrate 1	24.6	5.0	200.4	81.90	5.93	8.06	4.6	6.5	6.9
Rougher concentrate 2	19.7	4.0	181.8	82.00	5.99	8.51	3.7	5.2	5.8
Rougher conc. 1+2	44.3	8.9	382.2	81.94	5.96	8.26	8.4	11.7	12.6
Rougher concentrate 3	19.5	3.9	182.3	81.80	5.91	8.87	3.7	5.1	6.0
Rougher conc. 1+2+3	63.8	12.8	564.5	81.90	5.94	8.45	12.0	16.8	18.6
Rougher concentrate 4	16.7	3.4	160.0	81.70	5.88	9.17	3.1	4.4	5.3
Rougher conc. 1+2+3+4	80.5	16.2	724.5	81.86	5.93	8.60	15.2	21.2	23.9
Float tail	416.3	83.8	643.0	88.40	4.27	5.29	84.8	78.8	76.1
Total	496.8	100.0	1367.5	87.34	4.54	5.83	100.0	100.0	100.0

Table 19: Test procedure and metallurgical balance for B107

Test No: B107

Sample: Wabush Spiral Concentrate

Project: CRDPJ379600-08

Grind size: 80% Passing 117um

Date: October 8, 2010

Pulp density: 28 % solids

Operator: Marc

Objective: Scoping bench flotation test of Wabush Spiral Concentrate using Sodium Oleate and Sodium Silicate. Spiral Concentrate wet ground for 25 minutes

STAGE	TIME (min)	pH	ADDITION		COMMENTS	Conc pulp weight, g
			Reagent	g/tonne		
Slurry		7.3			JKTeck flotation machine, 1200 rpm 500 g sample in 1.5 L stainless steel cell	
Condition	3	11.8	Sodium Silicate	5000	2500 milligrams of Na ₂ SiO ₃ ·5H ₂ O in 50 ml water added, conditioned at natural pH	
Condition	3	10.0	Sodium Oleate	500 (Total)	Adjust pH to 10, then add 125 mg of Sodium Oleate in 25 ml water	
Rougher flotation						
Rougher float 1	1				Air flowrate 2, no frother	309.0
Rougher float 2	1					218.0
Condition	3	10.0			Readjust pH to 10, then add 125mg of Sodium Oleate in 25ml water, no frother	
Rougher float 3	1					233.2
Rougher float 4	1					183.7
		9.9			Record final pH	
					tailings pulp	828.4

Product	Solid weight		Water weight (g)	Assay (%)			Distribution (%)		
	(g)	(%)		Fe ₂ O ₃	MnO	SiO ₂	Fe ₂ O ₃	MnO	SiO ₂
Rougher concentrate 1	39.5	8.0	269.5	88.30	4.01	5.48	7.7	10.4	10.9
Rougher concentrate 2	26.4	5.3	191.6	87.70	3.94	5.82	5.1	6.8	7.8
Rougher conc. 1+2	65.9	13.3	461.1	88.06	3.98	5.62	12.9	17.2	18.7
Rougher concentrate 3	29.9	6.1	203.3	87.70	3.84	5.98	5.8	7.5	9.0
Rougher conc. 1+2+3	95.8	19.4	664.4	87.95	3.94	5.73	18.7	24.7	27.8
Rougher concentrate 4	25.7	5.2	158.0	88.10	3.73	5.86	5.0	6.3	7.6
Rougher conc. 1+2+3+4	121.5	24.6	822.4	87.98	3.89	5.76	23.7	31.0	35.4
Float tail	372.4	75.4	456.0	92.50	2.83	3.43	76.3	69.0	64.6
Total	493.9	100.0	1278.4	91.39	3.09	4.00	100.0	100.0	100.0

Table 20: Test procedure and metallurgical balance for BI08

Test No: BI08

Sample: Wabush Spiral Concentrate

Project: CRDPJ379600-08

Grind size: 80% Passing 117um

Date: October 26, 2010

Pulp density: 25 % solids

Operator: Marc

Objective: Scoping bench flotation test of Wabush Spiral Concentrate using Sodium Oleate and Sodium Silicate. Spiral Concentrate wet ground for 25 minutes

STAGE	TIME (min)	pH	ADDITION		COMMENTS	Conc pulp weight, g
			Reagent	g/tonne		
Slurry		7.9			JKTeck flotation machine, 1200 rpm 500 g sample in 1.5 L stainless steel cell	
Condition	3	7.5	Tannic Acid	200	100 milligrams of Tannic acid in 25ml water	
Condition	3	11.7	Sodium Silicate	5000	2500 milligrams of Na ₂ SiO ₃ ·5H ₂ O in 50 ml water added, conditioned at natural pH	
Condition	3	10.0	Sodium Oleate	200 (Total)	Adjust pH to 10, then add 50 mg of Sodium Oleate in 25 ml water	
Rougher flotation						
Rougher float 1	1				Air flowrate 5, 2 drops DF250	140.4
Rougher float 2	1					168.3
Condition	3				Readjust pH to 10, then add 50mg of Sodium Oleate in 25ml water, 2 drops DF250	
Rougher float 3	1				Air flowrate 6	244.1
Rougher float 4	1					205.4
		9.9			Record final pH	
tailings pulp						1195.4

Product	Solid weight		Water weight (g)	Assay (%)			Distribution (%)		
	(g)	(%)		Fe ₂ O ₃	MnO	SiO ₂	Fe ₂ O ₃	MnO	SiO ₂
Rougher concentrate 1	12.6	2.6	127.8	86.40	4.22	5.82	2.4	3.3	3.5
Rougher concentrate 2	16.0	3.2	152.3	86.30	4.30	5.85	3.1	4.3	4.5
Rougher conc. 1+2	28.6	5.8	280.1	86.34	4.26	5.84	5.5	7.6	8.0
Rougher concentrate 3	21.6	4.4	222.5	86.30	4.23	5.66	4.2	5.7	5.9
Rougher conc. 1+2+3	50.2	10.2	502.6	86.33	4.25	5.76	9.7	13.3	13.9
Rougher concentrate 4	19.8	4.0	185.6	87.20	4.11	5.80	3.8	5.1	5.5
Rougher conc. 1+2+3+4	70.0	14.2	688.2	86.57	4.21	5.77	13.5	18.4	19.4
Float tail	423.7	85.8	771.7	91.60	3.09	3.97	86.5	81.6	80.6
Total	493.7	100.0	1459.9	90.89	3.25	4.23	100.0	100.0	100.0

Table 21: Test procedure and metallurgical balance for B109

Test No: B109

Sample: Wabush Spiral Concentrate
 Grind size: 80% Passing 117um
 Pulp density: 27 % solids

Project: CRDPJ379600-08
 Date: October 28, 2010
 Operator: Marc

Objective: Scoping bench flotation test of Wabush Spiral Concentrate using Sodium Oleate and Sodium Silicate. Spiral Concentrate wet ground for 25 minutes

STAGE	TIME (min)	pH	ADDITION		COMMENTS	Conc pulp weight, g
			Reagent	g/tonne		
Slurry		8.0			JKTeck flotation machine, 1200 rpm 500 g sample in 1.5 L stainless steel cell	
Condition	3	7.3	Tannic Acid	400	200 milligrams of Tannic Acid in 25ml water	
Condition	3	11.5	Sodium Silicate	5000	2500 milligrams of Na ₂ SiO ₃ ·5H ₂ O in 50 ml water added, conditioned at natural pH	
Condition	3	10.0	Sodium Oleate	200 (Total)	Adjust pH to 10, then add 50 mg of Sodium Oleate in 25 ml water	
Rougher flotation						
Rougher float 1	1				Air flowrate 6, 2 drops DF250	181.5
Rougher float 2	1					141.9
Condition	3	10.0			Readjust pH to 10, then add 50mg of Sodium Oleate in 25ml water	
Rougher float 3	1				3 drops DF250	128.2
Rougher float 4	1					121.8
		9.9			Record final pH	
					tailings pulp	1272.6

Product	Solid weight		Water weight (g)	Assay (%)			Distribution (%)		
	(g)	(%)		Fe ₂ O ₃	MnO	SiO ₂	Fe ₂ O ₃	MnO	SiO ₂
Rougher concentrate 1	25.2	5.1	156.3	89.00	3.69	5.08	5.0	6.4	6.7
Rougher concentrate 2	21.0	4.3	120.9	89.30	3.65	5.11	4.2	5.3	5.6
Rougher conc. 1+2	46.2	9.4	277.2	89.14	3.67	5.09	9.1	11.6	12.2
Rougher concentrate 3	13.3	2.7	114.9	88.70	3.72	5.16	2.6	3.4	3.6
Rougher conc. 1+2+3	59.5	12.1	392.1	89.04	3.68	5.11	11.7	15.0	15.8
Rougher concentrate 4	16.2	3.3	105.6	89.00	3.52	4.98	3.2	3.9	4.2
Rougher conc. 1+2+3+4	75.7	15.4	497.7	89.03	3.65	5.08	14.9	19.0	20.0
Float tail	417.3	84.6	855.3	92.00	2.83	3.69	85.1	81.0	80.0
Total	493.0	100.0	1353.0	91.54	2.96	3.90	100.0	100.0	100.0

Table 22: Test procedure and metallurgical balance for B110

Test No: B110

Sample: Wabush Spiral Concentrate
 Grind size: 80% Passing 117um
 Pulp density: 24 % solids

Project: CRDPJ379600-08
 Date: November 1, 2010
 Operator: Marc

Objective: Scoping bench flotation test of Wabush Spiral Concentrate using Sodium Oleate, Sodium Silicate, and Citric acid. Spiral Concentrate wet ground for 25 minutes

STAGE	TIME (min)	pH	ADDITION		COMMENTS	Conc pulp weight, g
			Reagent	g/tonne		
Slurry		7.3			JKTeck flotation machine, 1200 rpm 500 g sample in 1.5 L stainless steel cell	
Condition	3	6.5	Citric Acid	200	100 milligrams Citric Acid in 25ml water	
Condition	3	11.4	Sodium Silicate	5000	2500 milligrams of Na ₂ SiO ₃ ·5H ₂ O in 50 ml water added, conditioned at natural pH	
Condition	3	10.0	Sodium Oleate	200 (Total)	Adjust pH to 10, then add 50 mg of Sodium Oleate in 25 ml water	
Rougher flotation						
Rougher float 1	1				Air flowrate 5, 2 drops DF250	330.5
Rougher float 2	1					324.0
Condition	3	9.9 10.0			Readjust pH to 10, then add 50mg of Sodium Oleate in 25ml water, no frother	
Rougher float 3	1				Air 5, no frother	368.6
Rougher float 4	1					269.7
		9.9			Record final pH	
					tailings pulp	776.3

Product	Solid weight		Water weight (g)	Assay (%)			Distribution (%)		
	(g)	(%)		Fe2O3	MnO	SiO2	Fe2O3	MnO	SiO2
Rougher concentrate 1	41.3	8.3	289.2	86.80	4.36	6.28	8.0	10.6	11.3
Rougher concentrate 2	44.5	9.0	279.5	86.60	4.30	6.57	8.6	11.3	12.8
Rougher conc. 1+2	85.8	17.3	568.7	86.70	4.33	6.43	16.5	21.9	24.1
Rougher concentrate 3	39.4	7.9	329.2	87.10	4.12	6.28	7.6	9.6	10.8
Rougher conc. 1+2+3	125.2	25.2	897.9	86.82	4.26	6.38	24.1	31.4	34.9
Rougher concentrate 4	30.2	6.1	239.5	87.30	3.98	6.57	5.9	7.1	8.7
Rougher conc. 1+2+3+4	155.4	31.3	1137.4	86.92	4.21	6.42	30.0	38.5	43.6
Float tail	341.6	68.7	434.7	92.30	3.06	3.78	70.0	61.5	56.4
Total	497.0	100.0	1572.1	90.62	3.42	4.61	100.0	100.0	100.0

Table 23: Test procedure and metallurgical balance for B111

Test No: B111

Sample: Wabush Spiral Concentrate
Grind size: 80% Passing 117um
Pulp density: 25 % solids

Project: CRDPJ379600-08

Date: November 3, 2010

Operator: Marc

Objective: Scoping bench flotation test of Wabush Spiral Concentrate using Sodium Oleate and Sodium Silicate. Spiral Concentrate wet ground for 25 minutes

STAGE	TIME (min)	pH	ADDITION		COMMENTS	Conc pulp weight, g
			Reagent	g/tonne		
Slurry		7.3			JKTeck flotation machine, 1200 rpm 500 g sample in 1.5 L stainless steel cell	
Condition	3	6.0	Citric Acid	400	200 milligrams Citric Acid in 25ml water	
Condition	3	11.4	Sodium Silicate	5000	2500 milligrams of Na ₂ SiO ₃ ·5H ₂ O in 50 ml water added, conditioned at natural pH	
Condition	3	10.0	Sodium Oleate	200 (Total)	Adjust pH to 10, then add 50 mg of Sodium Oleate in 25 ml water	
Rougher flotation						
Rougher float 1	1				Air flowrate 3, no frother	330.1
Rougher float 2	1					241.1
Condition	3	10.0			Readjust pH to 10, then add 50mg of Sodium Oleate in 25ml water, no frother	
Rougher float 3	1					292.9
Rougher float 4	1					209.6
		9.9			Record final pH	
					tailings pulp	891.1

Product	Solid weight		Water weight (g)	Assay (%)			Distribution (%)		
	(g)	(%)		Fe ₂ O ₃	MnO	SiO ₂	Fe ₂ O ₃	MnO	SiO ₂
Rougher concentrate 1	39.8	8.0	290.3	87.90	3.94	5.54	7.7	10.2	11.1
Rougher concentrate 2	32.8	6.6	208.3	87.90	3.93	5.69	6.3	8.4	9.4
Rougher conc. 1+2	72.6	14.5	498.6	87.90	3.94	5.61	14.0	18.6	20.6
Rougher concentrate 3	32.0	6.4	260.9	88.20	3.83	5.71	6.2	8.0	9.2
Rougher conc. 1+2+3	104.6	20.9	759.5	87.99	3.90	5.64	20.1	26.6	29.8
Rougher concentrate 4	24.9	5.0	184.7	88.70	3.69	5.84	4.8	6.0	7.4
Rougher conc. 1+2+3+4	129.5	25.9	944.2	88.13	3.86	5.68	25.0	32.6	37.2
Float tail	370.9	74.1	520.2	92.40	2.79	3.35	75.0	67.4	62.8
Total	500.4	100.0	1464.4	91.29	3.07	3.95	100.0	100.0	100.0

Table 24: Test procedure and metallurgical balance for B112

Test No: B112

Sample: Wabush Spiral Concentrate
 Grind size: 80% Passing 117um
 Pulp density: 19 % solids

Project: CRDPJ379600-08
 Date: February 28, 2011
 Operator: Marc

Objective: Scoping bench flotation test of Wabush Spiral Concentrate using Sodium Oleate and Sodium Silicate. 500g Spiral Concentrate with 350ml distilled water ground for 25 minutes

STAGE	TIME (min)	pH	ADDITION		COMMENTS	Conc pulp weight, g
			Reagent	g/tonne		
Slurry		7.92			JKTeck flotation machine, 1200 rpm 500 g sample in 1.5 L stainless steel cell	
Condition	3	10.00	Sodium Oleate	200 (Total)	Adjust pH to 10, then add 50 mg of Sodium Oleate in 25 ml water	
Rougher flotation						
Rougher float 1	1				Air flowrate 2 no frother	423.0
Rougher float 2	1					313.8
Rougher float 3	1					228.1
Rougher float 4	1					157.3
Condition	3	9.56 10.00			Readjust pH to 10, then add 50mg of Sodium Oleate in 25ml water, no frother	
Rougher float 5	1				-Air flowrate 3	186.4
Rougher float 6	1				-Air flowrate increased to 5 -added water	227.7
Rougher float 7	1					168.5
Rougher float 8	1					165.6
		9.20			Record final pH	
					tailings pulp	718.8

Product	Solid weight		Water weight (g)	Assay (%)			Distribution (%)		
	(g)	(%)		Fe2O3	MnO	SiO2	Fe2O3	MnO	SiO2
Rougher concentrate 1	220.9	44.5	202.1	96.60	1.39	1.32	48.8	15.1	10.7
Rougher concentrate 2	133.3	26.9	180.5	93.90	2.79	2.57	28.6	18.3	12.5
Rougher conc. 1+2	354.2	71.4	382.6	95.58	1.92	1.79	77.4	33.4	23.2
Rougher concentrate 3:4	102.3	20.6	283.1	77.80	7.79	11.50	18.2	39.2	43.0
Rougher conc. 1+2+(3:4)	456.5	92.0	665.7	91.60	3.23	3.97	95.7	72.5	66.2
Rougher concentrate 5:8	35.8	7.2	712.4	53.10	15.60	25.80	4.3	27.5	33.8
Rougher conc. 1+2+(3:4)+(5:8)	492.3	99.2	1378.1	88.80	4.13	5.55	100.0	100.0	100.0
Float tail	3.8	0.8	715.0						
Total	496.1	100.0	2093.1	88.12	4.10	5.51	100.0	100.0	100.0

Table 25: Test procedure and metallurgical balance for B113

Test No: B113

Sample: Wabush Spiral Concentrate

Project: CRDPJ379600-08

Grind size: 80% Passing 117um

Date: May 3, 2011

Pulp density: 15 % solids

Operator: Marc

Objective: Scoping bench flotation test of Wabush Spiral Concentrate using Sodium Oleate and Sodium Silicate. 500g Spiral Concentrate with 350ml distilled water ground for 25 minutes

STAGE	TIME (min)	pH	ADDITION		COMMENTS	Conc pulp weight, g
			Reagent	g/tonne		
Slurry		7.65			JKTeck flotation machine, 1200 rpm 500 g sample in 1.5 L stainless steel cell	
Condition	3	11.00	Sodium Oleate	200 (Total)	Adjust pH to 11, then add 50 mg of Sodium Oleate in 25 ml water	
Rougher flotation						
Rougher float 1	1				Air 3	619.5
Rougher float 2	1					163.5
Rougher float 3	2				Air 5	318.1
Condition	3	10.52 11.00			Readjust pH to 11, then add 50mg of Sodium Oleate in 25ml water, no frother	
Rougher float 4	4				Air 4	1267.2
		10.28			Record final pH	
					tailings pulp	977.4

Product	Solid weight		Water weight (g)	Assay (%)			Distribution (%)		
	(g)	(%)		Fe2O3	MnO	SiO2	Fe2O3	MnO	SiO2
Rougher concentrate 1	323.3	65.4	296.2	96.90	1.35	1.27	70.2	24.4	17.5
Rougher concentrate 2	53.6	10.8	109.9	92.20	3.02	3.91	11.1	9.0	8.9
Rougher conc. 1+2	376.9	76.3	406.1	96.23	1.59	1.65	81.2	33.4	26.5
Rougher concentrate 3	36.8	7.4	281.3	83.80	5.16	8.77	6.9	10.6	13.8
Rougher conc. 1+2+3	413.7	83.7	687.4	95.13	1.91	2.28	88.1	44.1	40.2
Rougher concentrate 4	71.9	14.5	1195.3	67.70	11.10	17.40	10.9	44.6	53.4
Rougher conc. 1+2+3+4	485.6	98.3	1882.7	91.06	3.27	4.52	99.0	88.7	93.6
Float tail	8.6	1.7	968.8	49.90	23.60	17.40	1.0	11.3	6.4
Total	494.2	100.0	2851.5	90.35	3.62	4.74	100.0	100.0	100.0

Table 26: Test procedure and metallurgical balance for B114

Test No: B114

Sample: Wabush Spiral Concentrate
 Grind size: 80% Passing 117um
 Pulp density: 16 % solids

Project: CRDPJ379600-08
 Date: March 3, 2011
 Operator: Marc

Objective: Scoping bench flotation test of Wabush Spiral Concentrate using Sodium Oleate and Sodium Silicate. 500g Spiral Concentrate with 350ml distilled water ground for 25 minutes

STAGE	TIME (min)	pH	ADDITION		COMMENTS	Conc pulp weight, g
			Reagent	g/tonne		
Slurry		7.79			JKTeck flotation machine, 1200 rpm 500 g sample in 1.5 L stainless steel cell	
Condition	3	10.87	Sodium Silicate	1000	500 milligrams of Na ₂ SiO ₃ ·5H ₂ O in 50 ml water added, conditioned at natural pH	
Condition	3	11.00	Sodium Oleate	200 (Total)	Adjust pH to 11, then add 50 mg of Sodium Oleate in 25 ml water	
Rougher flotation						
Rougher float 1	0.5				Air flowrate 4	305.2
Rougher float 2	0.5					195.3
Rougher float 3	1				Added water	254.8
Rougher float 4	1					108.1
Rougher float 5						58.2
Condition	3	10.35			Readjust pH to 11, then add 50mg of Sodium Oleate in 25ml water, no frother	
Rougher float 6	0.5				Air flowrate 5 -bubbles appear empty	364.3
Rougher float 7	0.5					325.3
Rougher float 8	0.5				*voluminous froth, little control	255.3
Rougher float 9	0.5					68.4
		10.38			Record final pH	
					tailings pulp	1134.6

Product	Solid weight		Water weight (g)	Assay (%)			Distribution (%)		
	(g)	(%)		Fe2O3	MnO	SiO2	Fe2O3	MnO	SiO2
Rougher concentrate 1	45.1	9.3	260.1	88.90	3.99	5.22	9.0	12.2	12.2
Rougher concentrate 2	32.2	6.7	163.1	89.20	4.05	5.68	6.5	8.8	9.5
Rougher conc. 1+2	77.3	16.0	423.2	89.02	4.01	5.41	15.5	21.0	21.7
Rougher concentrate 3	44.2	9.1	210.6	89.10	3.61	5.66	8.9	10.8	13.0
Rougher conc. 1+2+3	121.5	25.1	633.8	89.05	3.87	5.50	24.4	31.9	34.6
Rougher concentrate 4:5	12.6	2.6	153.7	87.70	4.26	6.17	2.5	3.6	4.0
Rougher conc. 1+2+3+4:5	134.1	27.7	787.5	88.93	3.90	5.56	26.8	35.5	38.6
Rougher concentrate 6	45.2	9.4	319.1	92.90	2.53	3.62	9.5	7.8	8.5
Rougher conc. 1+2+3+4:5+6	179.3	37.1	1106.6	89.93	3.56	5.07	36.3	43.2	47.1
Rougher concentrate 7	32.9	6.8	292.4	90.20	3.22	5.17	6.7	7.2	8.8
Rougher conc. Sum 1 to 7	212.2	43.9	1399.0	89.97	3.51	5.09	43.0	50.4	55.9
Rougher concentrate 8:9	32.0	6.6	291.7	89.90	3.04	5.44	6.5	6.6	9.0
Rougher conc. Sum 1 to 8:9	244.2	50.5	1690.7	89.96	3.44	5.14	49.4	57.0	64.9
Float tail	239.2	49.5	895.4	93.90	2.65	2.83	50.6	43.0	35.1
Total	483.4	100.0	2586.1	91.91	3.05	3.99	100.0	100.0	100.0

Table 27: Test procedure and metallurgical balance for B115

Test No: B115

Sample: Wabush Spiral Concentrate
 Grind size: 80% Passing 117um
 Pulp density: 18 % solids

Project: CRDPJ379600-08

Date: March 5, 2011

Operator: Marc

Objective: Scoping bench flotation test of Wabush Spiral Concentrate using Sodium Oleate and Sodium Silicate. 500g Spiral Concentrate with 350ml distilled water ground for 25 minutes

STAGE	TIME (min)	pH	ADDITION		COMMENTS	Conc pulp weight, g
			Reagent	g/tonne		
Slurry		7.63			JKTeck flotation machine, 1200 rpm 500 g sample in 1.5 L stainless steel cell	
Condition	3	11.70	Sodium Silicate	5000	2500 milligrams of Na ₂ SiO ₃ ·5H ₂ O in 50 ml water added, conditioned at natural pH	
Condition	3	11.00	Sodium Oleate	200 (Total)	Adjust pH to 11, then add 50 mg of Sodium Oleate in 25 ml water	
Rougher flotation						
Rougher float 1	1				Air flowrate 1-1.5, no frother	240.8
Rougher float 2	1					200.3
Rougher float 3	1				Added water, Air flowrate 2-2.5	192.7
Rougher float 4	1					170.1
Condition	3	10.87 11.00			Readjust pH to 11, then add 50mg of Sodium Oleate in 25ml water, no frother	
Rougher float 5	1				Air flowrate 1-1.5	224.7
Rougher float 6	1					264.1
Rougher float 7	1					184.7
Rougher float 8	1					174.9
		10.97			Record final pH	
					tailings pulp	1017.2

Product	Solid weight		Water weight (g)	Assay (%)			Distribution (%)		
	(g)	(%)		Fe ₂ O ₃	MnO	SiO ₂	Fe ₂ O ₃	MnO	SiO ₂
Rougher concentrate 1	25.3	5.2	215.5	87.30	4.08	6.29	4.9	7.0	8.2
Rougher concentrate 2	21.8	4.4	178.5	87.40	3.98	6.46	4.2	5.9	7.3
Rougher conc. 1+2	47.1	9.6	394.0	87.35	4.03	6.37	9.2	12.8	15.5
Rougher concentrate 3:4	45.1	9.2	317.7	88.60	3.61	5.68	8.9	11.0	13.2
Rougher conc. 1+2+3:4	92.2	18.8	711.7	87.96	3.83	6.03	18.1	23.8	28.7
Rougher concentrate 5	14.5	3.0	210.2	87.60	3.87	6.17	2.8	3.8	4.6
Rougher conc. 1+2+3+4+5	106.7	21.8	921.9	87.91	3.83	6.05	20.9	27.6	33.3
Rougher concentrate 6	19.2	3.9	244.9	88.20	3.87	6.18	3.8	5.0	6.1
Rougher conc. Sum 1 to 6	125.9	25.7	1166.8	87.95	3.84	6.07	24.7	32.6	39.4
Rougher concentrate 7	16.4	3.3	168.3	88.20	3.39	5.92	3.2	3.8	5.0
Rougher conc. Sum 1 to 7	142.3	29.0	1335.1	87.98	3.79	6.05	27.9	36.4	44.5
Rougher concentrate 8	18.8	3.8	156.1	90.30	3.20	4.56	3.8	4.1	4.4
Rougher conc. Sum 1 to 8	161.1	32.9	1491.2	88.25	3.72	5.88	31.7	40.4	48.9
Float tail	329.1	67.1	688.1	93.20	2.68	3.01	68.3	59.6	51.1
Total	490.2	100.0	2179.3	91.57	3.02	3.95	100.0	100.0	100.0

Table 28: Test procedure and metallurgical balance for B116

Test No: B116

Sample: Wabush Spiral Concentrate

Project: CRDPJ379600-08

Grind size: 80% Passing 117um

Date: May 5, 2011

Pulp density: 14 % solids

Operator: Marc

Objective: Scoping bench flotation test of Wabush Spiral Concentrate using Sodium Oleate and Sodium Silicate. 500g Spiral Concentrate with 350ml distilled water ground for 25 minutes

STAGE	TIME (min)	pH	ADDITION		COMMENTS	Conc pulp weight, g
			Reagent	g/tonne		
Slurry		7.66			JKTeck flotation machine, 1200 rpm 500 g sample in 1.5 L stainless steel cell	
Condition	3	11.00	Tannic Acid	100	50 mg tannic acid in 25ml water	
Condition	3	11.00	Sodium Oleate	200 (Total)	Adjust pH to 11, then add 50 mg of Sodium Oleate in 25 ml water	
Rougher flotation						
Rougher float 1	1				Air 5 Voluminous froth difficult to control	761.5
Rougher float 2	1					311.9
Rougher float 3	5.5					1525.5
Conditioning	3				Readjust pH to 11, then add 50 mg of Sodium Oleate in 25 ml water (carried out 2 minutes into conc 3)	
		10.35			Record final pH	
					tailings pulp	1060.0

Product	Solid weight		Water weight (g)	Assay (%)			Distribution (%)		
	(g)	(%)		Fe2O3	MnO	SiO2	Fe2O3	MnO	SiO2
Rougher concentrate 1	219.2	44.2	542.3	94.00	2.44	2.94	46.1	28.7	25.8
Rougher concentrate 2	49.2	9.9	262.7	86.40	4.55	7.15	9.5	12.0	14.1
Rougher conc. 1+2	268.4	54.1	805.0	92.61	2.83	3.71	55.6	40.7	40.0
Rougher concentrate 3	205.4	41.4	1320.1	89.30	3.65	5.96	41.1	40.2	49.1
Rougher conc. 1+2+3	473.8	95.5	2125.1	91.17	3.18	4.69	96.7	80.8	89.0
Float tail	22.2	4.5	1037.8	66.50	16.10	12.30	3.3	19.2	11.0
Total	496.0	100.0	3162.9	90.07	3.76	5.03	100.0	100.0	100.0

Table 29: Test procedure and metallurgical balance for B118

Test No: B118

Sample: Wabush Spiral Concentrate

Project: CRDPJ379600-08

Grind size: 80% Passing 117um

Date: May 6, 2011

Pulp density: 20 % solids

Operator: Marc

Objective: Scoping bench flotation test of Wabush Spiral Concentrate using Sodium Oleate and Sodium Silicate. 500g Spiral Concentrate with 350ml distilled water ground for 25 minutes

STAGE	TIME (min)	pH	ADDITION		COMMENTS	Conc pulp weight, g
			Reagent	g/tonne		
Slurry		7.62			JKTeck flotation machine, 1200 rpm 500 g sample in 1.5 L stainless steel cell	
Condition	3	9.00	Sodium Oleate	200 (Total)	Adjust pH to 9, then add 50 mg of Sodium Oleate in 25 ml water	
Rougher flotation						
Rougher float 1	1				Air 5	500.9
Rougher float 2	1					130.7
Rougher float 3	2					237.3
Condition	3	8.10 9.00			Readjust pH to 9, then add 50mg of Sodium Oleate in 25ml water, no frother	
Rougher float 4	4				Air 5	590.8
		7.91			Record final pH	
					tailings pulp	1031.1

Product	Solid weight		Water weight (g)	Assay (%)			Distribution (%)		
	(g)	(%)		Fe2O3	MnO	SiO2	Fe2O3	MnO	SiO2
Rougher concentrate 1	277.1	55.7	223.8	97.30	1.24	1.07	60.7	17.9	11.0
Rougher concentrate 2	36.8	7.4	93.9	93.80	2.42	2.45	7.8	4.6	3.4
Rougher conc. 1+2	313.9	63.1	317.7	96.89	1.38	1.23	68.5	22.6	14.4
Rougher concentrate 3	21.4	4.3	215.9	84.50	5.70	7.21	4.1	6.4	5.7
Rougher conc. 1+2+3	335.3	67.4	533.6	96.10	1.65	1.61	72.5	28.9	20.1
Rougher concentrate 4	149.5	30.1	441.3	77.50	7.97	11.50	26.1	62.2	63.9
Rougher conc. 1+2+3+4	484.8	97.5	974.9	90.36	3.60	4.66	98.6	91.1	84.0
Float tail	12.6	2.5	1018.5	48.10	13.50	34.20	1.4	8.9	16.0
Total	497.4	100.0	1993.4	89.29	3.85	5.41	100.0	100.0	100.0

Table 30: Test procedure and metallurgical balance for B119

Test No: B119

Sample: Wabush Spiral Concentrate
 Grind size: 80% Passing 117um
 Pulp density: 21 % solids

Project: CRDPJ379600-08

Date: May 9, 2011

Operator: Marc

Objective: Scoping bench flotation test of Wabush Spiral Concentrate using Sodium Oleate and Sodium Silicate. 500g Spiral Concentrate with 350ml distilled water ground for 25 minutes

STAGE	TIME (min)	pH	ADDITION		COMMENTS	Conc pulp weight, g
			Reagent	g/tonne		
Slurry		7.80			JKTeck flotation machine, 1200 rpm 500 g sample in 1.5 L stainless steel cell	
Condition	3	9.00	Tannic Acid	100	50 mg Tannic Acid in 25ml of water	
Condition	3	9.00	Sodium Oleate	200 (Total)	Adjust pH to 9, then add 50 mg of Sodium Oleate in 25 ml water	
Rougher flotation						
Rougher float 1	1				Air 5	682.6
Rougher float 2	1					184.7
Rougher float 3	2				The next conditioning stage was not carried out as regardless of the addition of frother, not stable froth layer could be formed.	202.0
		8.17			Record final pH	
					tailings pulp	1305.9

Product	Solid weight		Water weight (g)	Assay (%)			Distribution (%)		
	(g)	(%)		Fe2O3	MnO	SiO2	Fe2O3	MnO	SiO2
Rougher concentrate 1	384.0	77.3	298.6	94.40	2.58	1.96	80.2	59.6	35.4
Rougher concentrate 2	51.8	10.4	132.9	85.60	5.19	7.13	9.8	16.2	17.4
Rougher conc. 1+2	435.8	87.7	431.5	93.35	2.89	2.57	90.1	75.8	52.7
Rougher concentrate 3	20.1	4.0	181.9	78.90	6.55	11.30	3.5	7.9	10.7
Rougher conc. 1+2+3	455.9	91.8	613.4	92.72	3.05	2.96	93.6	83.7	63.4
Float tail	40.8	8.2	1265.1	71.30	6.63	19.10	6.4	16.3	36.6
Total	496.7	100.0	1878.5	90.96	3.35	4.29	100.0	100.0	100.0

Table 31: Test procedure and metallurgical balance for BI21

Test No: BI21

Sample: Wabush Spiral Concentrate

Project: CRDPJ379600-08

Grind size: 80% Passing 117um

Date: May 10, 2011

Pulp density: 21 % solids

Operator: Marc

Objective: Scoping bench flotation test of Wabush Spiral Concentrate using Sodium Oleate and Sodium Silicate. 500g Spiral Concentrate with 350ml distilled water ground for 25 minutes

STAGE	TIME (min)	pH	ADDITION		COMMENTS	Conc pulp weight, g
			Reagent	g/tonne		
Slurry		7.78			JKTeck flotation machine, 1200 rpm 500 g sample in 1.5 L stainless steel cell	
Condition	3	8.00	Sodium Oleate	200 (Total)	Adjust pH to 8, then add 50 mg of Sodium Oleate in 25 ml water -left at natural pH	
Rougher flotation		8.04				
Rougher float 1	1				Air 5 Concentrate all red slurry, no metallic sheen	240.4
Rougher float 2	1					149.3
		7.67			Record final pH Flotation was carried out for 6 more minutes, but analysis was limited to two concentrates	
					tailings pulp	2073.5

Product	Solid weight		Water weight (g)	Assay (%)			Distribution (%)		
	(g)	(%)		Fe2O3	MnO	SiO2	Fe2O3	MnO	SiO2
Rougher concentrate 1	74.2	14.6	166.2	95.00	2.31	2.09	15.4	8.9	6.4
Rougher concentrate 2	33.1	6.5	116.2	93.70	2.76	2.68	6.8	4.7	3.6
Rougher conc. 1+2	107.3	21.1	282.4	94.60	2.45	2.27	22.2	13.6	10.0
Float tail	400.7	78.9	1672.8	88.90	4.17	5.48	77.8	86.4	90.0
Total	508.0	100.0	1955.2	90.10	3.81	4.80	100.0	100.0	100.0

Table 32: Test procedure and metallurgical balance for B122

Test No: B122

Sample: Wabush Spiral Concentrate

Project: CRDPJ379600-08

Grind size: 80% Passing 86um

Date: June 8, 2011

Pulp density: 16 % solids

Operator: Marc

Objective: Scoping bench flotation test of Wabush Spiral Concentrate using Sodium Oleate and Sodium Silicate. 500g Spiral Concentrate with 350ml distilled water ground for 35 minutes

STAGE	TIME (min)	pH	ADDITION		COMMENTS	Conc pulp weight, g
			Reagent	g/tonne		
Slurry		7.76			JKTeck flotation machine, 1200 rpm 500 g sample in 1.5 L stainless steel cell	
Condition	3	11.00	Sodium Oleate	200 (Total)	Adjust pH to 11, then add 50 mg of Sodium Oleate in 25 ml water	
Rougher flotation						
Rougher float 1	1				Air 3	551.7
Rougher float 2	2					674.6
Condition	3	10.61 11.00			Readjust pH to 11, then add 50mg of Sodium Oleate in 25ml water, no frother	
Rougher float 3	2				Air 7, 3 drops DF250	898.5
		10.53			Record final pH	
					tailings pulp	959.8

Product	Solid weight		Water weight (g)	Assay (%)			Distribution (%)		
	(g)	(%)		Fe2O3	MnO	SiO2	Fe2O3	MnO	SiO2
Rougher concentrate 1	237.3	47.5	314.4	96.00	1.60	1.52	49.8	24.8	18.5
Rougher concentrate 2	182.7	36.6	491.9	92.70	2.88	3.29	37.0	34.3	30.9
Rougher conc. 1+2	420.0	84.1	806.3	94.56	2.16	2.29	86.8	59.1	49.4
Rougher concentrate 3	70.2	14.1	828.3	77.50	7.47	11.80	11.9	34.2	42.5
Rougher conc. 1+2+3	490.2	98.1	1634.6	92.12	2.92	3.65	98.6	93.3	91.9
Float tail	9.4	1.9	950.4	66.00	11.00	16.70	1.4	6.7	8.1
Total	499.6	100.0	2585.0	91.63	3.07	3.90	100.0	100.0	100.0

Table 33: Test procedure and metallurgical balance for B123

Test No: B123

Sample: Wabush Spiral Concentrate

Project: CRDPJ379600-08

Grind size: 80% Passing 117um

Date: June 9, 2011

Pulp density: 19 % solids

Operator: Marc

Objective: Scoping bench flotation test of Wabush Spiral Concentrate using Sodium Oleate and Sodium Silicate. 500g Spiral Concentrate with 350ml distilled water ground for 25 minutes

STAGE	TIME (min)	pH	ADDITION		COMMENTS	Conc pulp weight, g
			Reagent	g/tonne		
Slurry		7.78			JKTeck flotation machine, 1200 rpm 500 g sample in 1.5 L stainless steel cell	
Condition	3	9.00	Potato Starch	250	12.5 ml 1 wt% solution, no pH adjustment necessary with starch addition	
Condition	3	9.00	Sodium Oleate	200 (Total)	Readjust pH to 9, then add 50 mg of Sodium Oleate in 25 ml water	
Rougher flotation						
Rougher float 1	1				Airflow 2	523.1
Rougher float 2	2					505.2
Condition	3	8.51 9.00			Readjust pH to 9, then add 50mg of Sodium Oleate in 25ml water, no frother	
Rougher float 3	2				Airflow 2, 2 drops DF250	718.5
		8.25			Record final pH	
					tailings pulp	827.0

Product	Solid weight		Water weight (g)	Assay (%)			Distribution (%)		
	(g)	(%)		Fe2O3	MnO	SiO2	Fe2O3	MnO	SiO2
Rougher concentrate 1	288.3	57.8	234.8	97.80	0.87	0.80	62.1	15.6	11.4
Rougher concentrate 2	124.4	24.9	380.8	91.10	3.44	3.35	25.0	26.8	20.6
Rougher conc. 1+2	412.7	82.7	615.6	95.78	1.64	1.57	87.1	42.5	32.1
Rougher concentrate 3	80.3	16.1	638.2	67.50	10.90	16.40	11.9	54.9	65.2
Rougher conc. 1+2+3	493.0	98.8	1253.8	91.17	3.15	3.98	99.0	97.4	97.3
Float tail	5.8	1.2	821.2	75.10	7.17	9.35	1.0	2.6	2.7
Total	498.8	100.0	2075.0	90.99	3.20	4.05	100.0	100.0	100.0

Table 34: Test procedure and metallurgical balance for B124

Test No: B124

Sample: Wabush Spiral Concentrate

Project: CRDPJ379600-08

Grind size: 80% Passing 117µm

Date: July 5, 2011

Pulp density: 17 % solids

Operator: Marc

Objective: Scoping bench flotation test of Wabush Spiral Concentrate using Sodium Oleate and Sodium Silicate. 500g Spiral Concentrate with 350ml distilled water ground for 25 minutes

STAGE	TIME (min)	pH	ADDITION		COMMENTS	Conc pulp weight, g
			Reagent	g/tonne		
Slurry		7.83			JKTeck flotation machine, 1200 rpm 500 g sample in 1.5 L stainless steel cell	
Condition	3	11.00	CuSO4	50	Adjust pH to 11, add 25mg CuSO4 directly to slurry	
Condition	3	11.00	Sodium Oleate	200 (Total)	Adjust pH to 11, then add 50 mg of Sodium Oleate in 25 ml water	
Rougher flotation						
Rougher float 1	1				Air 3	717.1
Rougher float 2	2					531.9
Condition	3	10.62 11.00			Readjust pH to 11, then add 50mg of Sodium Oleate in 25ml water, no frother	
Rougher float 3	2				Air 5	593.1
		10.78			Record final pH	
					tailings pulp	984.2

Product	Solid weight		Water weight (g)	Assay (%)			Distribution (%)		
	(g)	(%)		Fe2O3	MnO	SiO2	Fe2O3	MnO	SiO2
Rougher concentrate 1	350.3	71.2	366.8	95.10	2.24	1.54	74.8	46.7	24.7
Rougher concentrate 2	107.2	21.8	424.7	84.00	5.68	8.04	20.2	36.2	39.5
Rougher conc. 1+2	457.5	93.0	791.5	92.50	3.05	3.06	95.0	82.9	64.2
Rougher concentrate 3	28.2	5.7	564.9	66.20	7.73	22.20	4.2	13.0	28.7
Rougher conc. 1+2+3	485.7	98.7	1356.4	90.97	3.32	4.17	99.2	95.9	92.9
Float tail	6.2	1.3	978.0	57.70	11.20	25.10	0.8	4.1	7.1
Total	491.9	100.0	2334.4	90.55	3.42	4.44	100.0	100.0	100.0

Table 35: Test procedure and metallurgical balance for B125

Test No: B125

Sample: Wabush Spiral Concentrate

Project: CRDPJ379600-08

Grind size: 80% Passing 86um

Date: July 5, 2011

Pulp density: 19 % solids

Operator: Marc

Objective: Scoping bench flotation test of Wabush Spiral Concentrate using Sodium Oleate and Sodium Silicate. 500g Spiral Concentrate with 350ml distilled water ground for 35 minutes

STAGE	TIME (min)	pH	ADDITION		COMMENTS	Conc pulp weight, g
			Reagent	g/tonne		
Slurry		7.62			JKTeck flotation machine, 1200 rpm 500 g sample in 1.5 L stainless steel cell	
Condition	3	9.00	Potato Starch	250	12.5 ml 1 wt% solution, no pH adjustment necessary with starch addition	
Condition	3	9.00	Sodium Oleate	200 (Total)	Adjust pH to 11, then add 50 mg of Sodium Oleate in 25 ml water	
Rougher flotation						
Rougher float 1	1				Air 5	577.3
Rougher float 2	2					510.5
Condition	3	8.45 9.00			Readjust pH to 11, then add 50mg of Sodium Oleate in 25ml water, 5 drops DF-250	
Rougher float 3	2				Air 5	603.1
		8.25			Record final pH	
					tailings pulp	870.8

Product	Solid weight		Water weight (g)	Assay (%)			Distribution (%)		
	(g)	(%)		Fe2O3	MnO	SiO2	Fe2O3	MnO	SiO2
Rougher concentrate 1	299.6	60.3	277.7	97.00	1.40	1.13	64.2	25.4	16.1
Rougher concentrate 2	132.8	26.7	377.7	88.60	4.71	4.32	26.0	37.8	27.2
Rougher conc. 1+2	432.4	87.0	655.4	94.42	2.42	2.11	90.3	63.2	43.3
Rougher concentrate 3	57.2	11.5	545.9	67.40	9.58	18.80	8.5	33.1	51.0
Rougher conc. 1+2+3	489.6	98.5	1201.3	91.26	3.25	4.06	98.8	96.4	94.3
Float tail	7.6	1.5	863.2	72.00	7.88	15.60	1.2	3.6	5.7
Total	497.2	100.0	2064.5	90.97	3.32	4.24	100.0	100.0	100.0

Table 36: Test procedure and metallurgical balance for B126

Test No: B126

Sample: Wabush Spiral Concentrate
Grind size: NA
Pulp density: 16 % solids

Project: CRDPJ379600-08

Date: July 7, 2011

Operator: Marc

Objective: Scoping bench flotation test of Wabush Spiral Concentrate using Sodium Oleate and Sodium Silicate. 500g Spiral Concentrate with 350ml distilled water ground for 15 minutes

STAGE	TIME (min)	pH	ADDITION		COMMENTS	Conc pulp weight, g
			Reagent	g/tonne		
Slurry		7.45			JKTeck flotation machine, 1400 rpm 500 g sample in 1.5 L stainless steel cell	
Condition	3	11.00	Sodium Oleate	200 (Total)	Adjust pH to 11, then add 50 mg of Sodium Oleate in 25 ml water	
Rougher flotation						
Rougher float 1	1				Air 3	724.7
Rougher float 2	2					737.6
Condition	3	10.42 11.00			Readjust pH to 11, then add 50mg of Sodium Oleate in 25ml water, no frother	
Rougher float 3	2				Air 3	975.8
		10.60			Record final pH	
					tailings pulp	740.7

Product	Solid weight		Water weight (g)	Assay (%)			Distribution (%)		
	(g)	(%)		Fe2O3	MnO	SiO2	Fe2O3	MnO	SiO2
Rougher concentrate 1	233.1	47.3	491.6	94.30	2.05	2.84	48.7	31.2	32.7
Rougher concentrate 2	112.9	22.9	624.7	91.30	2.83	4.65	22.9	20.8	25.9
Rougher conc. 1+2	346.0	70.2	1116.3	93.32	2.30	3.43	71.6	52.0	58.6
Rougher concentrate 3	113.8	23.1	862.0	89.70	2.93	5.83	22.6	21.8	32.7
Rougher conc. 1+2+3	459.8	93.3	1978.3	92.42	2.46	4.02	94.2	73.8	91.3
Float tail	33.2	6.7	707.5	78.70	12.10	5.32	5.8	26.2	8.7
Total	493.0	100.0	2685.8	91.50	3.11	4.11	100.0	100.0	100.0

Table 37: Test procedure and metallurgical balance for B127

Test No: B127

Sample: Wabush Spiral Concentrate
 Grind size: 80% Passing 117um
 Pulp density: 20 % solids

Project: CRDPJ379600-08
 Date: August 29, 2011
 Operator: Marc

Objective: Scoping bench flotation test of Wabush Spiral Concentrate using Sodium Oleate and Sodium Silicate. 500g Spiral Concentrate with 350ml distilled water ground for 25 minutes

STAGE	TIME (min)	pH	ADDITION		COMMENTS	Conc pulp weight, g
			Reagent	g/tonne		
Slurry		7.67			JKTeck flotation machine, 1200 rpm 500 g sample in 1.5 L stainless steel cell	
Condition	3	9.65	Sodium Silicate	250	125 milligrams of Na ₂ SiO ₃ ·5H ₂ O in 25 ml water added, conditioned at natural pH	
Condition	3	10.15				
Condition	3	8.00	Potato Starch	250	12.5 ml 1 wt% solution, no pH adjustment	
Condition	3	8.00	Sodium Oleate	100	Readjust pH to 8, then add 50 mg of Sodium Oleate in 25 ml water	
Rougher flotation						
Rougher float 1	1				Air 3-4	542.5
Rougher float 2	3					564.0
Condition	3	7.93				
Condition	3	8.00	Potato Starch	100	5 ml 1 wt% solution	
Condition	3	8.00	Sodium Oleate	100	Readjust pH to 8, then add 50 mg of Sodium Oleate in 25 ml water 5 drops DF-250	
Rougher float 3	2				Air 4, 1min, then 7 1min	373.8
		7.92			Record final pH	
					tailings pulp	918.3

Product	Solid weight		Water weight (g)	Assay (%)			Distribution (%)		
	(g)	(%)		Fe ₂ O ₃	MnO	SiO ₂	Fe ₂ O ₃	MnO	SiO ₂
Rougher concentrate 1	304.3	62.2	238.2	96.50	1.61	1.07	66.8	27.1	14.1
Rougher concentrate 2	117.4	24.0	446.6	86.40	5.57	4.99	23.1	36.2	25.4
Rougher conc. 1+2	421.7	86.1	684.8	93.69	2.71	2.16	89.8	63.3	39.6
Rougher concentrate 3	38.6	7.9	335.2	58.20	11.00	27.50	5.1	23.5	46.1
Rougher conc. 1+2+3	460.3	94.0	1020.0	90.71	3.41	4.29	94.9	86.7	85.7
Float tail	29.2	6.0	889.1	76.10	8.21	11.30	5.1	13.3	14.3
Total	489.5	100.0	1909.1	89.84	3.69	4.70	100.0	100.0	100.0

Table 38: Test procedure and metallurgical balance for B128

Test No: B128

Sample: Wabush Spiral Concentrate

Project: CRDPJ379600-08

Grind size:

Date: September 24, 2011

Pulp density: 15 % solids

Operator: Marc

Objective: Scoping bench flotation test of Wabush Spiral Concentrate using Sodium Oleate.
500g Spiral Concentrate with 350ml distilled water ground for 30 minutes

STAGE	TIME (min)	pH	ADDITION		COMMENTS	Conc pulp weight, g
			Reagent	g/tonne		
Slurry		7.40			JKTeck flotation machine, 1200 rpm 500 g sample in 1.5 L stainless steel cell	
Condition	3	11.00	Sodium Oleate	100	Adjust pH to 11, then add 50 mg of Sodium Oleate in 25 ml water	
Rougher flotation						
Rougher float 1	1				Air 4, lots of froth	711.2
Rougher float 2	3					726.3
Condition	3	10.27 11.00	Sodium Oleate	50	Readjust pH to 11, then add 25 mg of Sodium Oleate in 25 ml water	
Rougher float 3	2				2 drops DF-250, Air 4, Heavy Froth	925.5
		10.85			Record final pH	
					tailings pulp	834.2

Product	Solid weight		Water weight (g)	Assay (%)			Distribution (%)		
	(g)	(%)		Fe2O3	MnO	SiO2	Fe2O3	MnO	SiO2
Rougher concentrate 1	232.1	47.3	479.1	93.20	2.63	2.73	49.1	33.6	26.9
Rougher concentrate 2	92.1	18.8	634.2	87.60	4.07	6.22	18.3	20.7	24.3
Rougher conc. 1+2	324.2	66.1	1113.3	91.61	3.04	3.72	67.5	54.3	51.2
Rougher concentrate 3	59.1	12.0	866.4	86.20	3.98	8.30	11.6	13.0	20.8
Rougher conc. 1+2+3	383.3	78.1	1979.7	90.78	3.18	4.43	79.0	67.3	72.0
Float tail	107.2	21.9	727.0	86.10	5.54	6.15	21.0	32.7	28.0
Total	490.5	100.0	2706.7	89.75	3.70	4.80	100.0	100.0	100.0

Table 39: Test procedure and metallurgical balance for B129

Test No: B129

Sample: Wabush Spiral Concentrate

Project: CRDPJ379600-08

Grind size: 80% passing 117um

Date: September 24, 2011

Pulp density: 16 % solids

Operator: Marc

Objective: Scoping bench flotation test of Wabush Spiral Concentrate using Sodium Oleate.
500g Spiral Concentrate with 350ml distilled water ground for 25 minutes

STAGE	TIME (min)	pH	ADDITION		COMMENTS	Conc pulp weight, g
			Reagent	g/tonne		
Slurry		7.38			JKTeck flotation machine, 1200 rpm 500 g sample in 1.5 L stainless steel cell	
Condition	3	12.00	Sodium Oleate	100	Adjust pH to 12, then add 50 mg of Sodium Oleate in 25 ml water	
Rougher flotation						
Rougher float 1	1				Air 4, thick red froth	519.3
Rougher float 2	3					614.2
Condition	3	11.60 12.00	Sodium Oleate	50	Readjust pH to 8, then add 25 mg of Sodium Oleate in 25 ml water	
Rougher float 3	2				Air 4, 3 drops DF-250, Thick red froth	811.6
		11.75			Record final pH	
					tailings pulp	1228.1

Product	Solid weight		Water weight (g)	Assay (%)			Distribution (%)		
	(g)	(%)		Fe2O3	MnO	SiO2	Fe2O3	MnO	SiO2
Rougher concentrate 1	64.5	12.9	454.8	86.30	4.37	6.08	12.5	16.7	18.2
Rougher concentrate 2	57.2	11.5	557.0	85.20	4.10	5.84	10.9	13.9	15.5
Rougher conc. 1+2	121.7	24.4	1011.8	85.78	4.24	5.97	23.4	30.6	33.7
Rougher concentrate 3	56.0	11.2	755.6	84.10	3.96	6.15	10.5	13.1	16.0
Rougher conc. 1+2+3	177.7	35.6	1767.4	85.25	4.15	6.02	33.9	43.7	49.7
Float tail	320.9	64.4	907.2	92.00	2.96	3.38	66.1	56.3	50.3
Total	498.6	100.0	2674.6	89.60	3.39	4.32	100.0	100.0	100.0

Table 40: Test procedure and metallurgical balance for B130

Test No: B130

Sample: Wabush Spiral Concentrate

Project: CRDPJ379600-08

Grind size: 80% passing 117µm

Date: October 4, 2011

Pulp density: 21 % solids

Operator: Marc

Objective: Scoping bench flotation test of Wabush Spiral Concentrate using Sodium Oleate.
500g Spiral Concentrate with 350ml distilled water ground for 25 minutes

STAGE	TIME (min)	pH	ADDITION		COMMENTS	Conc pulp weight, g
			Reagent	g/tonne		
Slurry		7.56			JKTeck flotation machine, 1200 rpm 500 g sample in 1.5 L stainless steel cell	
Condition	3		Potato Starch	250	Adjust pH to 9, add 12.5 ml 1 wt% solution	
Condition	3	9.00	Sodium Oleate	100	Adjust pH to 9, then add 50 mg of Sodium Oleate in 25 ml water	
Condition	3		Kerosene	100.00	50 mg kerosene emulsified in 100 ml H2O (15 drops)	
Rougher flotation					Air 4, stable froth	
Rougher float 1	1					593.4
Rougher float 2	3					375.3
		8.43			Record final pH	
					tailings pulp	1344.6

Product	Solid weight		Water weight (g)	Assay (%)			Distribution (%)		
	(g)	(%)		Fe2O3	MnO	SiO2	Fe2O3	MnO	SiO2
Rougher concentrate 1	330.6	67.3	262.8	97.90	1.27	1.14	71.8	27.1	18.3
Rougher concentrate 2	86.6	17.6	288.7	89.00	4.46	4.61	17.1	24.9	19.4
Rougher conc. 1+2	417.2	84.9	551.5	96.05	1.93	1.86	89.0	52.0	37.8
Float tail	74.3	15.1	1270.3	67.00	10.00	17.20	11.0	48.0	62.2
Total	491.5	100.0	1821.8	91.66	3.15	4.18	100.0	100.0	100.0

Table 41: Test procedure and metallurgical balance for B131

Test No: B131

Sample: Wabush Spiral Concentrate

Project: CRDPJ379600-08

Grind size: 80% passing 117um

Date: October 4, 2011

Pulp density: 20 % solids

Operator: Marc

Objective: Scoping bench flotation test of Wabush Spiral Concentrate using Sodium Oleate.
500g Spiral Concentrate with 350ml distilled water ground for 25 minutes

STAGE	TIME (min)	pH	ADDITION		COMMENTS	Conc pulp weight, g
			Reagent	g/tonne		
Slurry		7.46			JKTeck flotation machine, 1200 rpm 500 g sample in 1.5 L stainless steel cell	
Condition	3		NaH2PO4	50	Add 25mg NaH2PO4 to slurry	
Condition	3	9.00	Sodium Oleate	100	Readjust pH to 9, then add 50 mg of Sodium Oleate in 25 ml water	
Condition	3		Kerosene	100	50 mg kerosene emulsified in 100 ml H2O (15 drops)	
Rougher flotation						
Rougher float 1	1				Air 4	635.4
Rougher float 2	3					623.5
		8.55			Record final pH	
					tailings pulp	1196.9

Product	Solid weight		Water weight (g)	Assay (%)			Distribution (%)		
	(g)	(%)		Fe2O3	MnO	SiO2	Fe2O3	MnO	SiO2
Rougher concentrate 1	326.9	65.5	308.5	96.10	2.02	1.58	69.2	37.5	23.1
Rougher concentrate 2	150.8	30.2	472.7	82.70	5.91	9.56	27.5	50.6	64.5
Rougher conc. 1+2	477.7	95.8	781.2	91.87	3.25	4.10	96.6	88.0	87.7
Float tail	21.2	4.2	1175.7	71.90	9.94	13.00	3.4	12.0	12.3
Total	498.9	100.0	1956.9	91.02	3.53	4.48	100.0	100.0	100.0

Table 42: Test procedure and metallurgical balance for B132

Test No: B132

Sample: Wabush Spiral Concentrate

Project: CRDPJ379600-08

Grind size: 80% passing 117um

Date: November 15, 2011

Pulp density: 27 % solids

Operator: Marc

Objective: Scoping bench flotation test of Wabush Spiral Concentrate using Sodium Oleate.
500g Spiral Concentrate with 350ml distilled water ground for 25 minutes

STAGE	TIME (min)	pH	ADDITION		COMMENTS	Conc pulp weight, g
			Reagent	g/tonne		
Slurry		7.51			JKTeck flotation machine, 1200 rpm 500 g sample in 1.5 L stainless steel cell	
Condition	3	10.70 11.00	Potato Starch	1000	50 ml 1 wt% solution, no pH adjustment necessary with starch addition	
Condition	3	11.00	CaCl2	50ppm Ca2+	207.7 mg CaCl2 anhydrous	
Condition	3	11.00	Sodium Oleate	100	Adjust pH to 11, then add 50 mg of Sodium Oleate in 25 ml water	
Rougher flotation						
Rougher float 1	1				Air 10, 10 drops MBC	175.7
Rougher float 2	1				Air 10, 10 drops MBC, possible spill over	232.7
					Record final pH	
					tailings pulp	1362.2

Product	Solid weight		Water weight (g)	Assay (%)			Distribution (%)		
	(g)	(%)		Fe2O3	MnO	SiO2	Fe2O3	MnO	SiO2
Rougher concentrate 1	23.3	4.8	152.4	78.40	5.81	12.50	4.4	5.4	9.2
Rougher concentrate 2	18.8	3.9	213.9	80.80	6.54	9.21	3.6	4.9	5.5
Rougher conc. 1+2	42.1	8.7	366.3	79.47	6.14	11.03	8.0	10.4	14.7
Float tail	444.4	91.3	917.8	86.50	5.02	6.08	92.0	89.6	85.3
Total	486.5	100.0	1284.1	85.89	5.12	6.51	100.0	100.0	100.0

Table 43: Test procedure and metallurgical balance for B133

Test No: B133

Sample: Wabush Spiral Concentrate

Project: CRDPJ379600-08

Grind size: 80% passing 117um

Date: November 16, 2011

Pulp density: 24 % solids

Operator: Marc

Objective: Scoping bench flotation test of Wabush Spiral Concentrate using Sodium Oleate.
500g Spiral Concentrate with 350ml distilled water ground for 25 minutes

STAGE	TIME (min)	pH	ADDITION		COMMENTS	Conc pulp weight, g
			Reagent	g/tonne		
Slurry		7.69			JKTeck flotation machine, 1200 rpm 500 g sample in 1.5 L stainless steel cell	
Condition	3	7.00	Armeen 18D	10	5 ml 0.1 wt% solution	
Rougher flotation						
Rougher float 1	1	7.00			Air 5, 2 drops MIBC	203.4
Condition	3	7.00	Armeen 18D	10		
Rougher float 2	1				Air 5, no frother	110.4
Condition	3	7.00	Armeen 18D	10		
Rougher float 3	1				Air 6, no frother	209.9
		6.93			Record final pH	
					tailings pulp	1466.0

Product	Solid weight		Water weight (g)	Assay (%)			Distribution (%)		
	(g)	(%)		Fe2O3	MnO	SiO2	Fe2O3	MnO	SiO2
Rougher concentrate 1	18.7	3.9	184.7	86.20	5.34	5.18	3.7	5.5	4.2
Rougher concentrate 2	8.2	1.7	102.2	86.30	5.58	5.53	1.6	2.5	2.0
Rougher conc. 1+2	26.9	5.5	286.9	86.23	5.41	5.29	5.3	8.0	6.2
Rougher concentrate 3	14.8	3.0	195.1	85.60	5.36	6.27	2.9	4.3	4.0
Rougher conc. 1+2+3	41.7	8.6	482.0	86.01	5.39	5.64	8.2	12.3	10.2
Float tail	443.8	91.4	1022.2	90.00	3.62	4.65	91.8	87.7	89.8
Total	485.5	100.0	1504.2	89.66	3.77	4.73	100.0	100.0	100.0

Table 44: Test procedure and metallurgical balance for B135

Test No: B135

Sample: Wabush Spiral Concentrate

Project: CRDPJ379600-08

Grind size: 80% passing 117um

Date: November 19, 2011

Pulp density: 24 % solids

Operator: Marc

Objective: Scoping bench flotation test of Wabush Spiral Concentrate using Sodium Oleate.
500g Spiral Concentrate with 350ml distilled water ground for 25 minutes

STAGE	TIME (min)	pH	ADDITION		COMMENTS	Conc pulp weight, g
			Reagent	g/tonne		
Slurry		7.60			JKTeck flotation machine, 1200 rpm 500 g sample in 1.5 L stainless steel cell	
Condition	3	10.00	Potato Starch	1500	75 ml 1 wt% solution	
Condition	3	10.00	Armeen 18D	20	10 ml 0.1wt% solution	
Rougher flotation						
Rougher float 1	2				Air 10, 10 drops MIBC	339.6
Condition	3	9.57 10.00	Armeen 18D	40	20ml 0.1 wt% solution	
Rougher float 2	3				Air 10, 10 drops MIBC	249.2
Condition	3	9.50 10.00	Armeen 18D	100	50 ml 0.1 wt% solution	
Rougher float 3	3				Air 10, no MIBC	224.5
		9.65			Record final pH	
					tailings pulp	1255.2

Product	Solid weight		Water weight (g)	Assay (%)			Distribution (%)		
	(g)	(%)		Fe2O3	MnO	SiO2	Fe2O3	MnO	SiO2
Rougher concentrate 1	22.6	4.6	317.0	68.80	4.28	23.80	3.5	5.8	25.0
Rougher concentrate 2	19.3	3.9	229.9	54.80	3.34	40.00	2.4	3.9	35.9
Rougher conc. 1+2	41.9	8.5	546.9	62.35	3.85	31.26	5.9	9.7	61.0
Rougher concentrate 3	22.0	4.5	202.5	68.40	4.46	23.90	3.4	5.9	24.5
Rougher conc. 1+2+3	63.9	13.0	749.4	64.43	4.06	28.73	9.3	15.7	85.4
Float tail	428.2	87.0	827.0	94.20	3.26	0.73	90.7	84.3	14.6
Total	492.1	100.0	1576.4	90.33	3.36	4.37	100.0	100.0	100.0

Table 45: Test procedure and metallurgical balance for B136

Test No: B136

Sample: Wabush Spiral Concentrate

Project: CRDPJ379600-08

Grind size: 80% passing 117um

Date: December 8, 2011

Pulp density: 18 % solids

Operator: Marc

Objective: Scoping bench flotation test of Wabush Spiral Concentrate using Sodium Oleate.
500g Spiral Concentrate with 350ml distilled water ground for 25 minutes

STAGE	TIME (min)	pH	ADDITION		COMMENTS	Conc pulp weight, g
			Reagent	g/tonne		
Slurry		7.54			JKTeck flotation machine, 1200 rpm 500 g sample in 1.5 L stainless steel cell	
Condition	3	11.00	Sodium Oleate	100	Adjust pH to 11, then add 50 mg of Sodium Oleate in 25ml of water	
Rougher flotation						
Rougher float 1	2				Air 5, no frother, thick stable froth	891.1
Condition	3	10.67	Potato Starch	250	12.5ml 1 wt% solution	
Rougher float 2	2	11.00			Air 5, not frother, strong white froth	437.7
Condition	3	10.64	Sodium Oleate	100	Adjust pH to 11, then add 50 mg of Sodium Oleate in 25ml of water	
Rougher float 3	2	11.00			Air 5, no frother, thick reddish/white froth	766.0
		10.77			Record final pH	
					tailings pulp	621.1

Product	Solid weight		Water weight (g)	Assay (%)			Distribution (%)		
	(g)	(%)		Fe2O3	MnO	SiO2	Fe2O3	MnO	SiO2
Rougher concentrate 1	359.1	73.4	532.0	94.30	2.49	2.25	76.7	49.7	35.6
Rougher concentrate 2	10.1	2.1	427.6	71.50	7.49	17.00	1.6	4.2	7.6
Rougher conc. 1+2	369.2	75.4	959.6	93.68	2.63	2.65	78.3	53.9	43.1
Rougher concentrate 3	31.1	6.4	734.9	78.50	5.77	12.60	5.5	10.0	17.2
Rougher conc. 1+2+3	400.3	81.8	1694.5	92.50	2.87	3.43	83.9	63.9	60.4
Float tail	89.2	18.2	531.9	79.80	7.27	10.10	16.1	36.1	39.6
Total	489.5	100.0	2226.4	90.18	3.67	4.64	100.0	100.0	100.0

Table 46: Test procedure and metallurgical balance for B137

Test No: B137

Sample: Wabush Spiral Concentrate
 Grind size: 80% passing 117um
 Pulp density: 17 % solids

Project: CRDPJ379600-08
 Date: December 8, 2011
 Operator: Marc

Objective: Scoping bench flotation test of Wabush Spiral Concentrate using Sodium Oleate.
 500g Spiral Concentrate with 350ml distilled water ground for 25 minutes

STAGE	TIME (min)	pH	ADDITION		COMMENTS	Conc pulp weight, g
			Reagent	g/tonne		
Slurry		7.31			JKTeck flotation machine, 1200 rpm 500 g sample in 1.5 L stainless steel cell	
Condition	3	11.00	Sodium Oleate	100	Adjust pH to 11, then add 50 mg of Sodium Oleate in 25ml of water	
Rougher flotation						
Rougher float 1	2				Air 5, no frother, stable froth	924.0
Condition	3	10.63 11.00	Potato Starch	500	25ml 1 wt% solution	
Rougher float 2	2				Air 5, no frother, stable reddish froth Thinner froth than B136	413.8
Condition	3	10.82 11.00	Sodium Oleate	100	Adjust pH to 11, then add 50 mg of Sodium Oleate in 25ml of water	
Rougher float 3	2				Air 5, no frother, thick red froth	854.8
		10.85			Record final pH	
					tailings pulp	690.3

Product	Solid weight		Water weight (g)	Assay (%)			Distribution (%)		
	(g)	(%)		Fe2O3	MnO	SiO2	Fe2O3	MnO	SiO2
Rougher concentrate 1	341.7	70.5	582.3	93.20	2.66	3.08	74.6	42.4	38.5
Rougher concentrate 2	11.9	2.5	401.9	69.10	9.52	16.10	1.9	5.3	7.0
Rougher conc. 1+2	353.6	73.0	984.2	92.39	2.89	3.52	76.6	47.6	45.5
Rougher concentrate 3	27.6	5.7	827.2	67.40	9.64	18.10	4.4	12.4	18.3
Rougher conc. 1+2+3	381.2	78.6	1811.4	90.58	3.38	4.57	80.9	60.1	63.7
Float tail	103.5	21.4	586.8	78.60	8.28	9.58	19.1	39.9	36.3
Total	484.7	100.0	2398.2	88.02	4.43	5.64	100.0	100.0	100.0

Table 47: Test procedure and metallurgical balance for B138

Test No: B138

Sample: Wabush Spiral Concentrate

Project: CRDPJ379600-08

Grind size: 80% passing 117um

Date: December 12, 2011

Pulp density: 11 % solids

Operator: Marc

Objective: Scoping bench flotation test of Wabush Spiral Concentrate using Sodium Oleate.
500g Spiral Concentrate with 350ml distilled water ground for 25 minutes

STAGE	TIME (min)	pH	ADDITION		COMMENTS	Conc pulp weight, g
			Reagent	g/tonne		
Slurry		7.68			JKTeck flotation machine, 1200 rpm 500 g sample in 1.5 L stainless steel cell	
Condition	3	11.00	Sodium Oleate	100	Adjust pH to 11, then add 50 mg of Sodium Oleate in 25ml of water	
Rougher flotation						
Rougher float 1	2				Air 5, no frother	941.8
Condition	3	10.78 11.00	Potato Starch	250	12.5 ml 1 wt% solution	
Rougher float 2	2				Air 5, no frother	481.4
Condition	3	10.73 11.00	Sodium Oleate	100	Adjust pH to 11, then add 50 mg of Sodium Oleate in 25ml of water	
Rougher float 3	4				Air 5, no frother	1142.7
Condition	3	10.67 11.00	Sodium Oleate	100	Adjust pH to 11, then add 50 mg of Sodium Oleate in 25ml of water	
Rougher float 4	4				Air 5, no frother	1102.2
		10.82			Record final pH	
					tailings pulp	819.9

Product	Solid weight		Water weight (g)	Assay (%)			Distribution (%)		
	(g)	(%)		Fe2O3	MnO	SiO2	Fe2O3	MnO	SiO2
Rougher concentrate 1	403.5	82.3	538.3	95.30	2.08	1.82	85.7	53.4	37.1
Rougher concentrate 2	7.2	1.5	474.2	68.10	8.31	19.20	1.1	3.8	7.0
Rougher conc. 1+2	410.7	83.8	1012.5	94.83	2.19	2.12	86.8	57.2	44.1
Rougher concentrate 3	30.8	6.3	1111.9	75.60	6.47	14.70	5.2	12.7	22.9
Rougher conc. 1+2+3	441.5	90.1	2124.4	93.48	2.49	3.00	92.0	69.8	67.0
Rougher concentrate 4	29.4	6.0	1072.9	80.10	4.98	12.50	5.2	9.3	18.6
Rougher conc. 1+2+3+4	470.8	96.0	3197.3	92.65	2.64	3.59	97.3	79.1	85.6
Float tail	19.4	4.0	800.5	63.10	16.90	14.70	2.7	20.9	14.4
Total	490.2	100.0	3997.8	91.48	3.21	4.03	100.0	100.0	100.0

Table 48: Test procedure and metallurgical balance for B139

Test No: B139

Sample: Wabush Spiral Concentrate

Project: CRDPJ379600-08

Grind size: 80% passing 117um

Date: December 13, 2011

Pulp density: 11 % solids

Operator: Marc

Objective: Scoping bench flotation test of Wabush Spiral Concentrate using Sodium Oleate.
500g Spiral Concentrate with 350ml distilled water ground for 25 minutes

STAGE	TIME (min)	pH	ADDITION		COMMENTS	Conc pulp weight, g
			Reagent	g/tonne		
Slurry		7.62			JKTeck flotation machine, 1200 rpm 500 g sample in 1.5 L stainless steel cell	
Condition	3	11.00	Sodium Oleate	100	Adjust pH to 11, then add 50 mg of Sodium Oleate in 25ml of water	
Rougher flotation						
Rougher float 1	2				Air 5, no frother	815.3
Condition	3	10.79	Potato Starch	150	7.5 ml 1 wt% solution	
Rougher float 2	2	11.00			Air 5, no frother	548.0
Condition	3	10.67	Sodium Oleate	100	Adjust pH to 11, then add 50 mg of Sodium Oleate in 25ml of water	
Rougher float 3	4	11.00			Air 5, no frother	1188.7
Condition	3	11.00	Sodium Oleate	100	Adjust pH to 11, then add 50 mg of Sodium Oleate in 25ml of water	
Rougher float 4	4				Air 5, no frother	1177.2
		10.73			Record final pH	
					tailings pulp	942.8

Product	Solid weight		Water weight (g)	Assay (%)			Distribution (%)		
	(g)	(%)		Fe2O3	MnO	SiO2	Fe2O3	MnO	SiO2
Rougher concentrate 1	369.2	75.1	446.1	95.90	1.79	1.67	79.3	38.8	28.6
Rougher concentrate 2	15.1	3.1	532.9	66.40	8.18	21.30	2.2	7.2	14.9
Rougher conc. 1+2	384.3	78.2	979.0	94.74	2.04	2.44	81.6	46.0	43.6
Rougher concentrate 3	82.1	16.7	1106.6	80.60	5.57	11.00	14.8	26.8	41.9
Rougher conc. 1+2+3	466.4	94.9	2085.6	92.25	2.66	3.95	96.4	72.8	85.5
Rougher concentrate 4	18.3	3.7	1158.9	68.30	13.00	14.00	2.8	14.0	11.9
Rougher conc. 1+2+3+4	484.7	98.6	3244.5	91.35	3.05	4.33	99.2	86.8	97.4
Float tail	7.0	1.4	935.8	49.60	32.30	7.99	0.8	13.2	2.6
Total	491.7	100.0	4180.3	90.75	3.47	4.38	100.0	100.0	100.0

Table 49: Test procedure and metallurgical balance for B140

Test No: B140

Sample: Wabush Spiral Concentrate

Project: CRDPJ379600-08

Grind size: 80% passing 117um

Date: January 16, 2012

Pulp density: 20 % solids

Operator: Marc

Objective: Scoping bench flotation test of Wabush Spiral Concentrate using Sodium Oleate.
500g Spiral Concentrate with 350ml distilled water ground for 25 minutes

STAGE	TIME (min)	pH	ADDITION		COMMENTS	Conc pulp weight, g
			Reagent	g/tonne		
Slurry		7.80			JKTeck flotation machine, 1200 rpm 500 g sample in 1.5 L stainless steel cell	
Condition	3	11.00	Sodium Oleate	100	Adjust pH to 11, then add 50 mg of Sodium Oleate in 25ml of water	
Rougher flotation						
Rougher float 1	3				Air 2 Used level scraper rather than handled scraper	757.3
Rougher float 2	3				Air 3	423.0
		10.45			Record final pH	
					tailings pulp	1259.0

Product	Solid weight		Water weight (g)	Assay (%)			Distribution (%)		
	(g)	(%)		Fe2O3	MnO	SiO2	Fe2O3	MnO	SiO2
Rougher concentrate 1	347.3	70.6	410.0	95.30	2.05	1.95	73.5	46.0	33.7
Rougher concentrate 2	101.5	20.6	321.5	88.40	4.24	5.60	19.9	27.8	28.2
Rougher conc. 1+2	448.8	91.2	731.5	93.74	2.55	2.78	93.4	73.9	61.9
Float tail	43.3	8.8	1215.7	68.60	9.33	17.70	6.6	26.1	38.1
Total	492.1	100.0	1947.2	91.53	3.14	4.09	100.0	100.0	100.0

Table 50: Test procedure and metallurgical balance for BI41

Test No: BI41

Sample: Wabush Spiral Concentrate

Project: CRDPJ379600-08

Grind size: 80% passing 117um

Date: January 23, 2012

Pulp density: 20 % solids

Operator: Marc

Objective: Scoping bench flotation test of Wabush Spiral Concentrate using Sodium Oleate.
500g Spiral Concentrate with 350ml distilled water ground for 25 minutes

STAGE	TIME (min)	pH	ADDITION		COMMENTS	Conc pulp weight, g
			Reagent	g/tonne		
Slurry		8.14	Potato Starch	250	12.5ml 1wt% solution in primary grinding	
					JKTeck flotation machine, 1200 rpm 500 g sample in 1.5 L stainless steel cell	
Condition	3	9.00	Sodium Oleate	100	Adjust pH to 9, then add 50 mg of Sodium Oleate in 25ml of water	
Rougher flotation						
Rougher float 1	3				Air 3	377.0
Rougher float 2	3				Air 5	152.8
Grind Tail	4	8.36			Grind Tails for 3min at 60% solids in ball mill (total slurry ~250g, sample was dried)	
		7.74	Potato Starch	50	2.5 ml 1wt% solution to prior to regrind	
Rougher float 3	2				Air 3, 2 drops MIBC	144.3
Condition	3	9.00	Sodium Oleate	50	Adjust pH to 9, then add 25 mg of Sodium Oleate in 25ml of water	
Rougher float 4	2				Air 3	213.3
Condition	3	8.73 9.00	Sodium Oleate	50	Adjust pH to 9, then add 25 mg of Sodium Oleate in 25ml of water	
Rougher float 5	2				Air 3	166.7
		8.58			Record final pH	
					tailings pulp	1491.7

Product	Solid weight		Water weight (g)	Assay (%)			Distribution (%)		
	(g)	(%)		Fe2O3	MnO	SiO2	Fe2O3	MnO	SiO2
Rougher concentrate 1	237.9	49.5	139.1	98.10	0.64	0.51	54.0	8.9	5.6
Rougher concentrate 2	70.3	14.6	82.5	96.80	1.33	0.87	15.7	5.4	2.8
Rougher conc. 1+2	308.2	64.1	221.6	97.80	0.80	0.59	69.7	14.3	8.5
Rougher concentrate 3	26.1	5.4	118.2	87.50	5.24	4.50	5.3	8.0	5.5
Rougher conc. 1+2+3	334.3	69.6	339.8	97.00	1.14	0.90	75.0	22.3	13.9
Rougher concentrate 4	92.2	19.2	121.1	79.70	8.33	8.05	17.0	44.8	34.5
Rougher conc. 1+2+3+4	426.5	88.8	460.9	93.26	2.70	2.44	92.0	67.0	48.4
Rougher concentrate 5	35.8	7.4	130.9	62.50	11.00	21.60	5.2	22.9	35.9
Rougher conc. 1+2+3+4+5	462.3	96.2	591.8	90.88	3.34	3.93	97.2	90.0	84.4
Float tail	18.3	3.8	1473.4	66.80	9.41	18.40	2.8	10.0	15.6
Total	480.6	100.0	1934.3	89.96	3.57	4.48	100.0	100.0	100.0

Table 51: Test procedure and metallurgical balance for B142

Test No: B142

Sample: Wabush Spiral Concentrate
Grind size: 80% passing 117um
Pulp density: 19 % solids

Project: CRDPJ379600-08

Date: January 21, 2012

Operator: Marc

Objective: Scoping bench flotation test of Wabush Spiral Concentrate using Sodium Oleate.
 500g Spiral Concentrate with 350ml distilled water ground for 25 minutes

STAGE	TIME (min)	pH	ADDITION		COMMENTS	Conc pulp weight, g
			Reagent	g/tonne		
Slurry		7.85			JKTeck flotation machine, 1200 rpm 500 g sample in 1.5 L stainless steel cell	
Condition	3	11.00	Sodium Oleate	100	Adjust pH to 11, then add 50 mg of Sodium Oleate in 25ml of water	
Rougher flotation						
Rougher float 1	2				Air 3 Used level scraper rather than handled scraper	648.8
Grind Tail	4	10.74			Grind Tails for 3min at 60% solids in ball mill (total slurry ~250g, sample was dried)	
Rougher float 2	1	8.91			Air 3, 2 drops MIBC	170.4
Condition	3	11.00	Sodium Oleate	50	Adjust pH to 11, then add 25 mg of Sodium Oleate in 25ml of water	
Rougher float 3	1				Air 3	361.1
Rougher float 4	1				Air 3	191.3
		10.80			Record final pH	
					tailings pulp	1196.7

Product	Solid weight		Water weight (g)	Assay (%)			Distribution (%)		
	(g)	(%)		Fe2O3	MnO	SiO2	Fe2O3	MnO	SiO2
Rougher concentrate 1	341.0	70.7	307.8	96.20	1.54	1.78	74.2	36.1	31.8
Rougher concentrate 2	11.7	2.4	158.7	84.20	5.22	7.42	2.2	4.2	4.5
Rougher conc. 1+2	352.7	73.2	466.5	95.80	1.66	1.97	76.4	40.3	36.3
Rougher concentrate 3	80.3	16.7	280.8	85.70	5.49	6.38	15.6	30.3	26.8
Rougher conc. 1+2+3	433.0	89.8	747.3	93.93	2.37	2.79	92.0	70.6	63.1
Rougher concentrate 4	17.5	3.6	173.8	81.20	6.44	9.35	3.2	7.7	8.6
Rougher conc. 1+2+3+4	450.5	93.5	921.1	93.43	2.53	3.04	95.2	78.3	71.7
Float tail	31.5	6.5	1165.2	67.80	10.00	17.20	4.8	21.7	28.3
Total	482.0	100.0	2086.3	91.76	3.02	3.97	100.0	100.0	100.0

Appendix II: Grinding and Passing Size

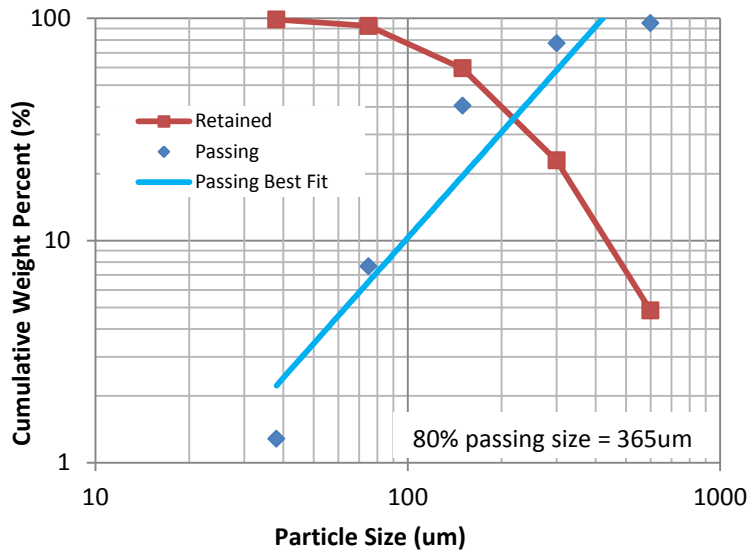


Figure 52: Size analysis of Wabush Spiral Concentrate as received with no grinding

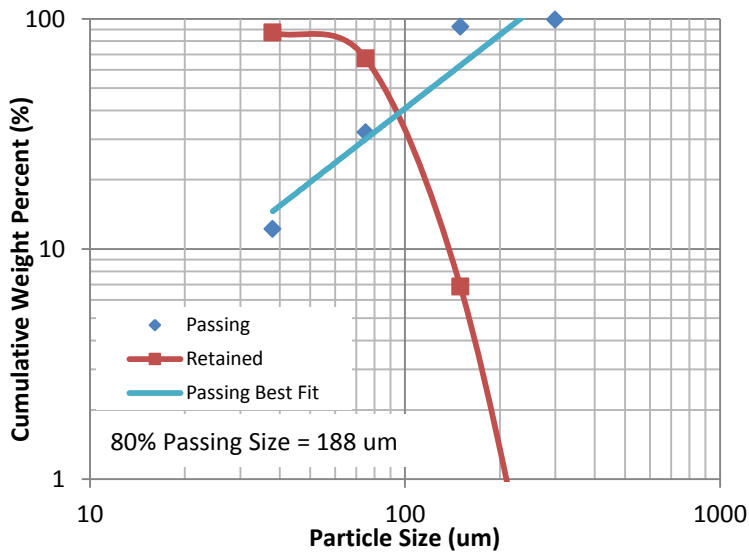


Figure 53: Size analysis of Wabush Spiral Concentrate after 20 minutes of dry grinding using a ball mill

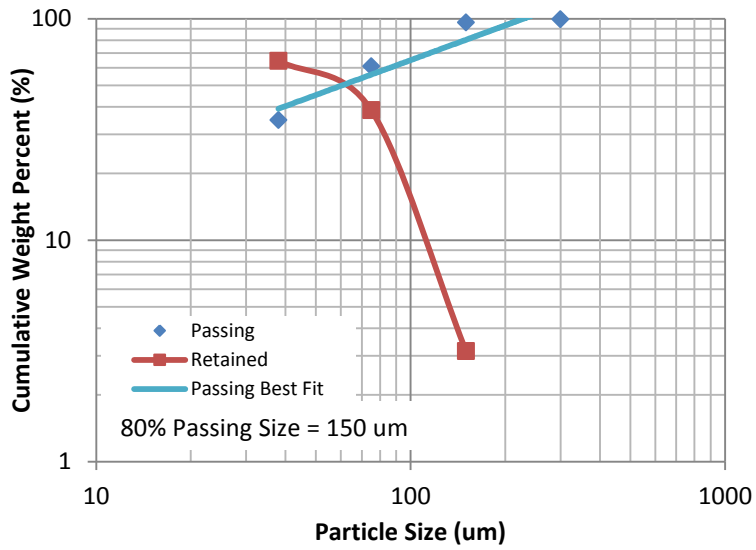


Figure 54: Size analysis of Wabush Spiral Concentrate after 25 minutes of dry grinding using a ball mill

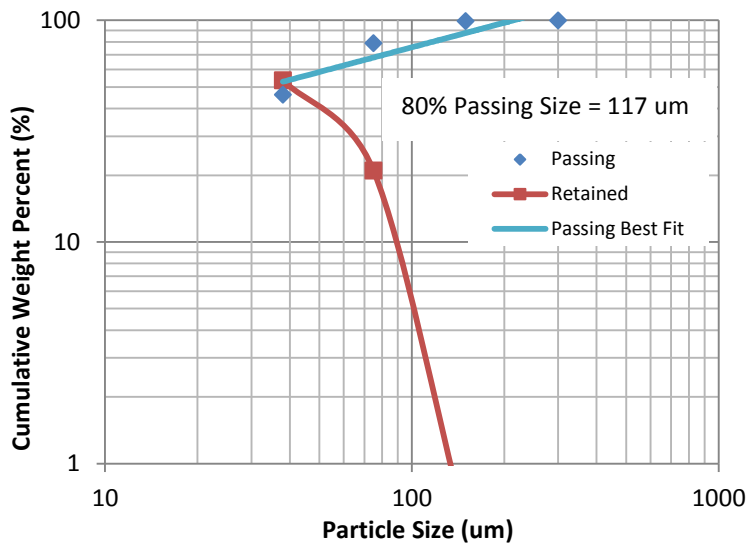
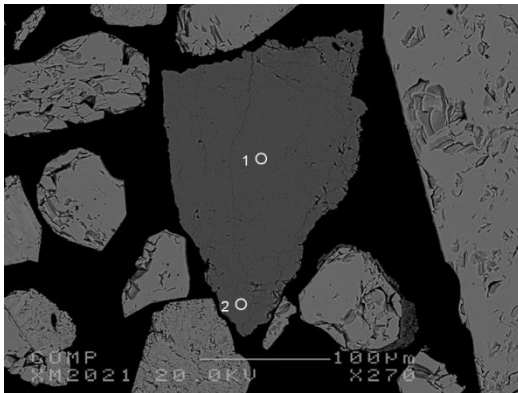


Figure 55: Size analysis of Wabush Spiral Concentrate after 35 minutes of wet grinding at 60% solids using a ball mill

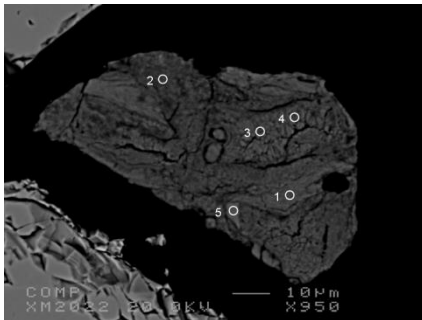
Appendix III: Mineralogical Analysis by CANMET

The content of a mineralogical study carried out on Wabush spiral concentrate and BI13 tails by Dr. Allen Pratt is included in this section. Details of the study can be found in Section 4.1.2.



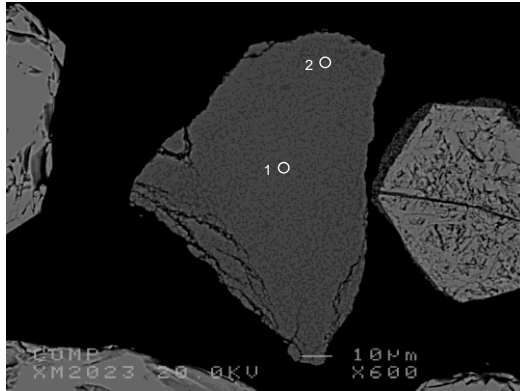
wt%	1	+/-	2	+/-
MnO2	95.78	1.07	94.93	1.06
Fe2O3	0.19	0.06	0.57	0.07
K2O	4.96	0.11	4.86	0.11
Total	100.93		100.36	
mol%				
MnO2	95.34		95.19	
Fe2O3	0.10		0.31	
K2O	4.56		4.50	
Total	100.00		100.00	

Figure CANMET 1: Back scattered electron image 1 of Wabush spiral concentrate with EPMA analysis



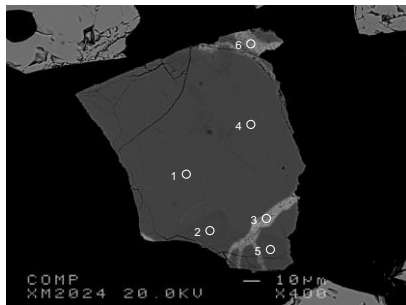
wt%	1	+/-	2	+/-	3	+/-	4	+/-	5	+/-
MnO2	89.09	1.03	91.24	1.05	98.29	1.08	97.89	1.08	90.13	1.04
Fe2O3	6.27	0.16	4.68	0.14	1.48	0.09	1.50	0.09	4.77	0.14
K2O	0.24	0.03	0.06	0.02	0.06	0.02	0.06	0.02	1.58	0.07
Total	95.60		95.98		99.83		99.45		96.48	
mol%										
MnO2	96.08		97.23		99.13		99.12		95.69	
Fe2O3	3.68		2.72		0.81		0.83		2.76	
K2O	0.24		0.05		0.05		0.05		1.55	
Total	100.00		100.00		100.00		100.00		100.00	

Figure CANMET 2: Back scattered electron image 2 of Wabush spiral concentrate with EPMA analysis



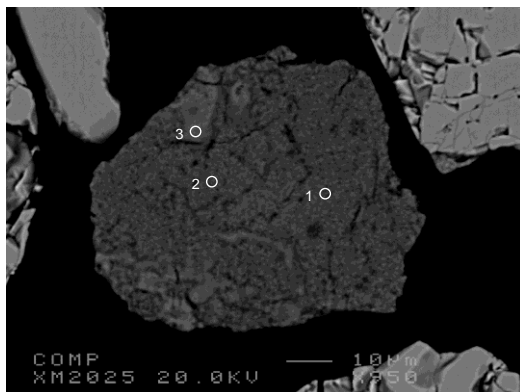
wt%	1	+/-	2	+/-
MnO2	99.67	1.09	99.26	1.08
Fe2O3	0.39	0.07	0.44	0.07
K2O	0.78	0.05	0.79	0.05
Total	100.84		100.49	
mol%				
MnO2	99.07		99.04	
Fe2O3	0.21		0.24	
K2O	0.72		0.73	
Total	100.00		100.00	

Figure CANMET 3: Back scattered electron image 3 of Wabush spiral concentrate with EPMA analysis



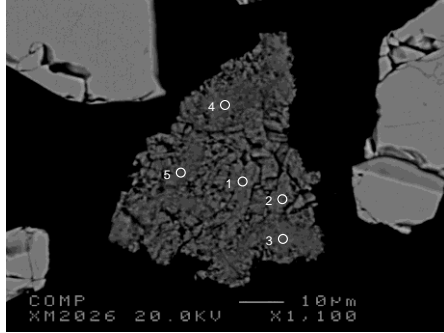
wt%	1	+/-	2	+/-	3	+/-	4	+/-	5	+/-	6	+/-
MnO2	99.94	1.09	99.35	1.08	83.33	1.00	99.53	1.08	97.59	1.07	83.17	1.07
Fe2O3	0.77	0.08	1.68	0.10	1.75	0.10	1.11	0.08	2.28	0.11	2.44	0.11
K2O	0.10	0.02	0.11	0.02	0.09	0.02	0.09	0.02	0.11	0.03	2.06	0.03
BaO					13.59	0.33	0.32	0.10	0.31	0.10	11.97	0.10
Total	100.81		101.14		98.76		101.05		100.29		99.64	
mol%												
MnO2	99.49		98.99		90.51		99.14		98.47		89.25	
Fe2O3	0.42		0.91		1.03		0.60		1.25		1.42	
K2O	0.09		0.10		0.09		0.08		0.10		2.04	
BaO					8.37		0.18		0.18		7.28	
Total	100.00		100.00		100.00		100.00		100.00		100.00	

Figure CANMET 4: Back scattered electron image 4 of Wabush spiral concentrate with EPMA analysis



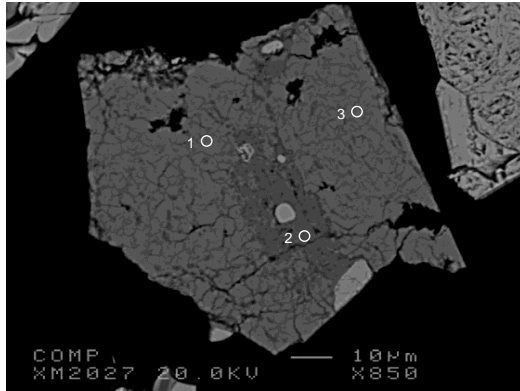
wt%	1	+/-	2	+/-	3	+/-
MnO2	94.23	1.06	92.75	1.05	3.07	0.20
Fe2O3	1.78	0.10	2.84	0.11	79.05	0.53
K2O	0.01	0.02	0.00	0.00	0.00	0.00
BaO	0.00	0.00	0.09	0.09	0.02	0.09
Total	96.02		95.68		82.14	
mol%						
MnO2	98.97		98.30		6.66	
Fe2O3	1.02		1.64		93.32	
K2O	0.01		0.00		0.00	
BaO	0.00		0.06		0.02	
Total	100.00		100.00		100.00	

Figure CANMET 5: Back scattered electron image 5 of Wabush spiral concentrate with EPMA analysis



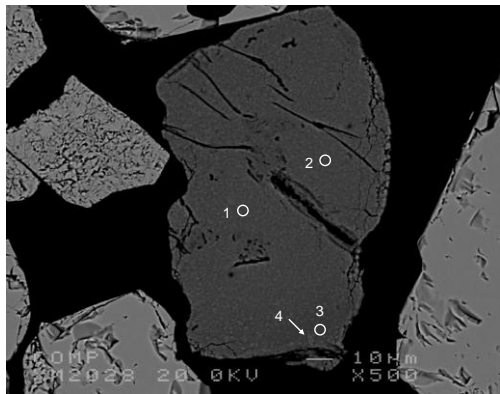
wt%	1	+/-	2	+/-	3	+/-	4	+/-	5	+/-
MnO2	94.80	1.06	94.21	1.06	5.32	0.26	27.69	0.58	39.18	0.69
Fe2O3	3.63	0.13	4.13	0.13	75.76	0.52	58.12	0.45	48.61	0.41
K2O	0.00	0.00	0.00	0.00	0.00	0.00	0.00	0.00	0.00	0.00
BaO	0.08	0.09	0.00	0.00	0.00	0.00	0.00	0.00	0.02	0.09
Total	98.50		98.34		81.08		85.81		87.80	
mol%										
MnO2	97.92		97.67		11.43		46.67		59.68	
Fe2O3	2.04		2.33		88.57		53.33		40.31	
K2O	0.00		0.00		0.00		0.00		0.00	
BaO	0.04		0.00		0.00		0.00		0.01	
Total	100.00		100.00		100.00		100.00		100.00	

Figure CANMET 6: Back scattered electron image 6 of Wabush spiral concentrate with EPMA analysis



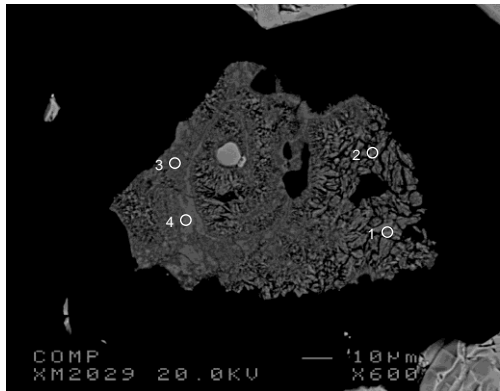
wt%	1	+/-	2	+/-	3	+/-
MnO2	100.09	1.09	2.61	0.19	99.59	1.09
Fe2O3	0.87	0.08	76.93	0.52	0.87	0.08
K2O	0.13	0.03	0.00	0.00	0.09	0.02
BaO	0.06	0.09	0.02	0.09	0.00	0.00
Total	101.15		79.55		100.55	
mol%						
MnO2	99.38		5.87		99.44	
Fe2O3	0.47		94.11		0.47	
K2O	0.12		0.00		0.09	
BaO	0.03		0.02		0.00	
Total	100.00		100.00		100.00	

Figure CANMET 7: Back scattered electron image 7 of Wabush spiral concentrate with EPMA analysis



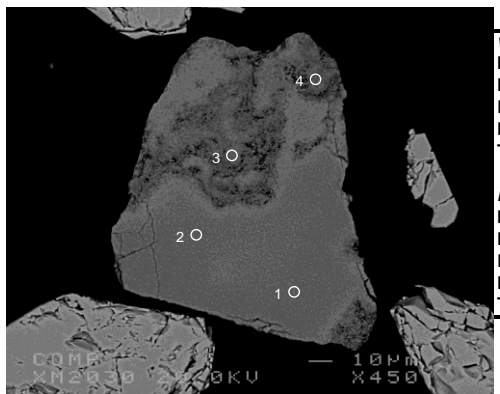
wt%	1	+/-	2	+/-	3	+/-	4
MnO2	99.34	1.08	98.85	1.09	99.22	1.08	98.94
Fe2O3	1.25	0.09	1.34	0.09	1.81	0.10	1.97
K2O	0.03	0.02	0.03	0.02	0.04	0.02	0.02
BaO	0.05	0.09	0.11	0.09	0.08	0.09	0.12
Total	100.67		100.33		101.14		101.04
<i>mol%</i>							
MnO2	99.26		99.18		98.94		98.85
Fe2O3	0.68		0.73		0.98		1.07
K2O	0.03		0.03		0.04		0.02
BaO	0.03		0.06		0.04		0.07
Total	100.00		100.00		100.00		100.00

Figure CANMET 8: Back scattered electron image 8 of Wabush spiral concentrate with EPMA analysis



wt%	1	+/-	2	+/-	3	+/-	4
MnO2	99.88	1.09	98.31	1.08	64.44	0.88	24.18
Fe2O3	0.47	0.07	0.79	0.08	25.65	0.30	62.25
K2O	0.00	0.00	0.00	0.00	0.00	0.00	0.00
BaO	0.10	0.09	0.08	0.09	0.01	0.08	0.06
Total	100.45		99.18		90.10		86.48
<i>mol%</i>							
MnO2	99.69		99.52		82.18		41.62
Fe2O3	0.25		0.43		17.81		58.33
K2O	0.00		0.00		0.00		0.00
BaO	0.06		0.05		0.01		0.05
Total	100.00		100.00		100.00		100.00

Figure CANMET 9: Back scattered electron image 9 of Wabush spiral concentrate with EPMA analysis



wt%	1	+/-	2	+/-	3	+/-	4
MnO2	92.30	1.05	91.94	1.05	91.98	1.05	90.59
Fe2O3	1.12	0.08	1.18	0.09	1.31	0.09	1.21
K2O	2.40	0.08	2.78	0.09	0.44	0.04	0.23
BaO	2.58	0.16	2.39	0.16	3.14	0.17	2.81
Total	98.40		98.29		96.87		94.84
<i>mol%</i>							
MnO2	95.56		95.27		96.95		97.35
Fe2O3	0.63		0.66		0.75		0.71
K2O	2.29		2.66		0.42		0.23
BaO	1.51		1.40		1.88		1.71
Total	100.00		100.00		100.00		100.00

Figure CANMET 10: Back scattered electron image 10 of Wabush spiral concentrate with EPMA analysis

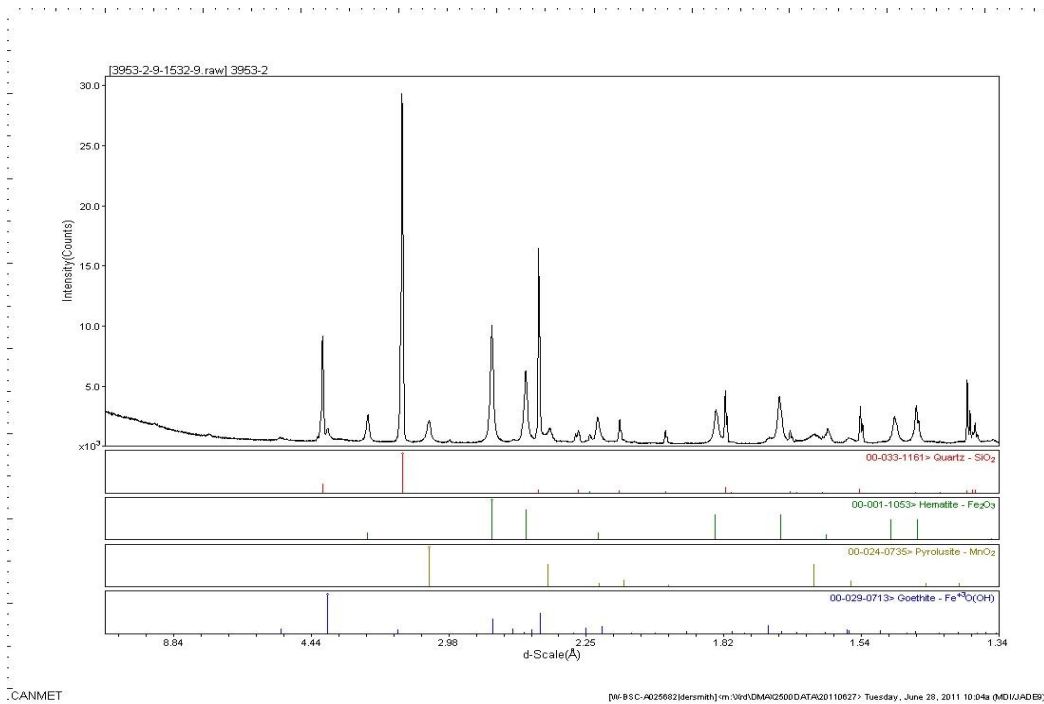
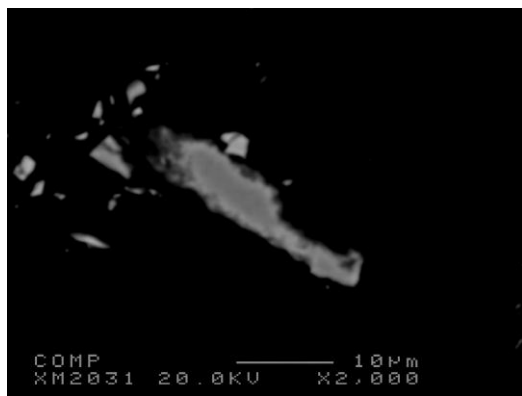
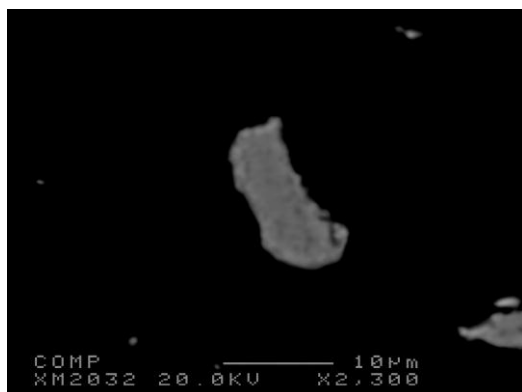


Figure CANMET 11: XRD spectra of BI13 tails



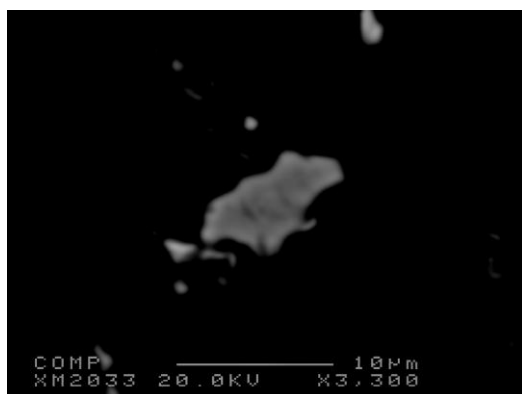
wt%	1	+/-
MnO2	92.78	1.05
Fe2O3	0.94	0.08
K2O	1.90	0.07
BaO	3.32	0.18
Total	98.94	
mol%		
MnO2	95.72	
Fe2O3	0.53	
K2O	1.81	
BaO	1.94	
Total	100.00	

Figure CANMET 12: Back scattered electron image 1 of BI13 tails with EPMA analysis



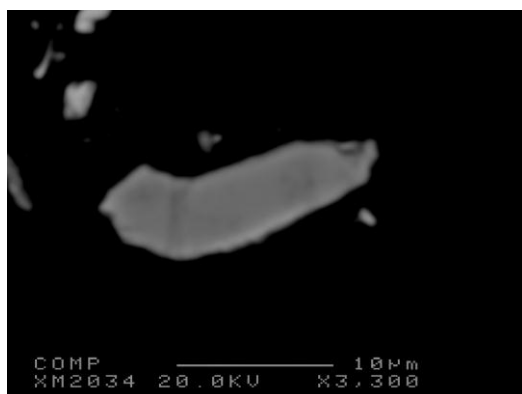
<i>wt%</i>	1	<i>+/-</i>
MnO2	95.26	1.07
Fe2O3	1.56	0.09
K2O	0.46	0.04
BaO	0.96	0.12
Total	98.23	
<i>mol%</i>		
MnO2	98.13	
Fe2O3	0.87	
K2O	0.44	
BaO	0.56	
Total	100.00	

Figure CANMET 13: Back scattered electron image 2 of BI13 tails with EPMA analysis



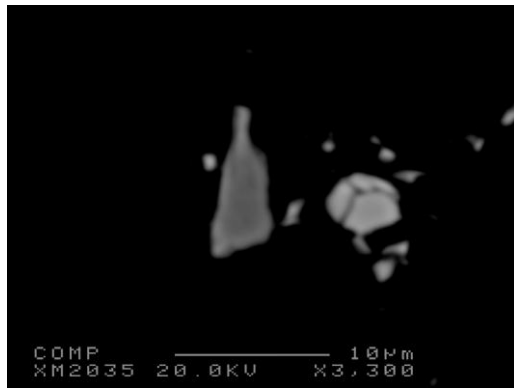
<i>wt%</i>	1	<i>+/-</i>
MnO2	96.41	1.07
Fe2O3	0.83	0.08
K2O	0.02	0.02
BaO	0.10	0.09
Total	97.37	
<i>mol%</i>		
MnO2	99.45	
Fe2O3	0.47	
K2O	0.02	
BaO	0.06	
Total	100.00	

Figure CANMET 14: Back scattered electron image 3 of BI13 tails with EPMA analysis



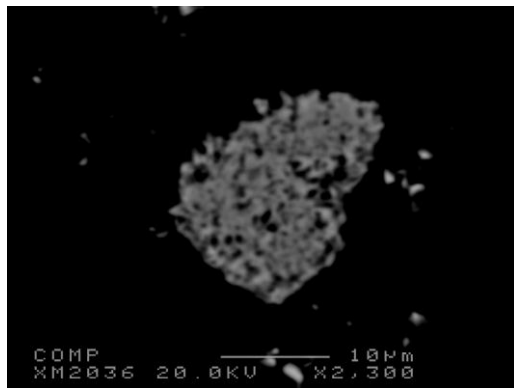
<i>wt%</i>	1	<i>+/-</i>
MnO2	91.01	1.05
Fe2O3	0.76	0.08
K2O	1.29	0.06
BaO	3.86	0.19
Total	96.92	
<i>mol%</i>		
MnO2	96.00	
Fe2O3	0.43	
K2O	1.26	
BaO	2.31	
Total	100.00	

Figure CANMET 15: Back scattered electron image 4 of BI13 tails with EPMA analysis



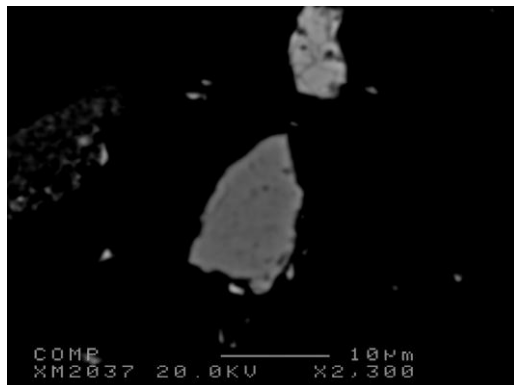
<i>wt%</i>	1	+/-
MnO2	95.82	1.06
Fe2O3	0.86	0.08
K2O	0.02	0.02
BaO	0.00	0.00
Total	96.70	
<i>mol%</i>		
MnO2	99.49	
Fe2O3	0.49	
K2O	0.02	
BaO	0.00	
Total	100.00	

Figure CANMET 16: Back scattered electron image 5 of BI13 tails with EPMA analysis



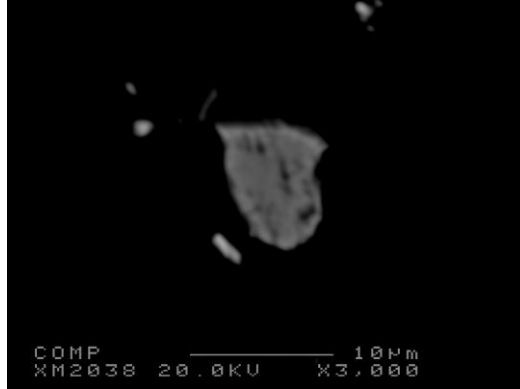
<i>wt%</i>	1	+/-
MnO2	82.44	1.00
Fe2O3	5.67	0.15
K2O	5.11	0.12
BaO	2.37	0.16
Total	95.59	
<i>mol%</i>		
MnO2	90.01	
Fe2O3	3.37	
K2O	5.15	
BaO	1.47	
Total	100.00	

Figure CANMET 17: Back scattered electron image 6 of BI13 tails with EPMA analysis



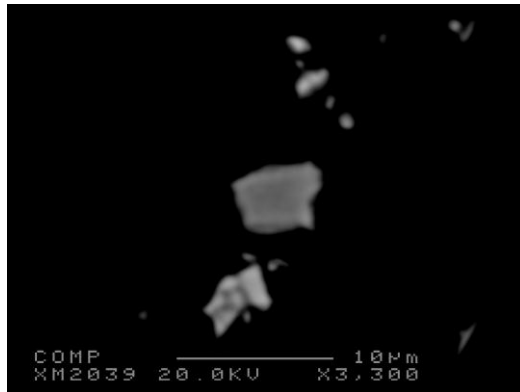
<i>wt%</i>	1	+/-
MnO2	90.36	1.04
Fe2O3	3.95	0.13
K2O	2.21	0.08
BaO	0.07	0.09
Total	96.59	
<i>mol%</i>		
MnO2	95.53	
Fe2O3	2.28	
K2O	2.16	
BaO	0.04	
Total	100.00	

Figure CANMET 18: Back scattered electron image 7 of BI13 tails with EPMA analysis



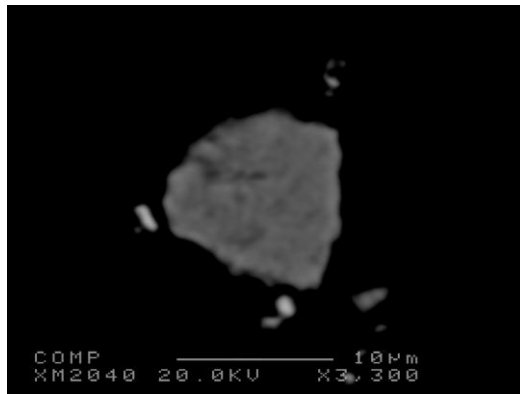
<i>wt%</i>	1	<i>+/-</i>
MnO2	98.89	1.09
Fe2O3	0.59	0.07
K2O	0.02	0.02
BaO	0.02	0.09
Total	99.52	
<i>mol%</i>		
MnO2	99.65	
Fe2O3	0.33	
K2O	0.02	
BaO	0.01	
Total	100.00	

Figure CANMET 19: Back scattered electron image 8 of BI13 tails with EPMA analysis



<i>wt%</i>	1	<i>+/-</i>
MnO2	87.13	1.02
Fe2O3	6.05	0.16
K2O	1.36	0.06
BaO	1.19	0.13
Total	95.73	
<i>mol%</i>		
MnO2	94.34	
Fe2O3	3.57	
K2O	1.36	
BaO	0.73	
Total	100.00	

Figure CANMET 20: Back scattered electron image 9 of BI13 tails with EPMA analysis



<i>wt%</i>	1	+/-
MnO2	86.72	1.01
Fe2O3	4.87	0.14
K2O	0.26	0.03
BaO	0.36	0.10
Total	92.21	
<i>mol%</i>		
MnO2	96.56	
Fe2O3	2.95	
K2O	0.27	
BaO	0.22	
Total	100.00	

Figure CANMET 21: Back scattered electron image 1 of BI13 tails with EPMA analysis

Appendix IV: Harris Exploration

The following is the mineralogical report as received from Harris Exploration Services:

Micron Geological Ltd,
4900 Skyline Drive,
North Vancouver,
BC, Canada, V7R 3J3

Tel (604) 980-4471
Email petlec@shaw.ca

March 10, 2011

To : Jeff Harris / Harris Exploration Services

From: Peter Le Couteur / Micron Geological Ltd

RE: MANGANESE IN SAMPLE “ B106 CON”

Objective

As you requested I analyzed a number of grains in a polished thin section of sample B106 with the objective of determining where the manganese is located.

Work done

I spent a little time scanning the polished thin section of the grain mount on a light microscope under transmitted and reflected light and, as you had already discovered, could not make any useful observations by that method that might help in upgrading the Mn in this sample. I marked a cross in ink on the section, labeled the quadrants 1 to 4 and scanned areas of about 0.5 by 0.4 mm in each quadrant with the SEM and made an X-ray map of these areas showing the distribution of Si, Mn, and Fe. Some of the minerals containing Mn and Si in these areas were analyzed on an AMRAY 1810 scanning electron microscope equipped with an EDAX “Genesis” energy dispersive X-ray analyzer. As the surfaces were uncoated and no standards used these analyses (“EDX” analyses) are semi-quantitative.

Results

The inked cross is shown in Figure 1 with the approximate locations of the 4 areas mapped . Each scanned area was first analyzed to determine the approximate chemical composition, with the results shown in Table 1.

Table HARRIS 1. EDX analyses of 4 mapped areas

Area	analysis	Na2O	MgO	Al2O3	SiO2	MnO	Fe2O3	Total
1	scan 0.54 x 0.43 mm		3	1	28	3	66	101
2	scan 0.54 x 0.43 mm	2	2	2	28	3	64	101
3	scan 0.54 x 0.43 mm	3	2		28	3	64	100
4	scan 0.54 x 0.43 mm	3	2		38	3	54	100

The analyses indicate that SiO₂ and Fe₂O₃ are the major constituents. The MnO level of 3% is about half the value noted in your letter .

The 4 mapped areas are shown in Figures 2 to 9 with paired images of the grains and the corresponding Xray map with locations of analyzed grains identified . In the back-scattered electron (“BSE”) images the majority brighter grey grains are mainly Fe oxide, with silicates appearing as darker grey . The Mn oxide grains are difficult to distinguish from the Fe oxide on the basis of their BSE grey-scale colour, but can be distinguished by their Xray emissions. On the Xray maps Mn is shown as yellow and Si as blue, with the majority Fe oxide grains shown as white . These maps indicate that, allowing for the inter-grain area covered by epoxy, silicates account for about 15 to 20% by area , Mn minerals about 2 to 5% and the remainder are Fe oxide.

Some of each of the grains containing Mn, Fe and Si were analyzed and these are located and numbered on the figures and listed in Table 2. These analyses indicate that :

1 The Fe mineral is an Fe oxide that consists essentially of only Fe and O, and does not appear to contain any Mn, Ti etc.

2 Most, but not all, of the silicate grains are quartz .

3 Some constituents in the 18 grains that contain Mn may be from attached grains of silicates, but of the 16 grains with substantial MnO (>32% MnO):

6 contain only Mn and O (100% MnO)

4 contain MnO (84 to 96% MnO) with 4 to 6 % K₂O

5 consist mainly of MnO (79 to 96 % MnO), with some SiO₂ (8-16%)

It is difficult to identify these minerals from composition and appearance alone since there are a number of oxides of Mn (at least 8, including oxides and hydroxides), quite a few that contain some Si, and several (such as cryptomelane) that contain some K. If it is important to identify these minerals a concentrate with a higher Mn content should be made and scanned by XRD.

Conclusions

1 The Mn in the sample appears to occur mainly as Mn oxide minerals with high MnO contents, some with only Mn and O, others with K and Si. Although the compositions suggest several possibilities the identity of these minerals will require XRD scans.

2 The small amount of these high-Mn minerals observed is compatible with the low percentage of MnO (3%, 6%?) in the sample. No Mn was observed in the much more abundant Fe oxide.

3 Because the Mn occurs in separate Mn minerals with high Mn content, if the diluting Fe oxide and quartz can be removed a much higher grade of Mn could be achieved.

Table HARRIS 2 EDX analyses of grains located in Figure 2, 4, 6 and 8

Area	analysis	Na2O	MgO	Al2O3	SiO2	K2O	CaO	MnO	Fe2O3	Total
1	1					5		95		100
1	2				100					100
1	3				100					100
1	4							100		100
1	5								100	100
1	6				100					100
1	7				100					100
2	1				100					100
2	2	21			67		1	1	11	101
2	3				100					100
2	4								100	100
2	5					4		96		100
2	6								100	100
2	7								100	100
3	1				100					100
3	2				100					100
3	4				100					100
3	5				100					100
3	6				8			92		100
3	7								100	100
3	8					8		92		100
3	9							100		100
3	10				9			91		100
3	11								100	100
3	12								100	100
3	13				52			9	39	100
4	1	11				6		84		101
4	2							100		100
4	3				100					100
4	4				100					100
4	5	7			19			32	42	100
4	6							100		100
4	7				16			84		100
4	8							100		100
4	9				100					100
4	10								100	100
4	11			5	8			88		101
4	12							100		100
4	13			7	14			79		100

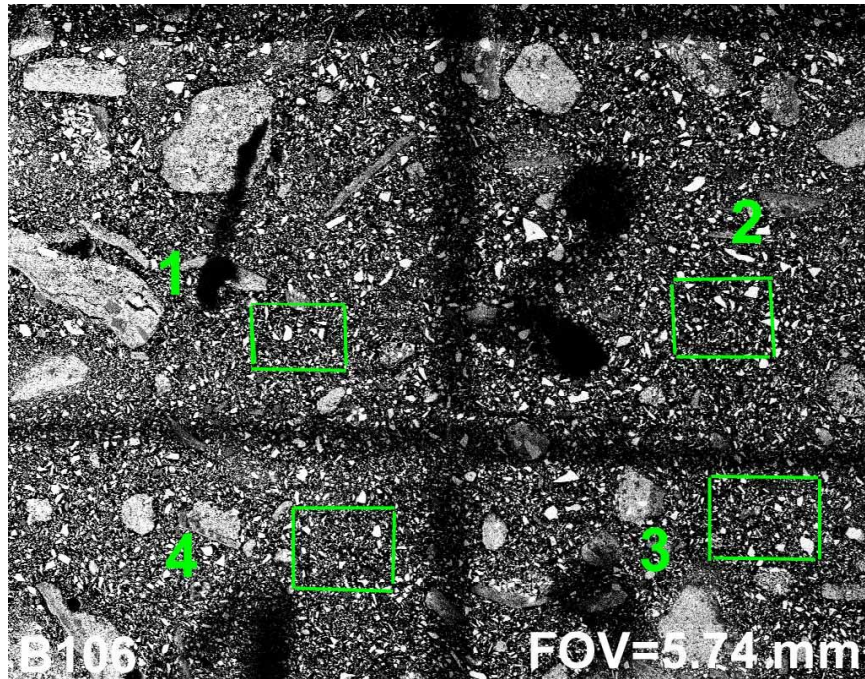


Figure HARRIS 1. BSE. Inked cross with quadrants 1 to 4 and green rectangles showing areas scanned and mapped and shown in Figures 2 to 9 .

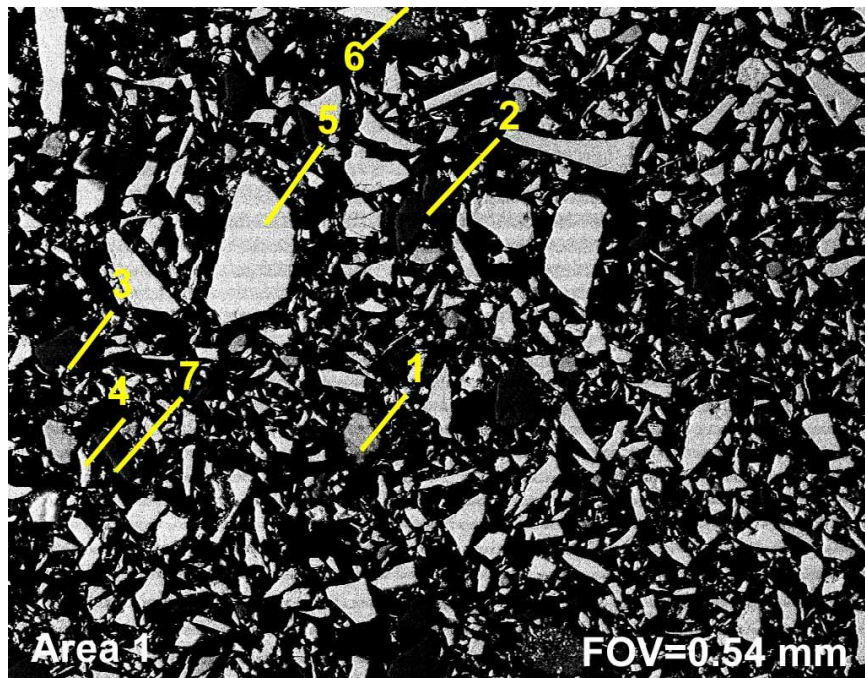


Figure HARRIS 2. BSE . Area 1. Analyses of marked grains in Table 2.

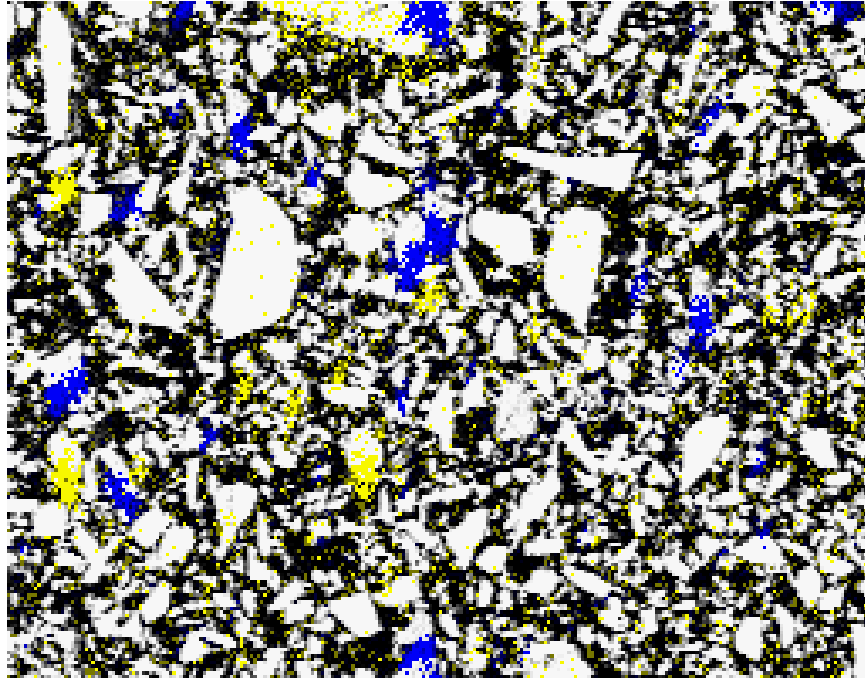


Figure HARRIS 3 .XRAY map . Same area as above figure. Yellow=Mn, blue=Si, white=Fe.

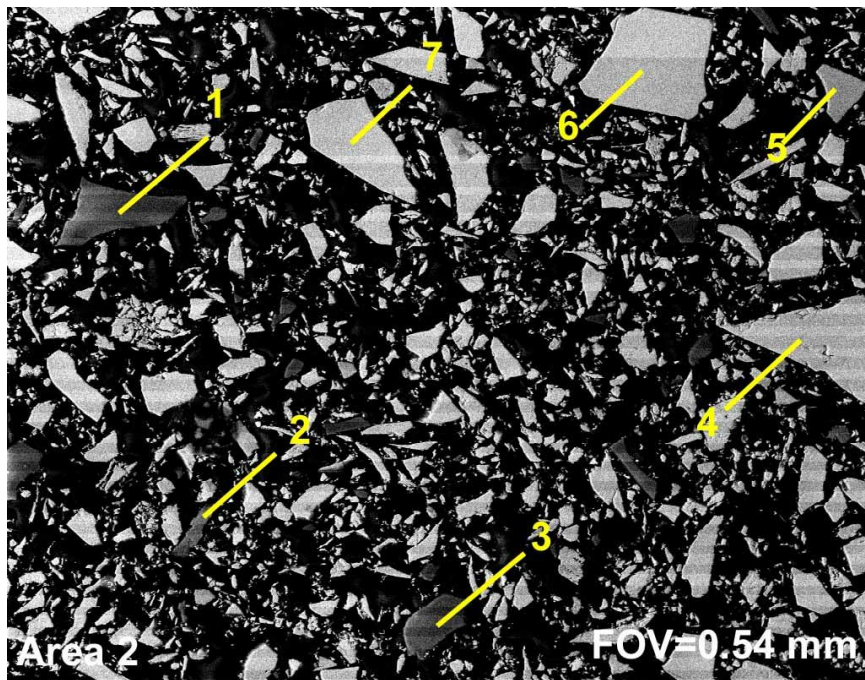


Figure HARRIS 4. BSE. Area 2.

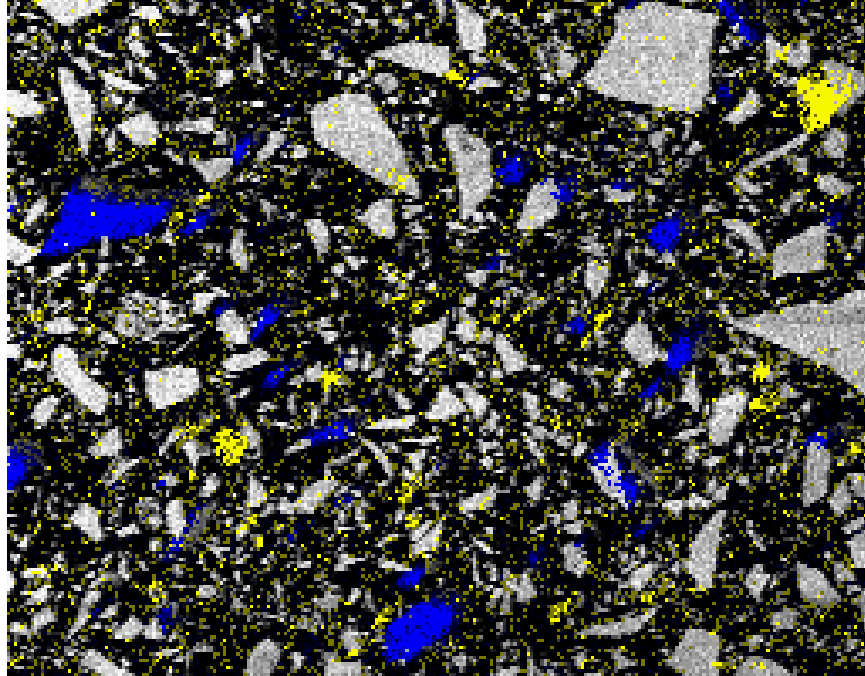


Figure HARRIS 5 .XRAY map . Same area as above figure. Yellow=Mn, blue=Si, white=Fe.

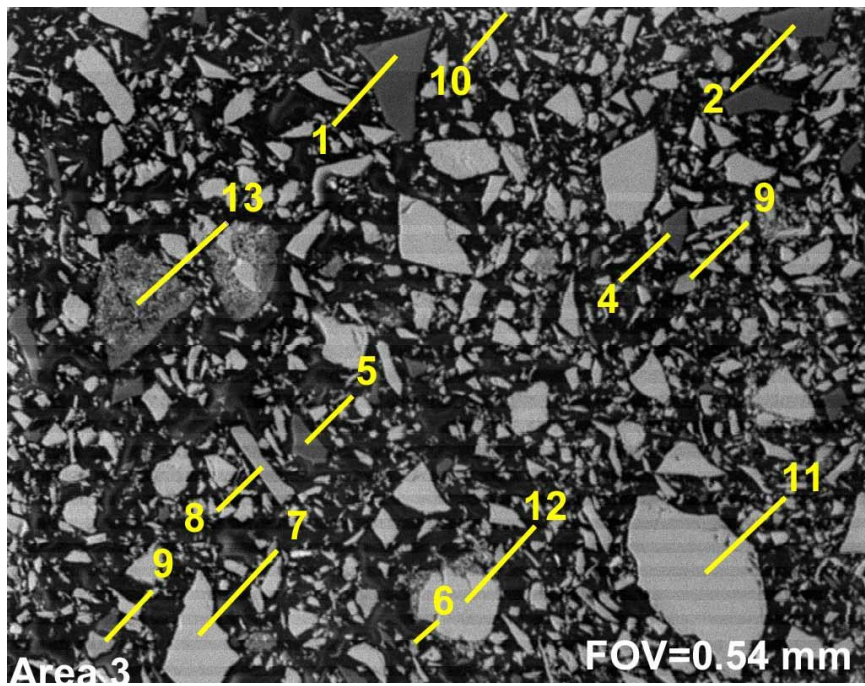


Figure HARRIS 6. BSE. Area 3.

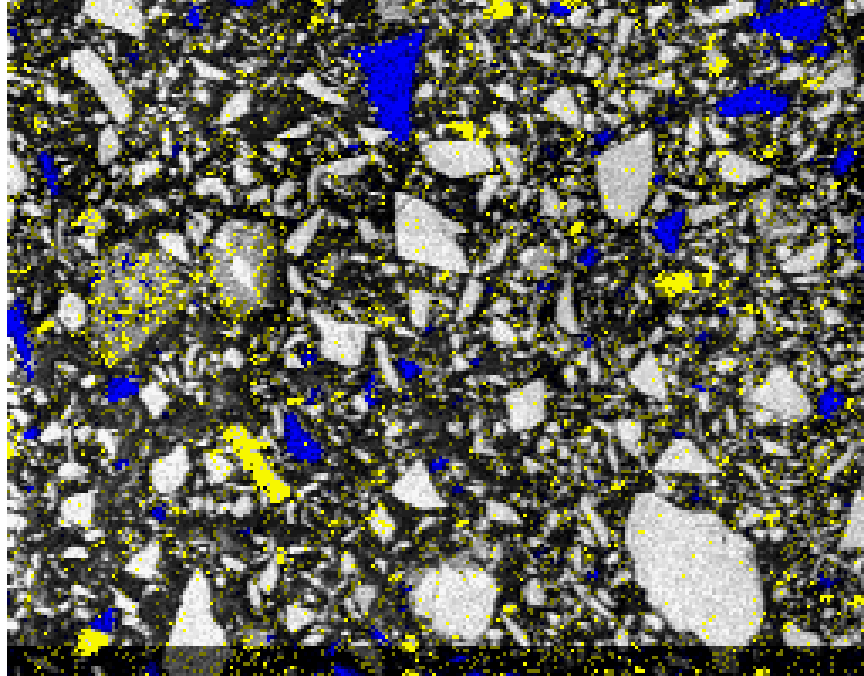


Figure HARRIS 7 .XRAY map . Same area as above figure. Yellow=Mn, blue=Si, white=Fe.

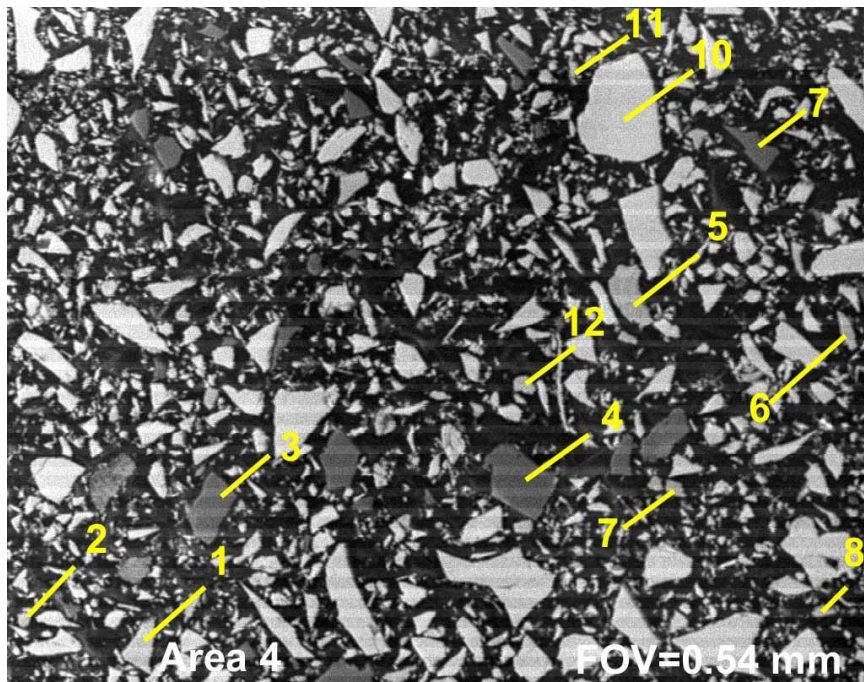


Figure HARRIS 8. BSE. Area 4.

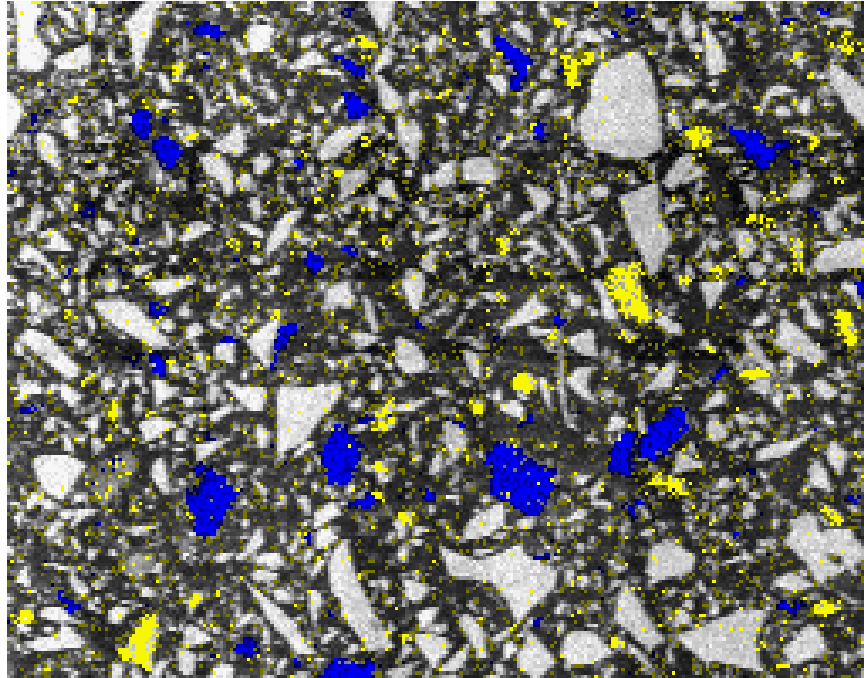


Figure HARRIS 9 .XRAY map . Same area as above figure. Yellow=Mn, blue=Si, white=Fe.

Appendix V: Micro-Scale Flotation

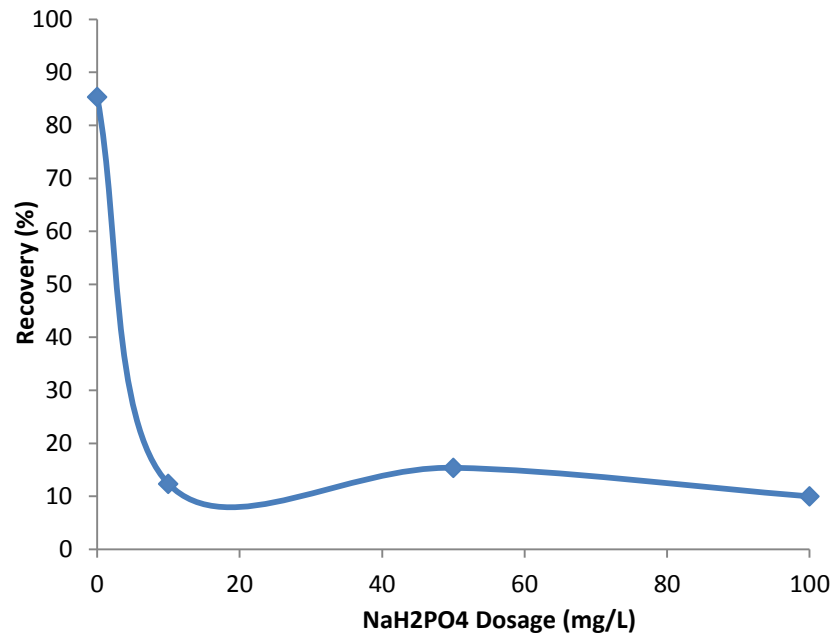


Figure 56: Micro-scale flotation recovery of pyrolusite as a function of NaH₂PO₄ dosage at pH 11 with a sodium oleate dosage of 5×10^{-5} mol/L

Appendix VI: FTIR Spectra

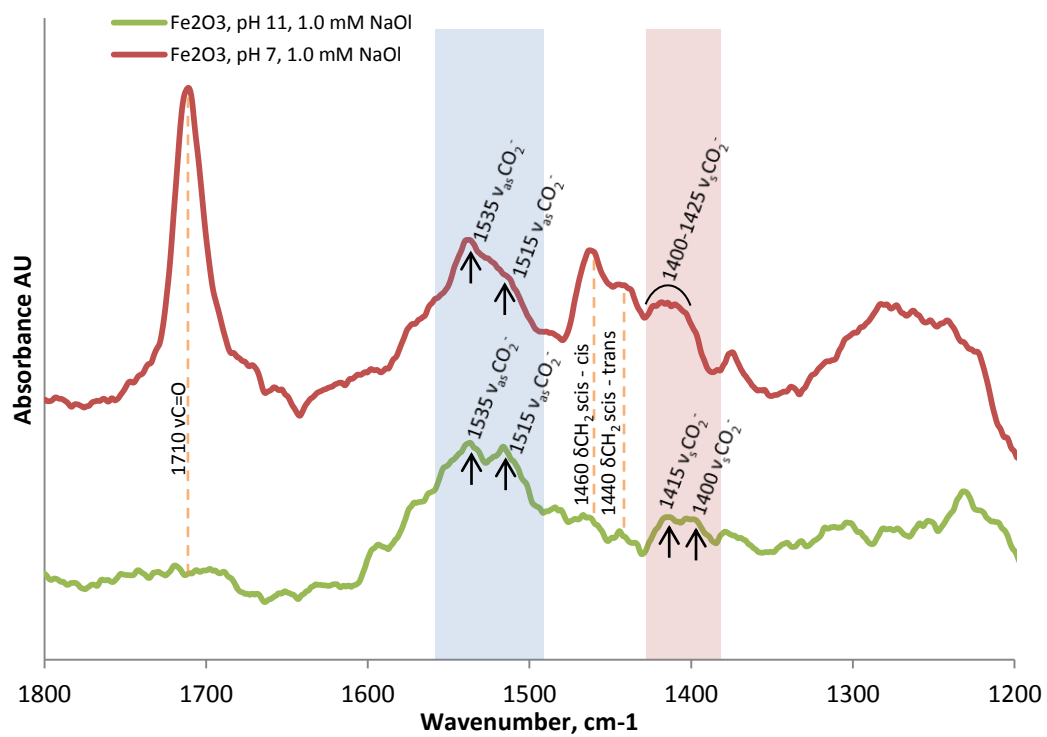


Figure 57: FTIR (DRIFTS) spectra of Fe₂O₃ (hematite) conditioned in 1.0 x 10⁻³ mol/L sodium oleate solution at pH 7 and 11 over a range of 1200 – 1800 cm⁻¹